SYNTHESIS AND REACTIVITY OF HETEROCYCLIC THIONE AND SELONE LIGANDS WITH A SATURATED BACKBONE

by

John R. Patterson

A thesis submitted to the faculty of
The University of North Carolina at Charlotte
in partial fulfillment of the requirements
for the degree of Master of Science in
Chemistry

Charlotte

2017

Approved by:

_____
Dr. Daniel Rabinovich

_____
Dr. Markus Etzkorn

_____
Dr. Thomas A. Schmedake

_____
Dr. Michael S. Matthews

ABSTRACT

JOHN R. PATTERSON Synthesis and Reactivity of Heterocyclic Thione and Selone Ligands with a Saturated Backbone (Under the direction of DR. DANIEL RABINOVICH)

The field of coordination chemistry is so pervasive that it finds use in nearly every branch of chemistry. Notable examples of metal complexes include hemoglobin, high utility catalysts, cancer medicines, and precursors to bulk and nanoscale materials. Previously within the Rabinovich group, the coordination chemistry of various unsaturated N-heterocyclic thione (NHT) and selone (NHSe) ligands has been explored. Utilizing the known analogous chemistry of N-heterocyclic carbenes (NHCs), there is evidence that saturated heterocycles are better sigma donors than their unsaturated counterparts. Exploration of this concept to deduce its consistency with NHT or NHSe ligands is still necessary, however. The focus of this project has been the synthesis and reactivity of saturated five-membered N-heterocyclic chalcogenones.

This work has explored the reactivity of these kinds of molecules by varying donor atom, sulfur or selenium, and the steric hindrance provided by the N-substituents. Examples of NHT or NHSe molecules with saturated backbones found in the literature lack large bulky aromatic N-groups. Research to better understand the coordination properties of these ligands has resulted in multiple experiments including synthetic, computational, spectroscopic, and crystallographic. Some coordination complexes with mercury(II), gold(I), compounds of iodine, and computational analysis has been attempted and the results will be discussed.

ACKNOWLEDGEMENTS

Thank you Mom and Dad, you created me. Luna, gerr woof bark wof. Margaret, you've been immeasurable. Терпе́ние и труд всё перетру́т. If I went back to where this started I'd argue it was in a measly intro class to nanoscale, I probably understood 10% of what that dude taught me, but it was vastly interesting. It's also pertinent to thank Drs. Lee and Park, who gave me opportunities that I literally never thought I'd have and access to knowledge that really accelerated my passion. Whether setting up a fresh lab bench, or learning about π back-bonding for the first time: both elevated me.

During my time in the Rabinovich lab, and UNC Charlotte, I've developed a sense of feel for this subject. It's been a long road, but not unlike any other journey that is worth the trek. The support from my advisor and committee members Drs. Rabinovich, Schmedake, Etzkorn, and Matthews really accelerated my progress. There are also a lot of underappreciated people in Burson that make my every day more reasonable for me, like Drs. Carlin and Merkert, or Drew Tobias. I really do appreciate them all, especially the ones that provide snacks and/or coffee. The students within this department are equally hard working, even in the harsh Burson conditions. I've had the pleasure of working with a handful of students on this project, a highschooler named Drew Peterson, and two undergraduates here in the department Grace and Ashley, who each helped my relearn the subject from their point of view. I've also made some good friends while growing here both within my lab that helped me every day and even some on the first floor. Beyond this department I'd like to thank Dr. James Golen at the University of Massachusetts Dartmouth who performed the XRD experiments for me and Dr. Ilia Guzei at the University of Wisconsin Madison for offering advice for SolidG analysis.

TABLE OF CONTENTS

LIST OF FIGURES

LIST OF TABLES

LIST OF SCHEMES

LIST OF ABBREVIATIONS

CSD	Cambridge Structural Database
DCM	Dichloromethane
DCE	Dichloroethane
DMSO	Dimethyl sulfoxide
EA	Elemental Analysis
ESI-MS	Electrospray Ionization Mass Spectrometry
NaHMDS	Sodium bis(trimethylsilyl)amide
h	Hour(s)
LUMO	Lowest unoccupied molecular orbital
HOMO	Highest occupied molecular orbital
IR	Infrared
NHC	N-Heterocyclic Carbene
NHT	N-Heterocyclic Thione
NHSe	N-Heterocyclic Selone
Mes	2,4,6-trimethylphenyl (Mesityl)
M.O.	Molecular orbital
Xy	2,6-dimethylphenyl (Xylyl)
Dipp	2,6-diisopropylphenyl
NMR	Nuclear Magnetic Resonance
THF	Tetrahydrofuran
XRD	X-Ray Diffraction

CHAPTER 1: INTRODUCTION

1.1 N-Heterocyclic Carbenes

Carbenes are sp^2 hybridized carbon atoms with only two atoms bonded to it, providing the carbon atom with two unbound electrons and two potential atomic orbital configurations for them. In the early exploration of these reactive species it was theorized that stabilization of free carbenes was possible for very short amounts of time, allowing for justification of reaction pathways involving carbenes or even free methylene. These reagents were utilized for many years for carbon insertion reactions and cyclopropanation reactions.[1] While metal complexes of carbenes started appearing in the literature in the late 1960's, many isolated by Schrock and Fischer, the true pioneers of N-heterocyclic carbene (NHC) ligands were the groups of Öfele and Wanzlick, Figure 1.1.[2-4] However, the first persistent carbene was isolated by Arduengo in 1991 (Figure 1.2).[5] The key difference between these isolable carbenes and complexes, known before, are the stabilization mechanisms.[6]

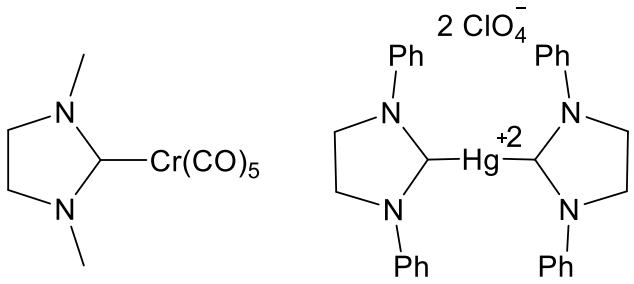

Figure 1.1: Öfele's NHC complex (left) and Wanzlick's NHC complex (right).

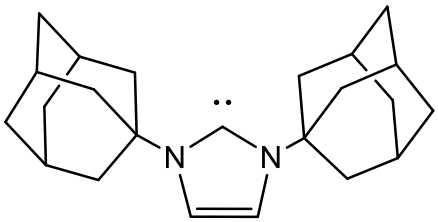

Figure 1.2: Arduengo's free NHC.

The classification of metal carbene complexes developed by Schrock and Fischer affords a clearer picture of why these molecules can be stable. There are two major effects that stabilize a carbene, namely inductive and mesomeric effects of the substituents on the carbene. Schrock carbenes are often noted as being excellent ancillary ligands for hard acid metals. Stabilization of the free electrons in the sp^2 and p_z orbitals, shown in Figure 1.3, is due to the increased inducing effect from Schrock carbenes compared to less electronegative moieties. The p_z and sp^2 orbitals are almost degenerate therefore; these carbenes exist in a triplet state. In contrast to Schrock carbenes, Fischer carbenes require π donating and σ withdrawing moieties that favor a singlet state in these carbenes, or two electrons paired in one sp^2 orbital due to sp^2 orbital to be slightly less energetically demanding that the p_z ortibal, as depicted in Figure 1.3. Fischer carbenes act like Lewis bases by donating the pair of electrons in the empty sp^2 orbtial into various bonding systems similar to amines, phosphines, esters, isonitriles, *etc*.

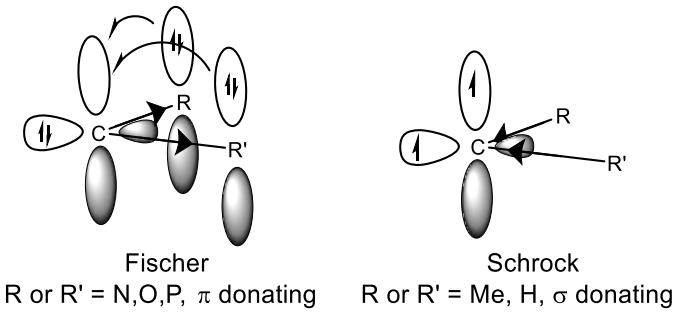

Figure 1.3: Comparison of the possible electronic stabilization factors of carbenes.

Also reported in the carbene literature is that a ring system supporting the Fischer carbene increases the electron donating character of the singlet pair on the carbene, specifically to a metal center while also stabilizing the molecule itself.[7] If one considers the natural angle of 120° for sp^2 hybridized carbons, a ring system supports the N-C-N atoms, keeping them near 120° of an internal angle. This was in fact a major reasoning for the stability of Wanzlick's carbene complex vs. complexes with noncyclic Fischer carbenes. This later resulted in a realization of NHCs as a whole new set of ligands, due to the benefits imparted by an empty atomic orbital on the carbene that allows for significant back bonding ability.[8]

NHCs are Fischer-type carbenes, with the added stability of two functional groups on the nitrogen moieties; one is a contiguous bond connecting the two nitrogen atoms to form the ring, while the other may be variable. These were first proposed by Öfele, *et al.*, Figure 1.1. When attempting to obtain various heterocyclic metal complexes it was noted that the addition of imidazolium salt to the metal hydride provided a stable yellow crystalline solid.[3] Using ^1H NMR spectroscopy the complex was determined to be a single entity with two peaks correlating to the equivalent imidazole hydrogens and N-substituted methyls. This was theorized to be *in situ* generated free carbene, which then reacted with the metal ion in the solution to produce the NMR signals. No structural data was obtained for this early NHC, however. In the same year, Wanzlick *et al*. were synthesizing mercury compounds of imidazolium salts similar to the ones Öfele had worked with, purposely attempting to make complexes of NHCs.[4] Wanzlick's earliest NHC complexes, Figure 1.1, were found to be homoleptic charged mercury(II) species with two NHC ligands stabilizing the complex. This reinforced the idea of carbenes being

a sigma fashion donating ligand, similar to isocyanides or phosphorous ligands, but no proof of such structures had yet been rendered without a metal attached to the carbene, leading to arguments of the existence of a free carbene.

The first structure of a free carbene was obtained by Arduengo *et al.*, Figure 1.2, proving dissenters of stable singlet carbenes wrong.[5] It was originally concluded that the steric bulk of the adamantyl groups was one of the major factors of keeping the carbene in a singlet ground state, congeners molecules without bulky substituents on the nitrogens were considered to not be stable. This was eventually proven wrong, as the variations on the Arduengo NHC quickly exploded, some examples shown in Figure 1.4,[4,9-17] and a surge of research went into these new excellent sigma donating and moderate π accepting ligands, due to their superiority to phosphorus based ligands. This inspired a very rapid development of these ligands in the scientific community due to their simplistic synthesis and favorable properties for homogeneous catalysis. Currently these ligands find use in applications ranging from homogeneous catalysis, metallo-pharmaceuticals, and organocatalysts to just name a few of the numerous uses for these ligands.[2,18-21]

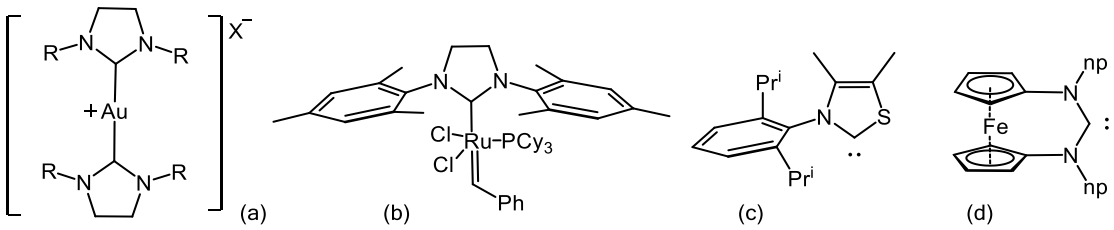

Figure 1.4: a) Organometallic antitumor medicine b) Grubbs' second generation olefin metathesis catalysis c) 2, 3-dihydrothiazol-2-ylide ligand d) ferrocenyl-substituted ylide carbene ligand.

1.2 Saturation Effects on NHC Systems

In a review on effects of both substituents and backbones on free carbenes, by Nolan *et al.* reported that there are two main factors that increase the basicity of the carbene; magnitude of σ induction from nitrogen atoms and internal carbene angle, typically dependent on sterics of the system.[7] Either more sigma donation into the nitrogen from substituents, or freedom of movement for the nitrogen atoms, allowing the internal carbene angle to get closer to the ideal 120°, is needed to increase basicity of the carbene.[22] Conveniently, it can be seen that by saturating the cyclic backbone an increase in basicity is achieved without losing any of the structural integrity of the system, actually increasing thermal stability.[23] The longer sp^3 carbon bonds will increase the internal angle, pushing the carbene into more of a sp^2 orientation. A secondary effect of this distortion in the planarity in the ring system is reducing the overlap of the nitrogen occupied p atomic orbitals. This physical geometry leads to less donation into the methine's empty p_z atomic orbital. Imidazolinium salts with mesityl functional groups are available by chemical suppliers, due to their incorporation with the second- and third-generation Grubbs' catalysts (Figure 1.5) and other similar NHC cross coupling homogeneous catalysts that find use in industry and research.[24]

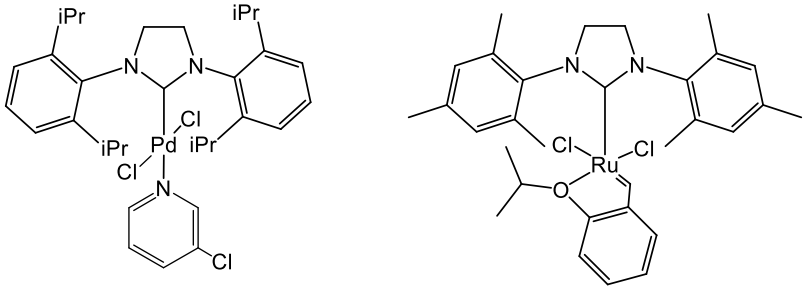

Figure 1.5: PEPPSI^{TM}SIPr and third generation of Grubbs' olefin metathesis catalyst.

1.3 NHT and NHSe ligands

The chalcogen family has one of the most abundant elements of the planet, oxygen. Oxygen is found everywhere in chemistry and tends to dominate the chalcogen chemistry currently known. The heavier members of group 16, namely sulfur, selenium, and tellurium, are typically found in minerals, thus the name chalcogen describing their generation from ores of copper, *Chalkós* in Greek. Tellurium is particularly of less interest to many molecular chemistries due to the poor Te-C bond overlap, leading to relatively few organo-tellurium molecules.[25] Very few biological systems utilize tellurium, but some are known, otherwise tellurium usage in human biology is neither abundant nor useful and potentially even dangerous.[26-27] The remaining chalcogens, S and Se, have many interesting atomic properties that are reflected their inclusion in many organic and inorganic systems.

In general, sulfur and selenium analogs of oxygen molecules are relatively stable, but they do have a 'slippery' nature in terms of bonding due to less electronegative nuclei allowing for easier transfer of valence electrons to carbon atoms. An example of this favorable electronic factor might be the use of sulfur in the eukaryotic and prokaryotic cells as a redox controlling agent in the thiolstat, a collection of redox sensitive cysteine proteins which together regulate cell activity.[28] While S and Se can often simply replace O in molecular systems, the congeners tend to have different properties, primarily polarizability offering chemistry like disulfide bonding used in many biological systems including the thiolstat. Another side effect of this electronic factor is that thio- and seleno-ketone molecules tend to be much less stable than their oxygen counterparts. Unlike the very common carbonyl group, the later chalcogenones form more polarizable

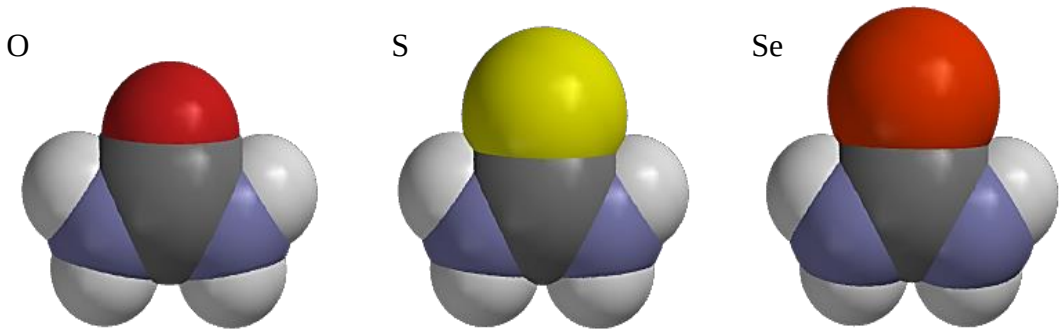

Figure 1.6: Left to right: urea, thiourea, and selenourea space-filling models.

bonds due to their lower electronegativity. This in turn allows for stronger bonds when attached to π accepting moieties, like NHCs, which has been noted in many instances. One example of how using sulfur or selenium in lieu of oxygen can change a molecule is seen in urea, one of the oldest known synthetic chemicals.[29] Heavier chalcogens have less overlap with the carbon atom, viewable in Figure 1.6, due to the higher repulsion from more electrons in them. This in turn creates a more polarized bond and increases the reactivity.

For example, urea is noted for high stability in multiple systems, whereas thio- or seleno-urea will undergo degradation to salts or other products under relatively mild conditions.[30] Some other interesting aspects of the heavier analogues of urea are the shortened C-N bond lengths, indicating delocalization of the nitrogen electron pair into the S or Se atom due to the low oxidation state on the nitrogen. Other studies have investigated delocalization abilities of the chalcogen elements in generic aromatic systems and found that sulfur and selenium are more well suited than oxygen to form aromatic systems with carbon.[31]

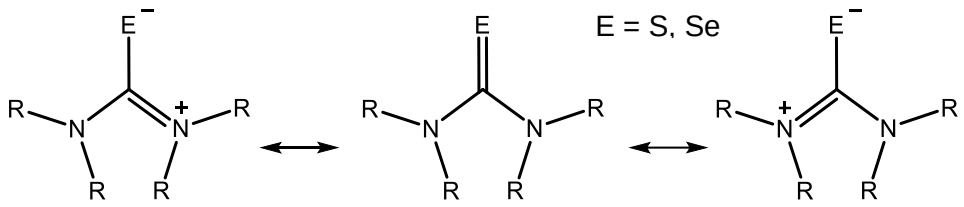

Figure 1.7: Zwitterionic resonance contributors of NHT and NHSe molecules.

While a small urea-like molecule loses stability with the heavier chalcogens, it can be expected that the higher oxidation on the nitrogen atoms would stabilize the chalcogenone bond. Such systems displaying zwitterionic type bonding have been studied by many groups exploring NHC systems, similar structure to urea, to stabilize the reactive carbene center which then reacts with a given chalcogen. Unlike the relatively weak urea stabilization, the NHC systems stabilized the chalcogen carbon bond on an energetic magnitude similar to that of other types of resonance stabilization energies.[13] This stabilizing effect of the new chalcogenone bond onto the singlet carbene does not show the same properties as the small urea type molecules with respect to heavier chalcogens. This is in part due to the zwitterionic resonance contributors of the new NHT or NHSe system, shown in Figure 1.7. This resonance is considered a stabilizing factor for the NHT or NHSe molecules, it has been reported that the zwitter-ionic state is a significant contributor in the heavier chalcogen variants.[32-33]

Figure 1.8 shows the proposed generic bonding of a NHC with elemental chalcogen. It can be seen that the donating and accepting nature of the methine carbon are good for bonding with the chalcogen atom, which is seen in the higher enthalpy of an NHT *vs.* a NHC.[13] These lone pairs on the chalcogen are most likely the orbitals that will be donating into a Lewis acid. Logically by having more electron density donated into the donor atom will benefit coordination to a metal ion. This supports two notions: N-C-N

moiety focuses electron density on the chalcogen via the methine carbon and if either of the nitrogen atoms are substituted with a proton then the charge placed onto the chalcogen will attract the hydrogen.

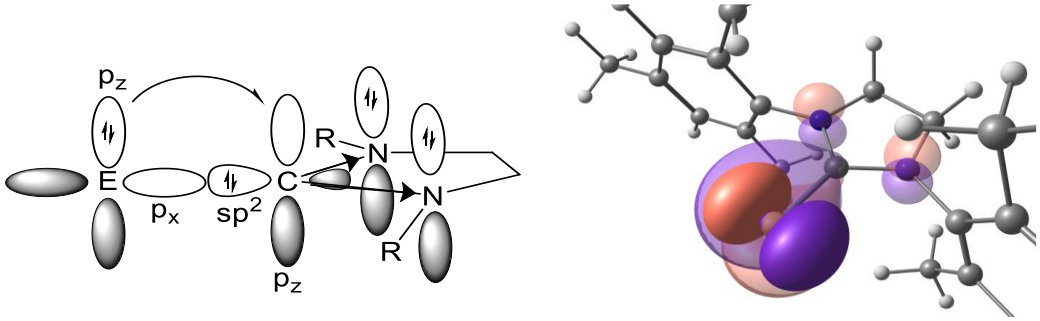

Figure 1.8: NHC and chalcogen frontier orbital interactions cartoon, left.
Right, NHT isosurface for HOMO (solid) and HOMO-1 (transparent).

1.4 Chalcogenone Coordination Chemistry

Coordination chemistry has been performed with thio- or seleno-keto donor ligands, but these seem to not form stable metal bonds unless bidentate. The structures that are known are primarily mercapto groups, with one of the donors being the thione or selone, with very few examples of the lone thio- or seleno-keto donor ligands.[34-36] The thione or seleone on standard alkyl molecules are just too unstable to donate electron pairs.[37] An example of this instability is seen in the results of attempted coordination chemistry with thio-keto type molecules, resulting in the formation of a platinum η^2 bond into the sulfur and carbon atoms of the thioketone.[38-39] This unexpected bonding was most likely caused by the lack of resonance stabilization and mild inductive substituents on the thione carbon leading to a more even shared π electron pair between carbon and sulfur.[38,40]

Thiones and selones of activated NHCs, unlike alkyl thio- or seleno-ketones. are much more stable as the strong sigma donation into the chalcogen atom and back π donation in the reverse to carbon stabilizes the system. The ylidic resonance coupled into the polarizability of the heavier chalcogen atom offers significantly higher stabilization as the chalcogen will take the negative. This electronic interaction has been noted and has been used by some investigators for various chemical applications. The bulk of this work, however, has focused on small N-substituted rings of various natures or molecules containing a thio- or seleno-urea moiety.[41] Most NHT or NHSe ligands found in the Cambridge Structural Database (CSD) have only hydrogen atom N-groups, or a single small N-substituent. Most examples of NHTs also tend to have an imidazole ring or benzene backbone, seen in Figure 1.9.

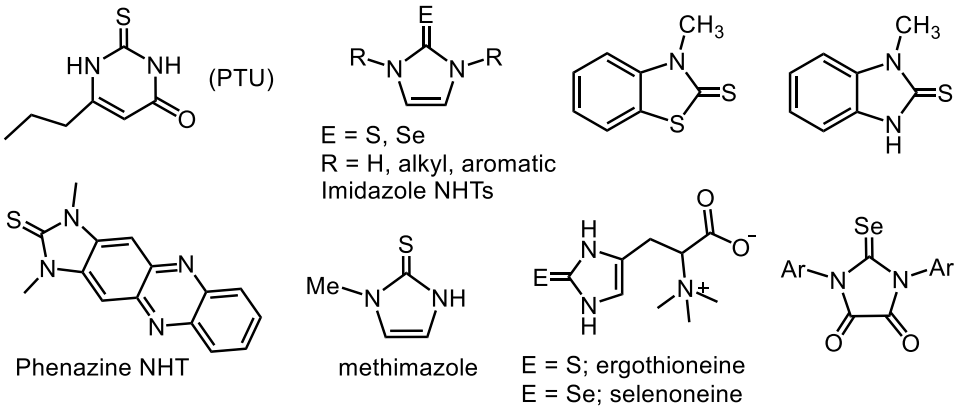

Figure 1.9: Examples of popular NHT and NHSe ligands.

These unsaturated NHT or NHSe systems have been widely explored, especially with small substituents, due to similarity of these molecules to some found in biological systems that are responsible for redox control in enzymes or elsewhere in cellular processes, like ergothioneine or seleoneine (Figure 1.9). Small unsaturated thoiones have been of particular interest due to the antithyroid medications methimazole and propyl-

thiouracil (PTU).[42-43] Yoon *et al.* used the donation properties in NHTs to design a functional phenazine NHT diagnostic molecule for hypochlorite in living cells, shown in Figure 1.8.[44] To stabilize their molecule to fluoresce small methyl N-substituents were required.

1.5 Saturated NHT and NHSe Ligands

Similar to NHC molecules, NHT or NHSe ligands with a saturated backbone should be more favorable Lewis bases. Thermal stability and higher solubility in organic solvents should be observed, akin to trends observed for NHCs. Of 300+ matches in CSD for saturated imidazole ring with S or Se, only 36 have alkyl substituted aromatic N-groups that would hinder nitrogen's reactivity in the molecules and impart "bulk" to the molecule as a whole. The majority within literature for saturated NHT or NHSe molecules has primarily been examples of smaller primary or secondary alkyl N-substituted thiones (Figure 1.10a). The bulk of what has been reported for these smaller variants of the NHT and NHSe molecules, typically deals with biological applications.[30,45]

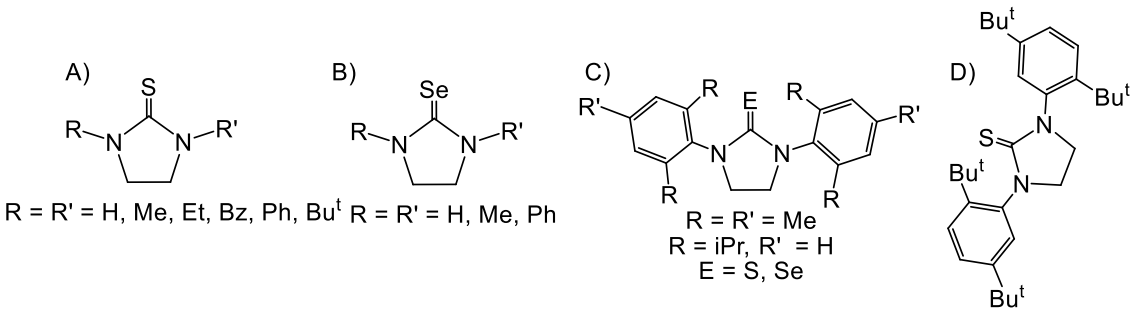

Figure 1.10: NHT or NHSe type molecules found in the CSD.

The analysis of the CSD for NHT or NHSe compounds draws attention to saturated systems, particularly the five-membered rings as there is an abundance of

literature on their unsaturated counterparts (Figure 1.9). Shown in Figure 1.10 are many examples of small NHT or NHSe molecules that are useful in biological or organic chemistries. However, to stabilize low-valent heavy metal complexes the usage of substituents larger than hydrogen on the nitrogen atoms of the heterocycle, to disable any bidentate nature, is necessary. These larger aromatic substituents should increase the stability of the ligand while also increasing electron density at the chalcogen donor atom.[4,9-17] Saturated NHSe ligands are sparse in literature, primarily appearing as diagnostic tools for analyze electronic properties of NHCs (Figure 1.10c).[46-48] Examples of these aromatic substituted saturated NHT or NHSe type molecules have been prepared in the literature, but the research is not heavily pursued.[2,15]

The bulky ligands that have been explored tend to be from classic NHC precursors, so primarily diisopropylphenyl or mesityl aromatic groups (Figure 1.9c). Some other bulky examples do exist, seen in Figure 1.10, but are limited to phenyl, t-butyl, and one particularly large bis(t-butyl)phenyl substituents, almost all from catalysis work previously done with NHTs.[10,49-50] The bulk of coordination chemistry done with the NHSe variants has been performed on gold(I) species by the Nolan groups to determine how coordination affects the donor atom.[51] The saturated bulky NHT ligands have some limited coordination chemistry reported. Hahn *et al.* synthesized silver NHC complexes that were found to decompose to the NHT of the original NHC, but no follow up research on the NHT products was published.[52]

Another line of research by Lan *et al.* computed donation ability and found that the delocalization of the nitrogen and methine into the chalcogen atom offers interesting electronics at the donor atom, particularly for palladium catalyzed reactions by increasing

the stability of the metal donating into empty π orbitals.[53] Yang *et al.* experimentally attempted this and indeed found that various palladium Heck reactions were quicker and required lower temperatures to complete various carbon carbon bond forming reactions when using a saturated NHT of the type seen in Figure 1.10d as a palladium ligand across many iodo-substrates.[54-55]

While the line of work published with palladium was impressive, the only other reactivity explored with these ligands to date are gold(I) complexes. Yang *et al.*, in a later publication, found NHT gold(I) complexes to be useful for catalyzing cyclization reactions of various alkyl chains with primary alkynes and alpha substituted carbonyl groups.[56] Similar gold(I) complexes were prepared by Che *et al.* and investigated for cellular toxicity and found particularly potent due to the potentially high binding affinity to thioredoxin reductase active sites, which control oxidation in cells; killing them if disabled.[57]

1.7 Project Objectives

The goals of this project are to synthesize new five-membered N-heterocyclic thione (NHT) and selone (NHSe) ligands with a saturated backbone and bulky aromatic N-substituents (Figure 1.11), with the goal of coordinating them to a variety of metals. The SIArE abbreviation is derived from NHC literature where ‘SI’ stands for saturated imidazole, Ar is the aromatic moiety in question, and the E at the end used to denote the chalcogen.

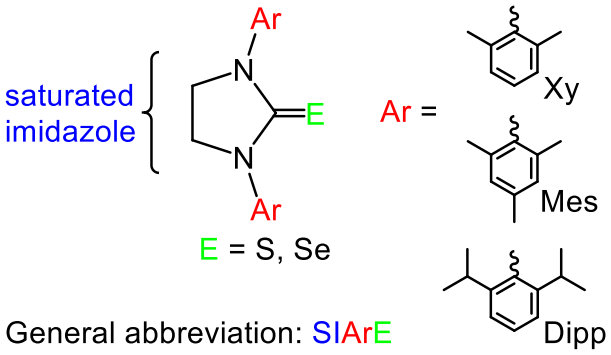

Figure 1.11: NHT and NHSe molecules of interest.

Examples of SIArE ligands shown here are known in literature, as previously mentioned, but the exploration of the synthesis and coordination chemistry is lacking. Coupling this fundamental empirical exploration with a focus on understanding the donating abilities of these saturated ligands will offer a basis for future work with these ligands. The results of the synthesis SIArE ligands and exploration into applications, different metal complexes including mercury(II) and gold(I), along with reactivity with iodine will be discussed herein.

CHAPTER 2: RESULTS AND DISCUSSION

2.1 Synthesis and Characterization of SIArE

Synthesis of the aforementioned SIArE ligands has been reported previously. Some of the papers reporting SIArE ligands were not focused on SIArE synthesis, instead having the ligand as an intermediate or by product. Of the papers purposely synthesizing them, they reported synthesis under N_2 atmosphere, but others show that this is not necessary. In essence all have slightly different variations on the synthesis, but often approach the synthesis in the same manner as that of NHC ligands.[16,47,50-52,54-55] Some of the earliest reports of SIArE synthesis comes from Hahn *et al.* during exploration of silver(I) NHC reactivity, finding that the NHTs SIMesS and SIDippS were the major products of reacting the respective silver complex with S_8. Obviously, this method is not practical for reactivity studies even though the conversion of the silver complex to thione is very favorable. Another more practical procedure was reported by Yang *et al.*, using diamine precursors and thiophosgene, Scheme 2.1. While affording reasonable yields for the desired SIMesS, the reaction involves a similar intermediate to the Arduengo NHC synthesis. By utilizing Arduengo's reported synthesis routes for free NHCs, Scheme 2.2 was conceived.[58-60]

Scheme 2.1: Yang *et al.* synthesis routes for SIMesS.

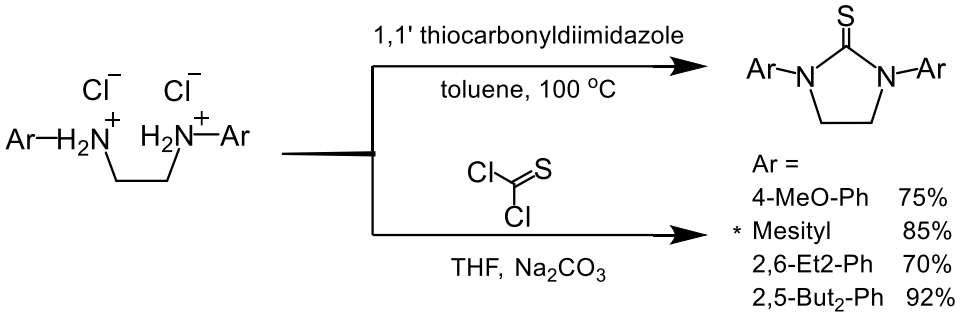

This seemed to be a valid and facile preparation; however a bottleneck occurred in the reduction of the diazadiene. Literature reported this synthesis step using various reducing agents, but only $NaBH_4$ and lithium aluminum hydride were explored for practical reasons.[61] When additions of dilute HCl were added to the reduced solution, to allow precipitation of the desired diamine salt, it seemed to cause some kind of decomposition or the initial reaction of the reducing agent caused some lysing event that was not predicted. The result for most reactions was no product or product containing heavy impurity. Therefore, the ring closing step was never attempted due to the previous synthesis step failing, until an alternative route was presented.

Scheme 2.2: Proposed synthesis route to SIArE.

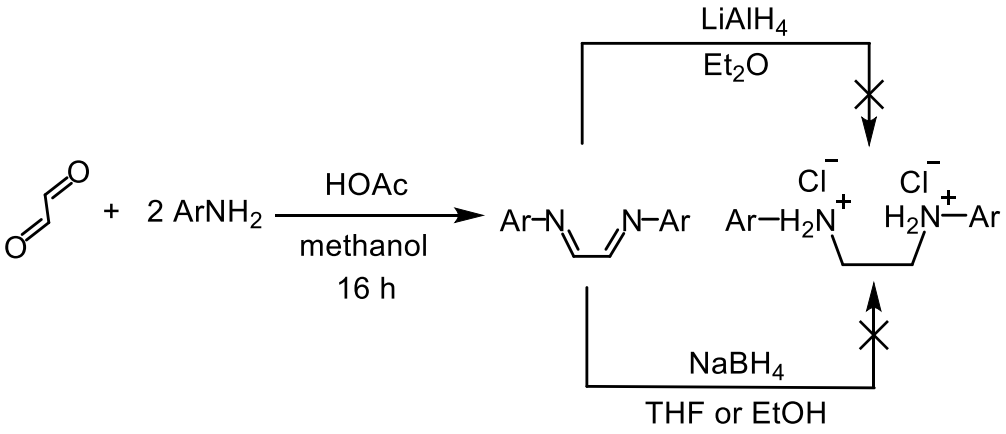

Ganter and Nolan, *et al.*, utilized a more elegant approach for the preparation of SIArSe molecules starting from imidazolinium salt precursors, but had poor yields unless using a small batch reaction, less than 100 mg. While the approach is rational, both report syntheses in a N_2 atmosphere and used strong bases, $KOBu^t$ and NaHMDS, which aren't desirable for facile preparation. The work-up of this reaction called for multiple steps, so an alternative work up was sought to increase the reported yield of *ca.* 50%.[12] We predicted that the last step could be substituted from another NHT synthesis reported by Arduengo where deprotonation was achieved using dry potassium carbonate in the presence of elemental chalcogen.[12] Grubbs and Kuhn patented an alternative synthesis for imidazolinium and other saturated NHC salts in 2008.[62]

Scheme 2.3: General ligand synthesis for SIArE.

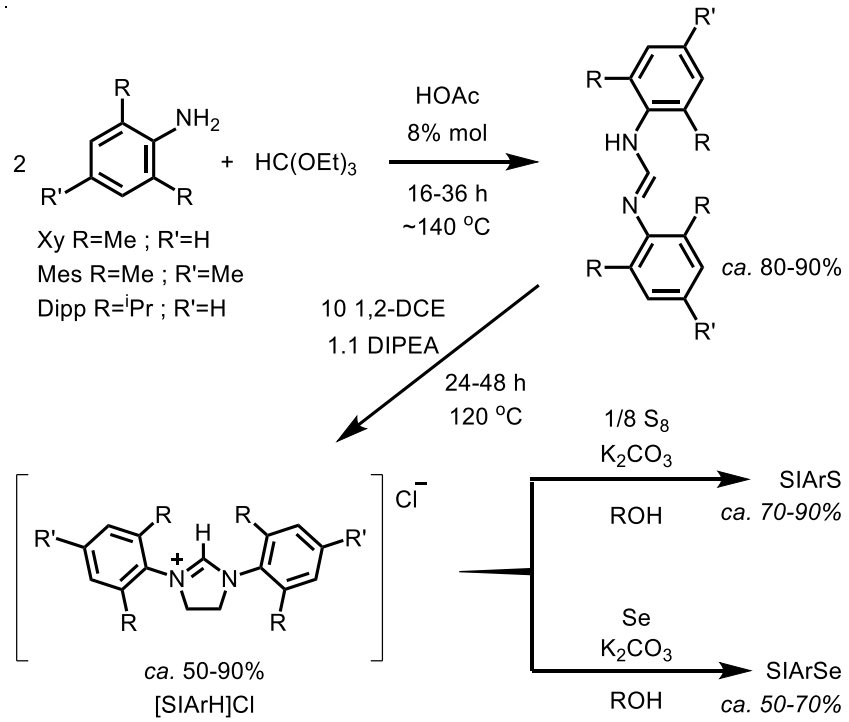

The saturated backbones, obtained from dihaloalkanes, are reacted with the front of a normal NHC ring, a formamidine, to synthesize imidazolinium salts, shown in Scheme 2.3. This synthesis is essentially the reverse of the Arduengo NHC synthesis, shown in Scheme 2.2.

The initial step to synthesize SIArE ligands is the synthesis of aromatic substituted formamidines. These are synthesized neat from one equivalent of triethylorthoformate and two equivalents of an alkyl substituted aniline, distilling ethanol in the presence of an acid catalyst. The pure fluffy white product is isolated easily with filtration. NMR spectroscopy revels an inherent isomerization property of these kind of formamidine molecules in solution, creating observable duplicate peaks in their ^{1}H NMR spectra.[63] This isomerization is primarily due to solvation and hydrogen bonding effects creating different arrangements of the molecule that are viewable in ^{1}H NMR, shown in Figure 2.1.

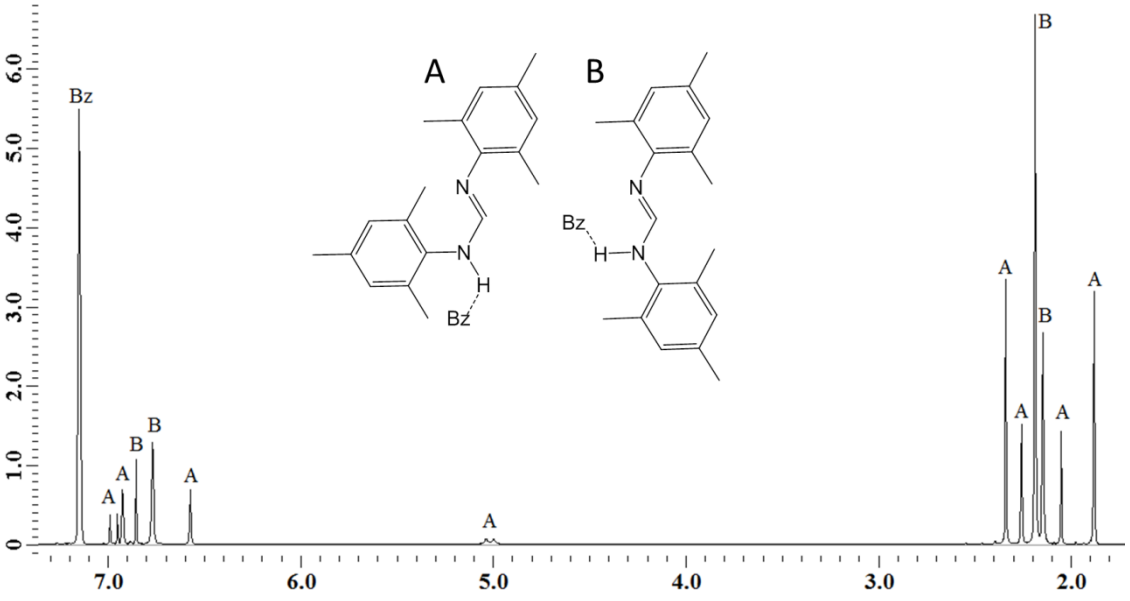

Figure 2.1: ^{1}H NMR spectrum of Mes formamidine in C_6D_6.

To synthesize imidazolinium salt from a formamidine starting compound a substitution reaction occurs after a base deprotonation. Deprotonation of the sp^3 nitrogen is accomplished with diisopropylethylamine (Hünig's base) due to its favorable solubility and weak nucleophilicity due to steric hindrance, which facilitates the substitution reaction with the dichloroethane. This reaction is performed under reduced pressure at high temperatures to expedite the alkane association onto the formamidine moiety. Purification of imidazolinium salt was reported as simple trituration using hot toluene for [SIMesH]Cl or cold acetone for [SIDippH]Cl. Hot toluene was found to be effective for the Mes imidazolinium salt, but acetone at 0 °C was observed to dissolve the [SIDippH]Cl product, resulting in poor yields. The Xy imidazolinium variant was not reported in the Grubbs' synthesis protocol, but synthesis was attempted in the same fashion as the Mes synthesis. This yielded clean formamidine with the same conditions as the Mes, but the salt synthesis was observed to yield impure material using toluene as a trituration solvent. Ethyl acetate was found to be sufficient to purify the solvent, by NMR analysis. After determining this, cold ethyl acetate was found to yield clean [SIDippH]Cl in yields above 50%.

Synthesis of the free ligand is accomplished with an addition of sulfur or selenium. shown in Scheme 2.3. Deprotonation of the methine proton using potassium carbonate allows a free pair of electrons on the carbon to act as a donation site onto atomic sulfur. Proton NMR spectrum of the chalcogenation reaction shows a definite loss of methine proton upon successful addition of chalcogen with the loss of the singlet around 9.5 ppm, shown in Figure 2.2.

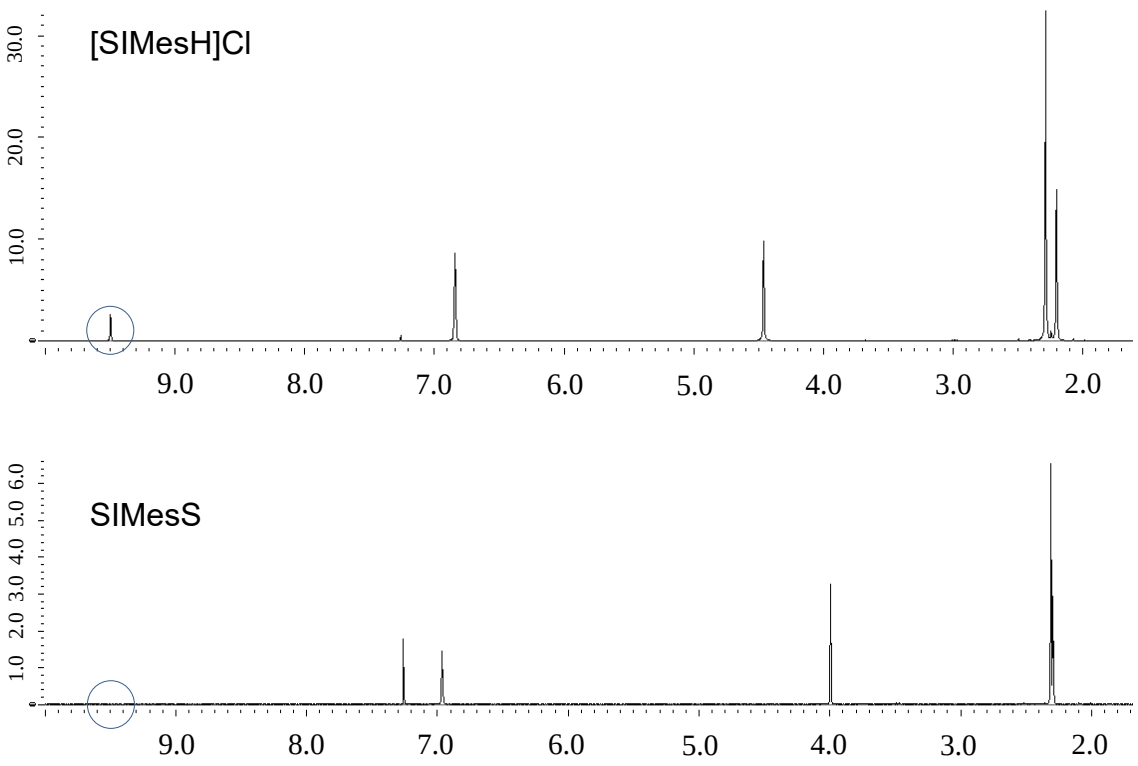

Figure 2.2: ^{1}H NMR spectra of SIMesHCl and SIMesS in $CDCl_3$.

The incorporation of sulfur onto the ring system is observed to increase electron shielding on the ring system and somewhat more shield the aromatic rings as well, presumably due to the larger number of electrons on the chalcogen. The most obvious change occurs in the methylene protons of the backbone, going from 4.5 ppm to 4 ppm after chalcogenation. The methyl peaks ortho to the ipso-carbon also become more shielded, but less significantly so, with -0.1 ppm downfield change typically in the SIMesE systems. This supports the electronic stabilizing effects of the zwitterionic resonance transferring to the chalcogen instead of the carbene carbon.

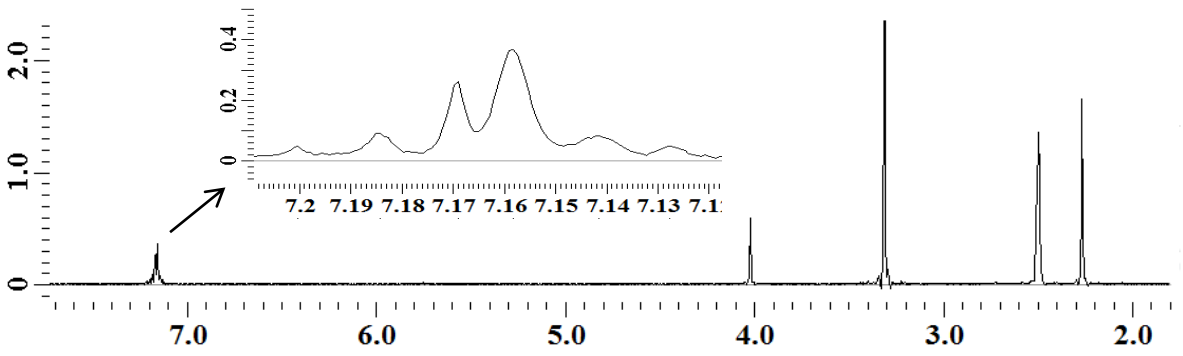

Figure 2.3: ^{1}H NMR spectrum of SIXySe in d_6-DMSO.

Shown in Figure 2.3 is a ^{1}H NMR spectrum of the SIXySe ligand. All the SIArE ligands share similar NMR characteristics. For example SIDippE ligands have near matching spectra to the SIXyE, but with two doublets in the 2 ppm range and a septet after 3.0 ppm. The mesityl derivatives are similar, but very simplistic due to the aromatic hydrogens being a singlet. The mesityl methyl's are not regiochemically identical, seen with two singlets around 2.3 ppm with 2:1 ratio, nor are the methyls of the diisopropylphenyls, thus giving rise to the two doublets.

Carbon NMR spectra of the SIArE lignads are, as expect similar, with minor differences seen in the respective ligands in the aromatic region in couple ^{13}C NMR, due to the various alkyl substituents. Figure 2.4 shows the decoupled and coupled NMR of SIXySe to deomonstrate the generic layout of SIArE ligand's carbom NMR. The early alky region always shows the backbone around 50 ppm and the various aromatic substituents more upfield. As mentioned the aromatic region is the only region that visbibly is altered by substituent, but always shows the 4 unique peaks for free ligands. Lastly, the C=E carbon tends to have a peak around 180 ppm for free ligands and always appears as a singlet.

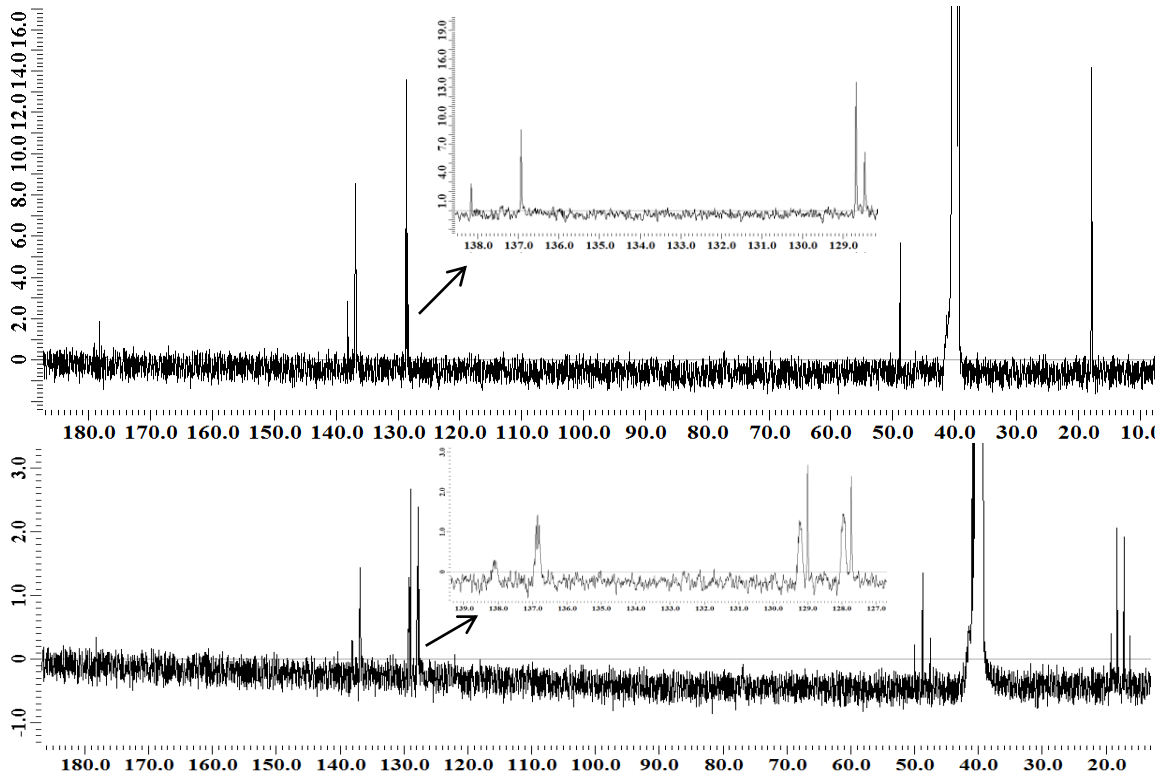

Figure 2.4: $^{13}C\{^{1}H\}$ (top) and ^{13}C NMR (bottom) spectra of SIXySe in d_6-DMSO.

Preperation of SIArSe is identical to the thione, just replacing grey selenium for S_8 in the reaction While the thione *vs.* the selone of these ligands should not be vastly different, it was observed that for almost all ^{1}H NMR spectra for SIArE both thione and selone were near identical in resonance shifts in both deuterated chloroform and DMSO. This fact along with the analysis of the ^{13}C NMR data showing a similar insignificant difference of the methine carbon shift was unexpected. For example the carbon of the *C*=E in SIDippS, 184.1 ppm, and SIDippSe, 184.3 ppm, are near identical in d_6-DMSO. It was brought into question if the alkyl substituents on the aromatic ring affect the electronics of the donor atoms. To test this ^{77}Se NMR spectroscopy experiments were performed and compared to literature values published by the Nolan and Ganter groups, Figure 2.5, finding identical values for SIMesSe and SIDippSe.[47-48,64] These experiments

do demonstrate a quantifiable difference of the electronic states as SIXySe, near identical to SIMesSe, produced a resonance 5 ppm downfield from SIMesSe. While quantifiable differences were observed, the ^{77}Se spectrum spans over 2000 ppm. With this fact in mind, it is apparent that the electronic shielding at the donor atoms for these ligands are very similar, but compared to selones without NHC heterocycles these ligands are far more shielded, by about 1000 ppm, explaining their potential as ligands.[65]

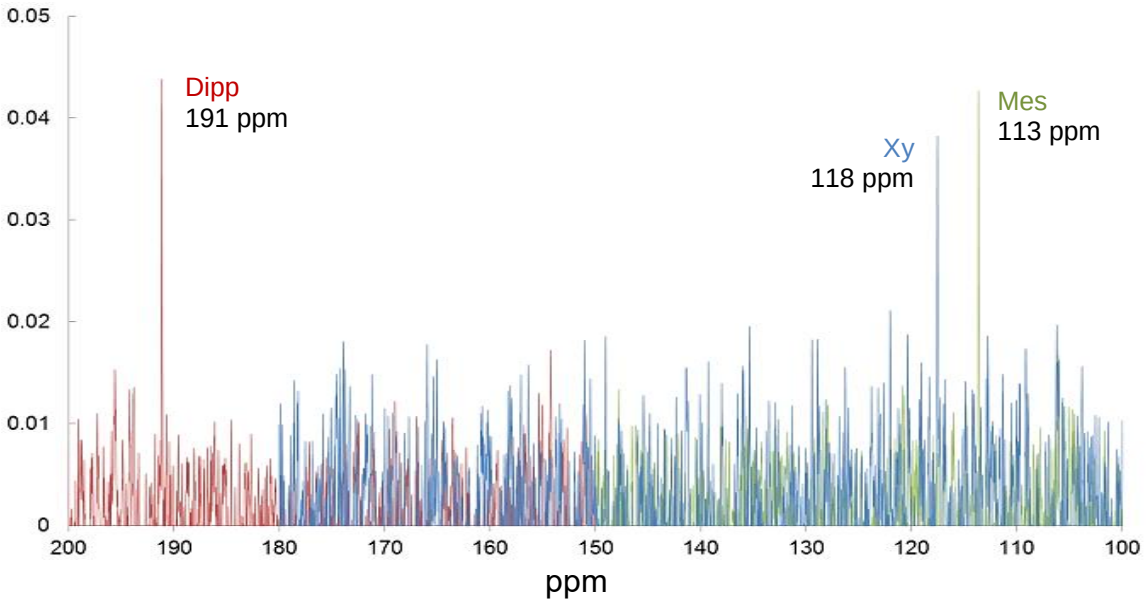

Figure 2.5: ^{77}Se NMR spectra of SIArSe in $CDCl_3$.

There is not an easy way to compare the donation of the selone ligands *vs.* the thiones. This is only made more difficult with the near matching spectroscopic data of any given SIArS *vs.* the analogous SIArSe. To attempt to compare these differences, computation methods were employed. As previously published, the enthalpy of thiourea compared to thioformaldehyde is stabilized by about 39.2 kcal/mol due to the ylidic-carbon allowing for resonance contributions.[53] Within the same study it was calculated

that the addition of a backbone that forces the nitrogen atoms to become slightly distorted in space, such as an ethylene subunit, causing a destabilization of the degenerate HOMO π orbitals of the ligand. This is not favorable for metal interactions and supports thioketone containing ligands being less coordinative to metal ions than thiourea containing ligands.

Theoretical work was done by Lan *et al.* on NHT systems and their Lewis base properties towards palladium catalysis.[53] To further this work, the same computation methods were employed using Hartree-Fock calculations and the 6-311G* basis set to avoid poor approximations of ionization potentials, Table 2.1. Minor differences of the calculated values of SIMesS compared to Lan *et al.* were attributed to the use of solid-state structures for the single point energy calculations. The HOMO-1 and HOMO difference for all the ligands are less than *ca.* 10 kcal/mol indicating these are near degenerate orbitals, and have been considered to both be participants in metal bonds. In general it is observed that the SIArSe ligands have slightly less stable HOMOs, possibly due to higher electron-electron repulsion of the selenium's core electrons. This, not calculated in the work done by Lan *et al.*, points to SIArSe potentially being a better donor into metal systems. Especially when considering the loss of accuracy in the calculated orbital energy due to the higher correlation energy in the SIArSe molecules.

Table 2. 1: Orbital Energies (kcal/mol) of SIArE Ligands Obtained from HF/6-311G* calculations in Gaussian '03

	SIXyS	SIXySe	SIMesS([53])	SIMesSe	SIDippS	SIDippSe
HOMO-1 (C=E ; p_z)	-192	-178	-192 (-193)	-176	-192	-179
HOMO (E ; p_x)	-187	-172	-184 (-187)	-169	-188	-173
LUMO	81	80	84 (94)	83	80	80

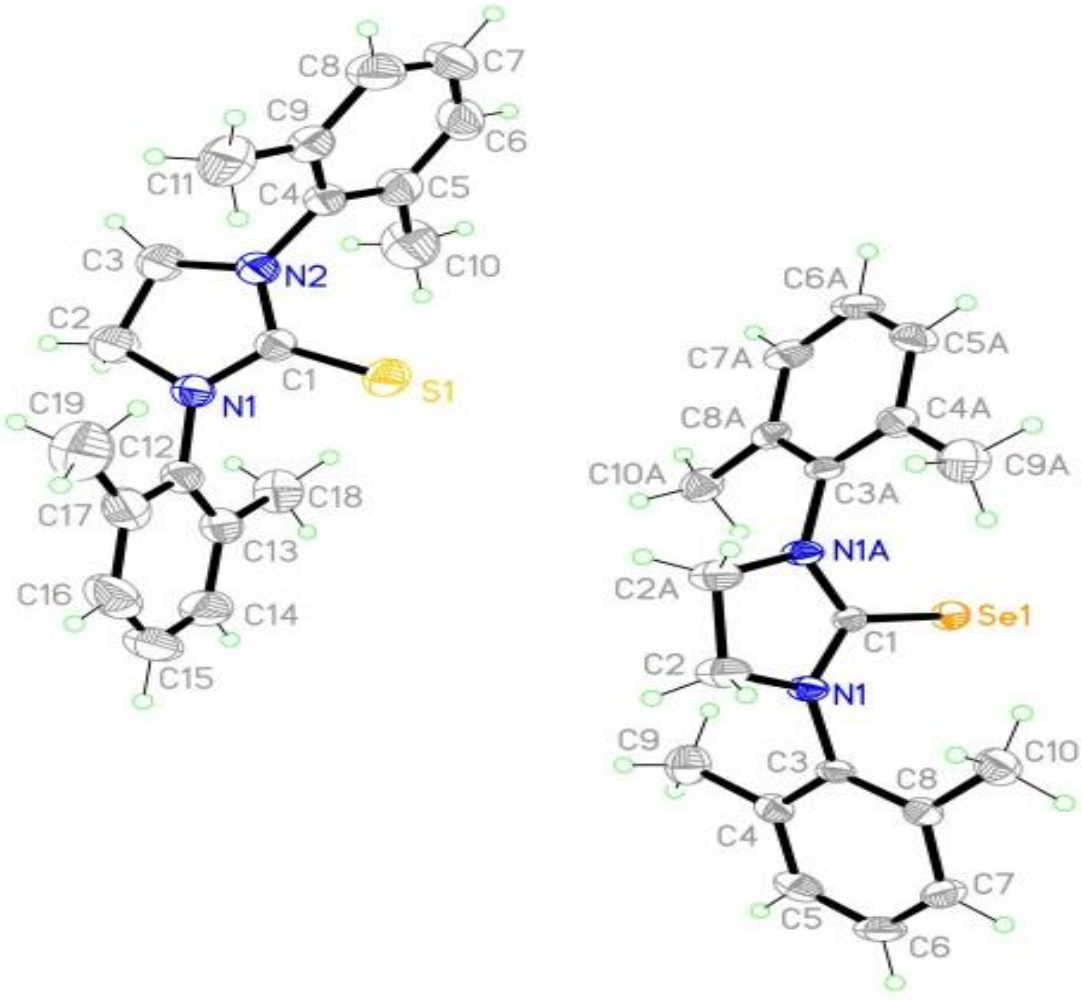

Figure 2.6: Molecular structures of SIXyS (left) and SIXySe (right).

Utilizing the Grubbs imidazolinium synthesis method, all desired ligand precursors were successfully prepared. The imidazolinium salts are generally utilized to generate a carbene in solution, which also occurs in the synthesis NHT and NHSe ligands, the final desired ligands.[66] After isolating the SIArE products they are found to be stable in open air for an extended amount of time. It's also been noted that these ligands are, in general, also very stable in organic solvent exposed to open air.[10,16,50,56-57,67] The synthesis, structure, and characterization of almost all of the SIArE molecules in this study have been reported previously, except for SIXySe.[66] Neither SIXyE ligands have been added to the CSD, however. Crystal structures of both SIXyE ligands were obtained, as shown in Figure 2.6, with selected bond lengths and angles for all six SIArE ligands included in Table 2.2.

Table 2.2: Selected Bond Lengths (Å) And Angles (°) For SIArE.
(Numbering scheme identical to SIXyS, Figure 2.6, above)

	SIXyS*	SIXySe*	SIMesS	SIMesSe	SIDippS	SIDippSe
Bond Lengths (Å)						
S-C(1)	1.672	1.836	1.670	1.829	1.661	1.815
C(1)-N(1)	1.346	1.346	1.360	1.343	1.348	1.343
C(1)-N(2)	1.348	1.346	1.360	1.343	1.353	1.354
Angles (°)						
N(1)-C(1)-N(2)	108.4	109.0	107.7	108.8	107.7	108.3
C(1)-N(1/2)-C(2/3)-C(3/2)	-4.4/ 4.4	-3.4/ 3.4	-11.4/ 11.4	-11.8/ 11.8	-0.3/ 0.3	-0.9/ 0.9

* This work

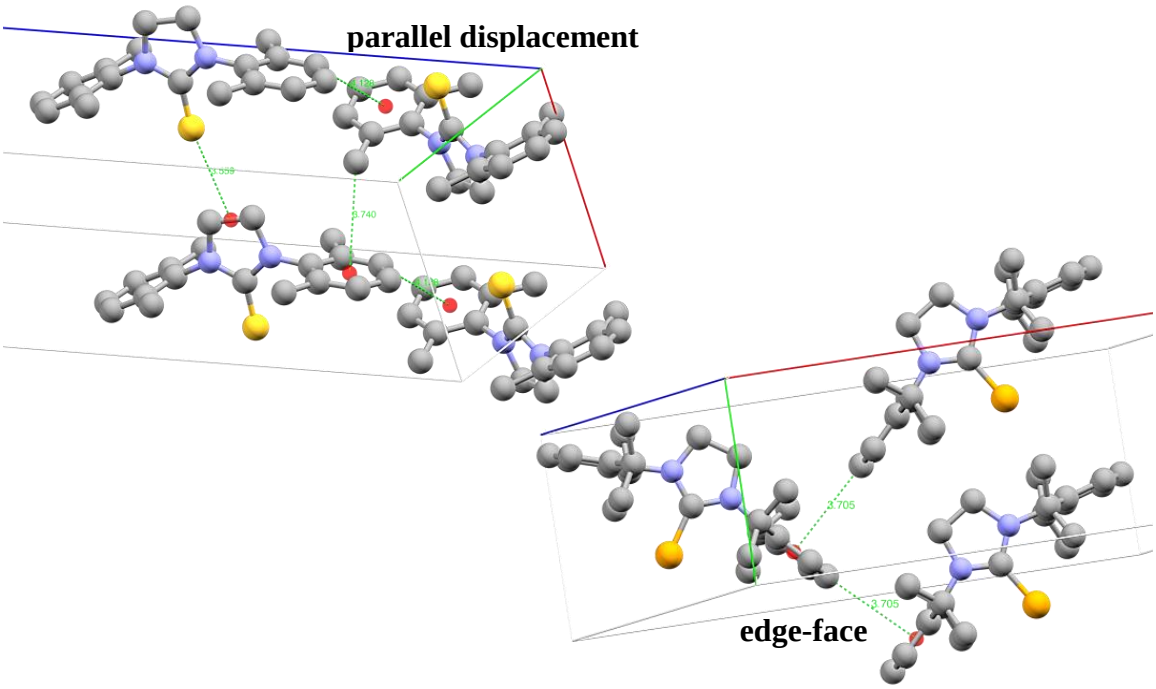

Figure 2.7: Representative 2D models of solid-state packing in SIXyE and SIMesE (left) and SIDippSe (right).

In general the molecules pack alkyl backbone to chalcogen. This arrangement of chalcogenone to backbone, Figure 2.7, shows a major dipole momentum of heteroring to the chalcogen. It is also noted that in solid-state the aromatic substituent bulk directly affects packing of the molecules. Figure 2.7 shows the general packing arrangements for SIMesE and SIXyE the aromatic substituents do not prevent face to face interactions of the aromatic rings orthogonal to the chalcogenone bond, which then is unhindered from weakly associating to the backbone of another molecule in the lattice. The isopropyl groups of SIDippE seem to make these face to face interactions unfavorable, forcing the molecules to stagger in solid-state respective to one another. The structure is stabilized by quadruple hydrogen interactions of the aromatic rings, these physical factors result in properties viewable in the structural data seen in Table 2.2. The torsion angle of the

SIDippE molecules is significantly smaller than that of SIXyE or SIMesE, as a result of fewer interactions between the aromatic rings in the solid-state structures.

Beyond the nature of packing perturbing the torsion of the rings the bond lengths and angles are all very close to one another. The C=S and C=Se bonds for the SIArE ligands are all between a true single, S-C = 1.81 and Se-C = 1.85 Å, and double bond, S=C = 1.55 and Se=C = 1.69 Å, seen in Table 2.2.[33,68] This supports the resonance hybrid proposed by Raper, as previously discussed, since the solid-state resides closer to a double bond than a single as described by Raper with other thiourea type molecular systems.

2.2 Iodine Adducts

Reactivity studies were considered using iodine to test the oxidation stability of the SIArE ligands. Similar work with smaller NHTs was originally done by Arduengo *et al.* and was further investigated by the Devillanova group.[11,69] Utilizing the soft nature of the chalcogen atom and the electronic stabilization offered by the heterocycle subunit, halogen hypervalent compounds were synthesized and studied. In Scheme 2.4 the general synthesis of NHT or NHSe with elemental iodine is shown.

Scheme 2.4: Synthesis of NHT and NHSe Iodine Compounds.

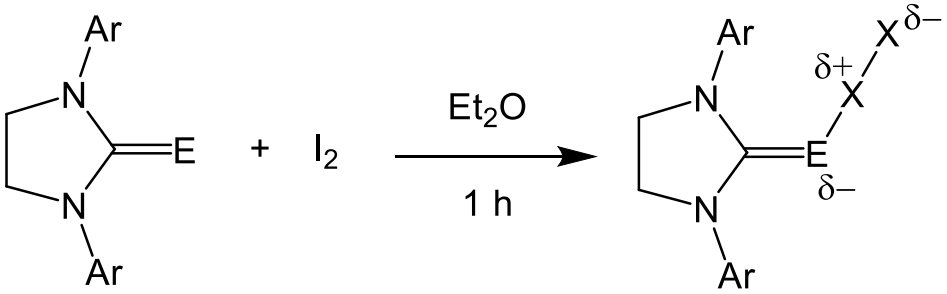

Analysis of the previous works mentioned indicates solid-state structures for the iodine compounds tended to favor the linear adduct, while the calculated bromine adducts favored the hypervalent, rare, T-shape geometry. This was investigated by Devillanova and the urea thione and selones have a stronger nucleophilic nature, allowing to cleave bromine, but only form adducts with iodine. In both of the papers, the NHTs were not substituted with aromatic bulky N-groups, just small methyl N-groups. Naturally, questions about what the SIArE ligands would do in such reactions arose, eventually leading to this line of work.

In efforts to continue this line of research the reactions of iodine with the SIArE ligands were performed. Synthesis was first done in diethyl ether, to more readily dissolve iodine. It was noticed that simply placing the solid iodine onto the amorphous ligand solid resulted in the slow formation of a new darkly coloured substance, but this was uncontrollable and deemed not useful for the synthesis of these compounds. In general the dark red compounds have good solubility in organic solvents, and display downfield shift, *ca.* 0.2 ppm, of the aromatic substituents and the saturated backbone, NMR spectra for SIDippSe and SIMesSe shown in Figures 2.9 and 2,10. It was noted that the ^{13}C NMR *C*=E was found to move upfield by over 5 ppm typically, which denotes a shielding effect post adduct formation. Beyond this the NMR spectra look similar to free ligand. Crystallization of these compounds was difficult due to some unclear sensitivty or reactivity. Of the six iodine compounds only three were successfully crystallized, Figure 2.8, from acetone mixtures of the filtrates.

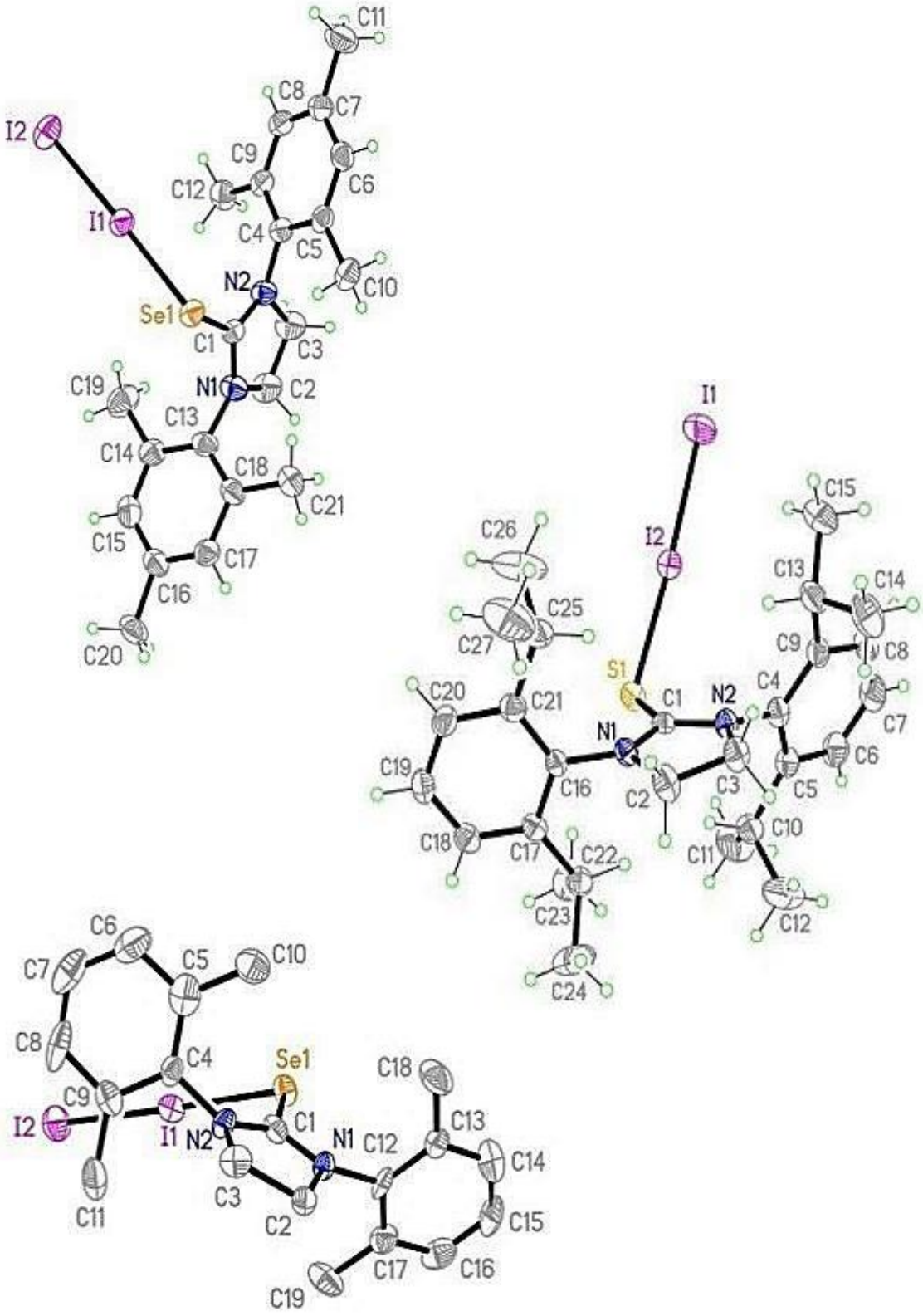

Figure 2.8: Molecular structures, top to bottom, of (SIMesSe)I_2, (SIDippS)I_2, and (SIXySe)I_2.

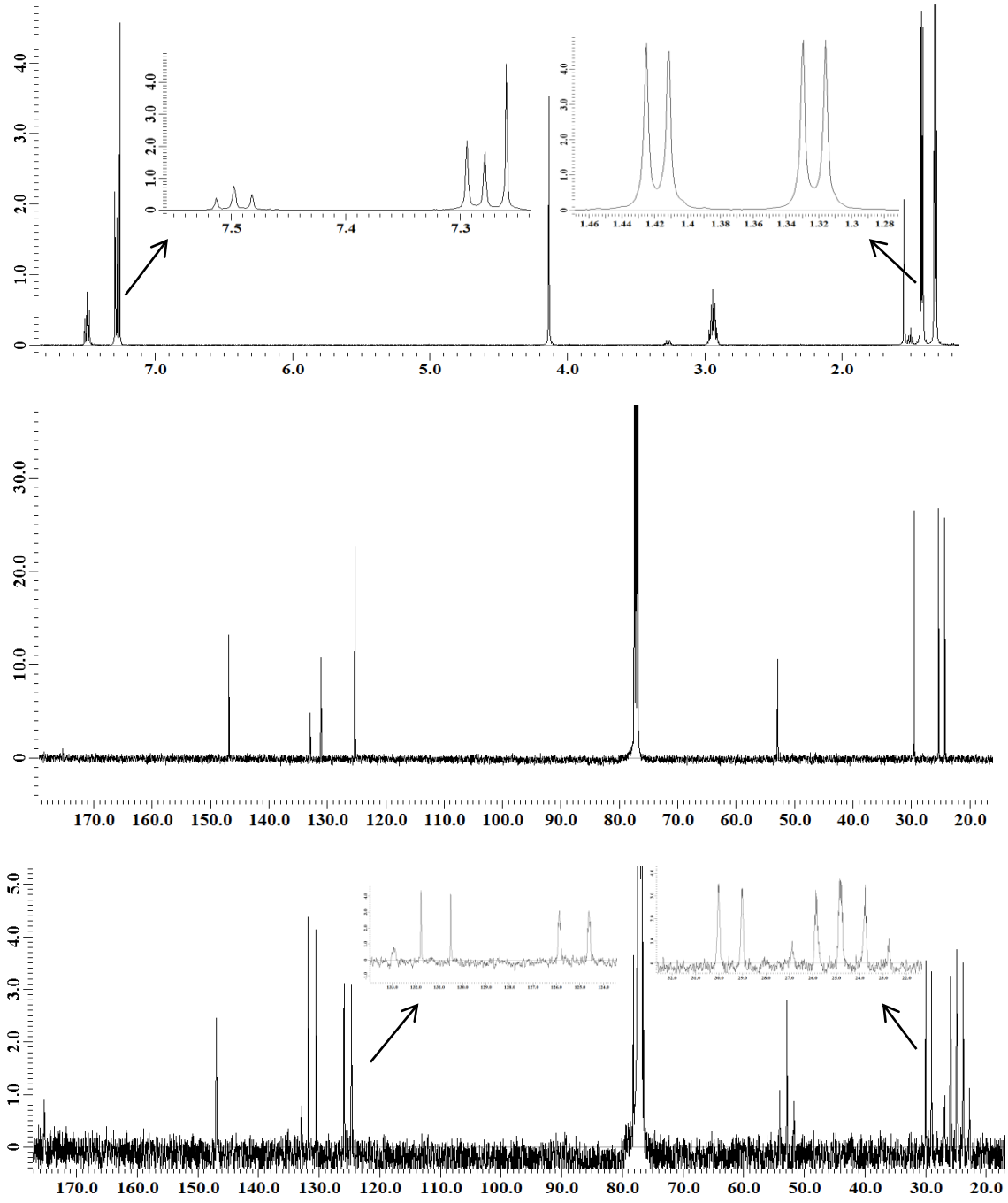

Figure 2.9: ^{1}H (top), $^{13}C\{^{1}H\}$ (middle), and ^{13}C (bottom) NMR spectra of $(SIDippS)I_2$ in $CDCl_3$.

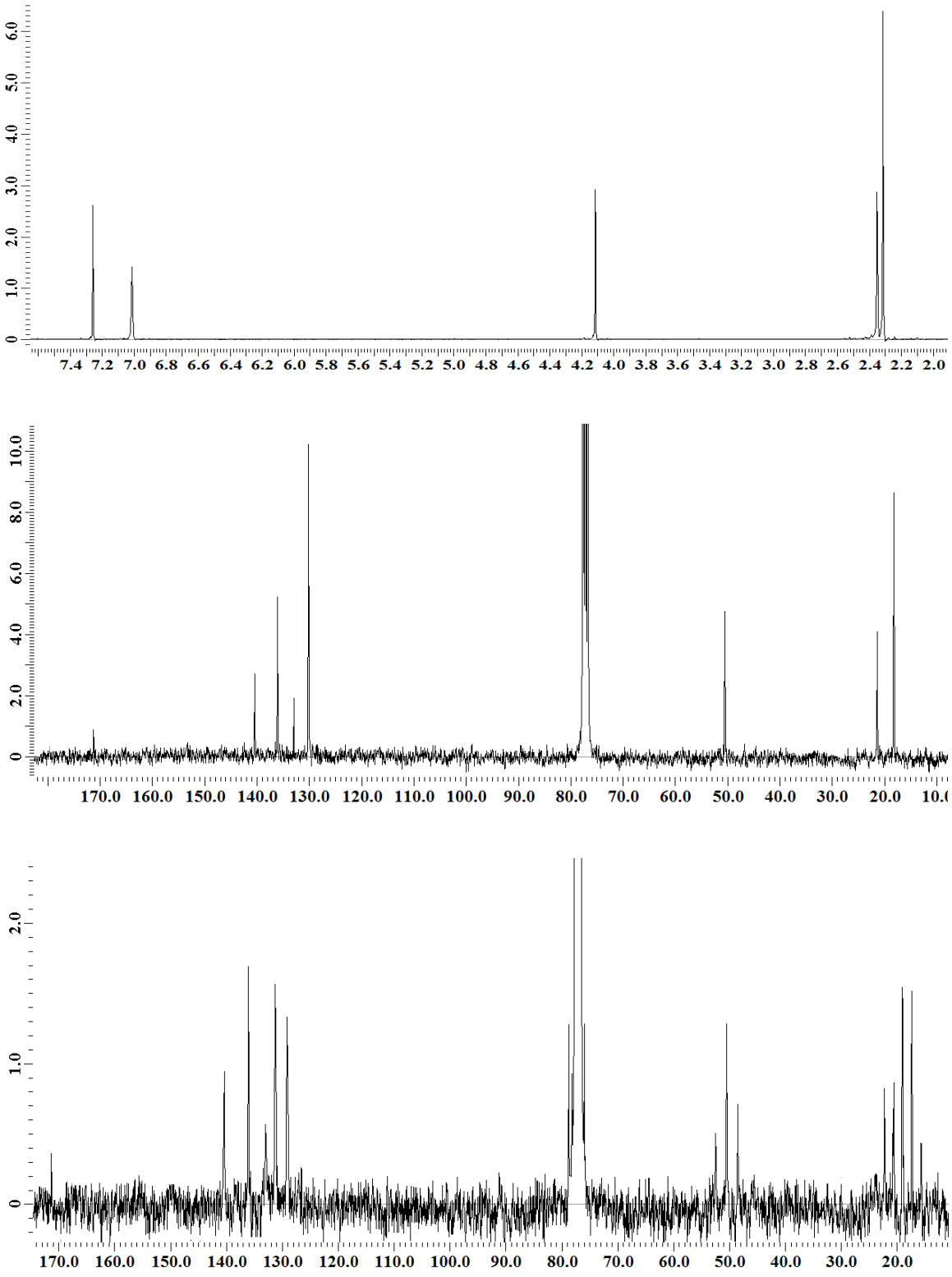

Figure 2.10: ^{1}H (top), $^{13}C\{^{1}H\}$ (middle), and ^{13}C (bottom) NMR spectra of (SIMesSe)I_2 in $CDCl_3$.

The result of the reaction in ether result in deep red products that are senseitive to low pressures and water. Due to the sensitivity of the compounds most were required to keep under dry conditions, but not in high vacuum. Most were found to be pure by elemental and spectroscopic analysis, only SIXySeI_2 was too unstable to isolate successfully.

Comparison in literature shows that free iodine has an I-I bond of 2.67 Å, the resulting strucutres of SIArEI_2 (Table 2.3) clearly show a weaking of the iodine bond and of the carbon chalcogen bond of the ligand in the solid-state.[70] This indicates a strong ionic bond to the halogen and further supports these particular lignad's ability to resist oxidation while still forming a strong ionic interaction. This elongation is also seen in reports from Godfrey and Devillanova where NHT or thione I_2 adducts were synthesized yielding elongated iodine bonds, usually by 0.2 Å. [69,71-72] One paper from Hope *et al.* isolated a small unstaturated NHT with diemthyl N-groups resulting in S-I of 2.68 Å and I-I of 2.75 Å.[73] This shows that SIArE seems to donate better into the σ* of iodine, mostly likely due to the more electronically rich donor atom of SIArE.

Table 2.3 : Selected Bond Lengths (Å) And Angles (°) for (SIArE)I_2.

	(SIXySe)I_2	(SIMesSe)I_2	(SIDippS)I_2
I(1)-E	2.79	2.76	2.68
E-C(1)	1.86	1.88	1.71
I-I(2)	2.89	2.92	2.88
E-I(1)-I(2)	177.9	178.1	173.4
I-E-C(1)	102.3	98.3	107.6
N(1)-C(1)-N(2)	111.2	110.7	110.8

2.3 Mercury(II) Complexes

Structural evidence for the binding character of SIArE ligands the coordination of mercury(II) halides with the SIArE ligands was desired for analysis. To obtain a series of crystal structures that may offer insight, mercury(II) halides were used. The particular use of this Lewis acid is that the soft nature would favor the formation of a new metal complex, allowing quick facile preparation and analysis. This is supported by the calculated HOMO for the SIArE ligands being less stable than, Table 2.1, the LUMO of HgI_2, -234 kcal/mol, thermodynamically allowing for the new bond. Shown in Scheme 2.5 is the reaction used to generate mercury complexes of NHT or NHSe ligands.

Scheme 2.5: General Reaction for the 1:1 SIArE Mercury(II) Complexes.

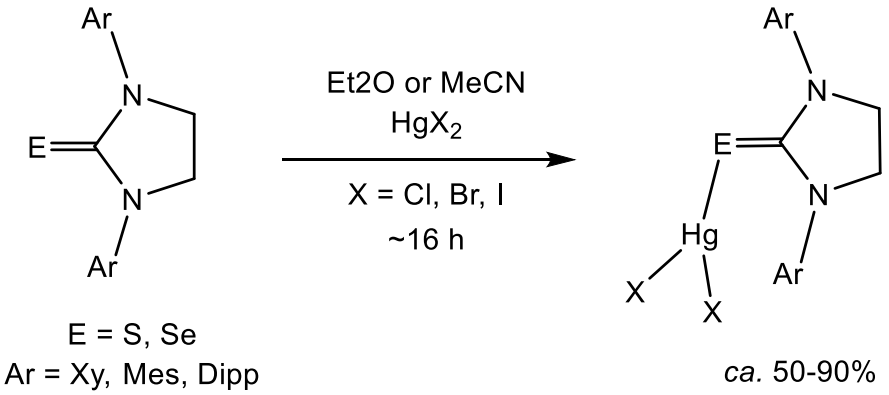

These reactions usually can be designed to be a mixture as product, allowing for simple filtration to isolate product materials. Metal complexes are usually are obtained in relatively high yields, limited by practical methods and scale of the reactions. To probe the coordination of the ligand 1:1 stoichiometric ratio is used for simplicity. To ensure the reaction is favored small amount of excess ligand was typically added to the system,

less than 0.1 extra equivalent most often. The SIXySe complexes were found to require the use of acetonitrile as a solvent.

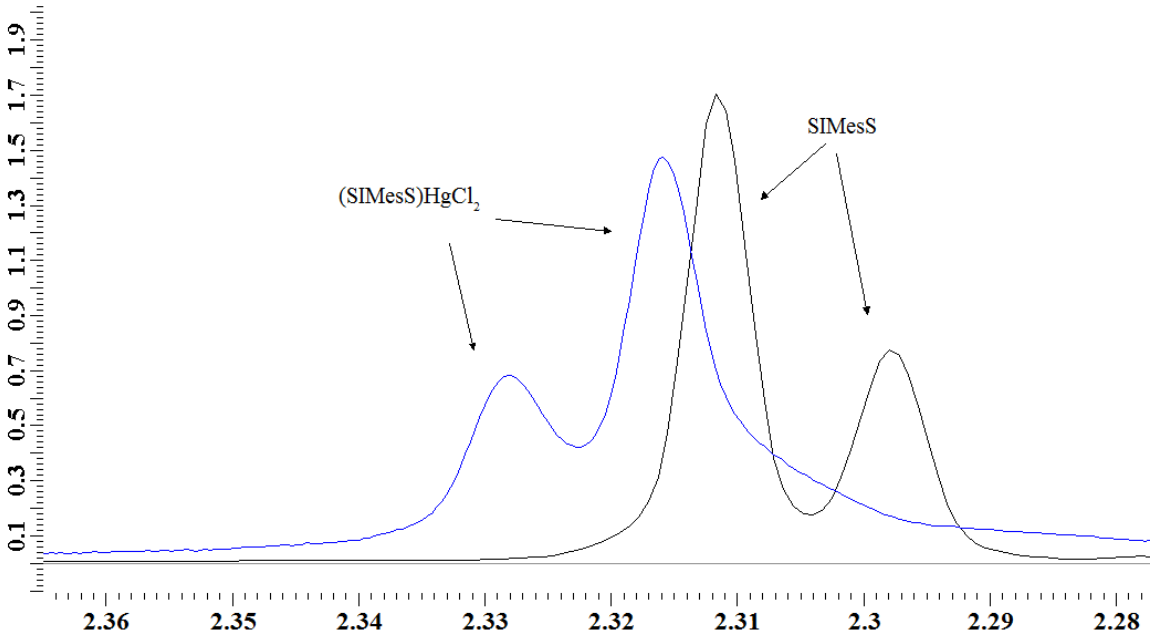

Figure 2.11: ^{1}H NMR spectra for (SIMesS)$HgCl_2$ (blue) overlaid with SIMesS (black) in $CDCl_3$.

Moderate to high yields of the reactions indicate that the reaction and formation of stable compounds occurred at room temperature readily with moderate mixing. Products are typically light yellow to white with solubility very similar to free ligand, readily dissolved in DMSO, dichloromethane, acetone, acetonitrile, tetrahydrofuran, and other organic solvents. Most often the product is quickly identified using ^{1}H NMR spectroscopy, due to deshielding of aromatic substituents and backbone peaks. In the SIMesE system's metal complexes, conveniently, an inversion of the mesityl methyl peak's shifts, example show in Figure 2.11. This has been observed for all SIMesE mercury(II) and gold(I) complexes, and is believed to be caused by inductive effect on the para mesityl methyl groups, causing a downfield shift, due to the attached metal

withdrawing electron density from the donor atom. The 18 new complexes have also been characterized by elemental analysis, IR spectroscopy, ^{13}C NMR spectroscopy, and XRD.

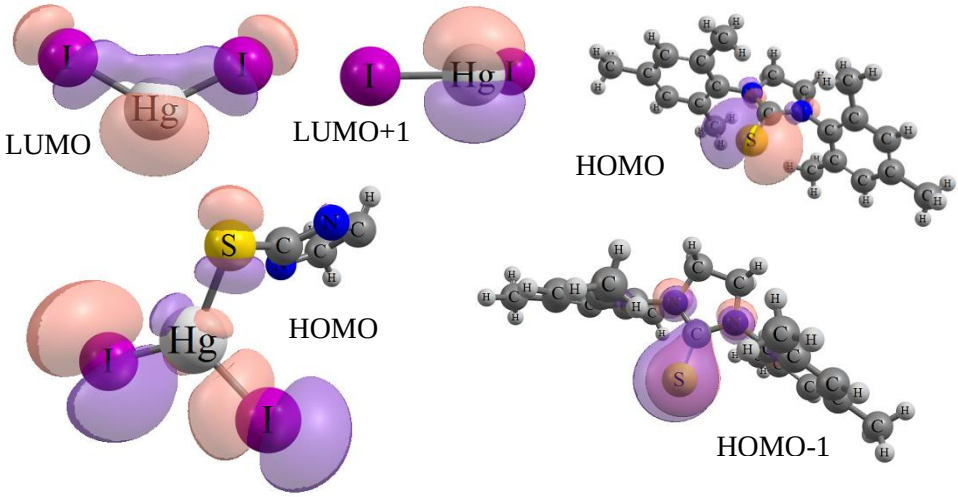

Figure 2.12: Molecular orbitals of HgI_2, SIMesS, and (SIMesS)HgI_2. (aromatic rings omitted from complex for clarity).

Some computational analysis has also been applied to the collected data to further understand the coordination preferences of the SIArE ligands. One such method was the use of Hartree-Fock SCF orbital calculations, using the same 6-311G*, allow for isosurface depictions of some relevant molecular orbitals to consider in the reaction between the NHT/NHSe and mercury dihalide. Shown in Figure 2.12 are the two lowest virtual orbitals of HgI_2, both considered to interact with the chalcogen as a σ and π bonding, respectively. Furthermore, the two highest occupied orbitals of the SIArE are calculated to be centered at the chalcogen atom and geometrically resemble p atomic orbitals. The minor difference between the HOMO and HOMO-1 of the ligand is attributed to the empty atomic orbital mesomerically stabilizing the M.O. The highest occupied orbital of the resulting complex is expected to be an anti-bonding orbital, since

there are 14 electrons on mercury. The calculated result is evidently a anti bonding d-orbital interaction between all three ligands on mercury.

2.3.1 Molecular Structures of (SIXyE)HgX_2

The synthesis of the SIXyE ligands were attempted despite not being described in the Grubbs' imidazolinium salt synthesis.[74] It was considered that the reactivity of the starting reagent 2,6-dimethylaniline would be very similar to that of the anilines used for the other two ligands. The steric hindrance around the donor chalcogen is expected to be identical to the mesityl analogs, but the lack of a para-ipso methyl group on the aromatic ring might allow for different arrangement of the ligands in solid-state or around a metal center. A draw back to the smaller molecular volume is a, minor, decrease solubility in common organic solvents. This is most likely the reason acetonitrile was required for the SIXySe syntheses, since the reactions attempted with diethyl ether yielded impure complexes; Et_2O was sufficiently polar for the SIXyS reactions, however. Single crystals of (SIXyE)HgX_2 (E = S, Se; X = Cl, Br, I) suitable for X-ray diffraction studies were obtained by the slow evaporation of solutions of the compounds in acetone (E = S; X = Cl: E = Se; X = Cl), THF (E = Se; X = Br, I), deuterated chloroform (E = S; X = I), or from the reaction's filtrate mixed with acetone (E = S; X = Br); the structures are shown in Figures 2.13 and 2.14.

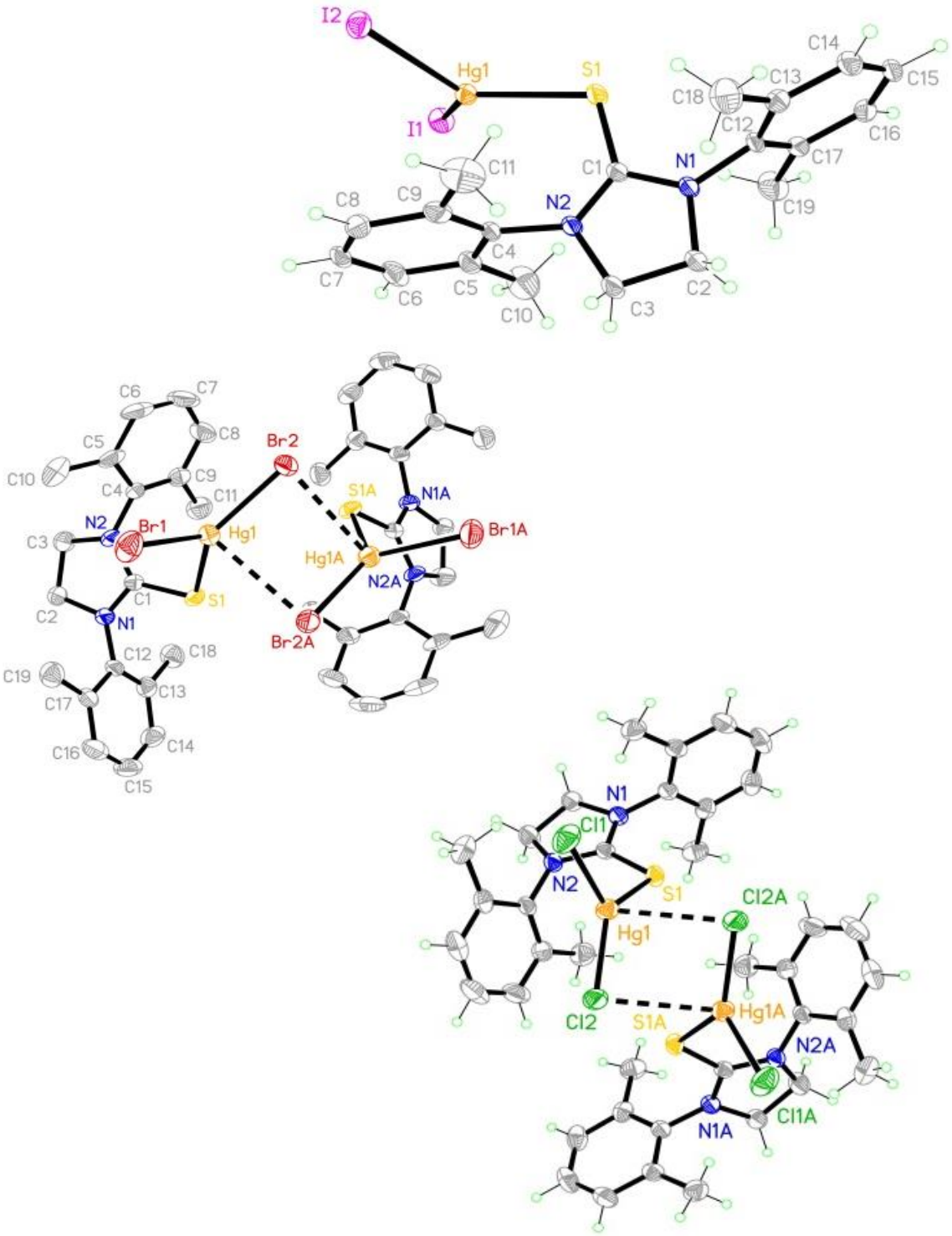

Figure 2.13: Molecular structures of (SIXyS)HgX_2 (X = Cl, Br, I).

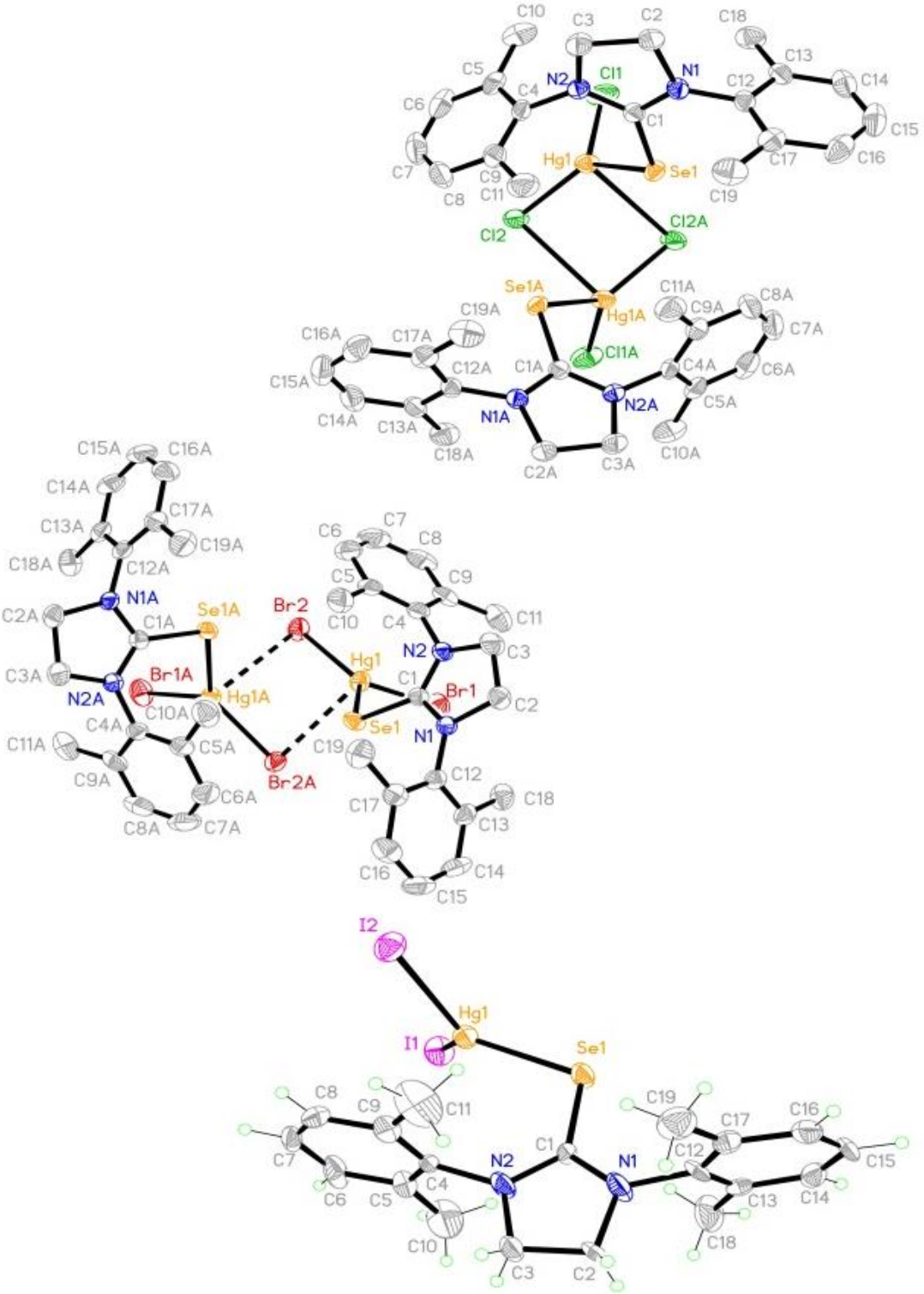

Figure 2.14: Molecular structure of (SIXySe)HgX_2 (X = Cl, Br, I).

The smallest aromatic substituted SIArE ligands, SIXyE, were found to produce monomeric complexes for mercury(II) iodide. However, the bromo and chloro variants yielded a slightly different solid-state structure potentially due to coulombic interactions allowed by less steric hindrance around the metal center. Shown in Figure 2.15 is the crystal packing representative of all the SIXyE mercury dimers. This configuration allows for pi-pi interactions between aromatic groups, *ca.* 4.3 Å, and in general aligns the organic and inorganic moieties together. The relatively close Hg-E bond distances 2.45 (Hg-S) and 2.54 (Hg-Se) Å may also promote the dimerization in solid-state. This notion is supported with the monomeric structures of SIXyE having longer Hg-E bonds (Table 2.3). Literature comparison of the mercury chalcogen bond lengths with small non-bulk aromatic substituted NHT or NHSe ligands shows the Hg-E bond lengths, in general to be shorter for the SIArE ligands. Structurally the smaller NHT or NHSe ligands tended to form four coordinate mercury(II) complexes, similar to some of the SIXyE complexes. However, the smaller ligands tended to have two NHT or NHSe ligands on one mercury(II) halide, unlike the SIXyE dimeric complexes. For these small NHT ligands the typical bond lengths are about 2.5 (Hg-S) and for the small NHSe ligands 2.6 (Hg-Se) Å, with any given HgI_2 have longer Hg-E bond lengths as seen in the SIXyE system.[75-79] The small unsaturated *vs.* the saturated NHT or NHSe ligands show insignificant differences in bond lengths to a given mercury(II) dihalide, with the difference on average being less than 0.01 Å. No evidence of a dimeric structure in solution was observed from ^{1}H NMR spectra for the SIXyE solid-state dimeric structures.

Table 2.4: Selected Bond Lengths (Å) and Angles (°) for (SIXyE)HgX_2.

E =	S			Se		
X =	Cl	Br	I	Cl	Br	I
Hg-E	2.45	2.46	2.51	2.53	2.54	2.59
E-C(1)	1.71	1.72	1.70	1.87	1.87	1.86
Hg-X(1)	2.40	2.51	2.69	2.42	2.52	2.70
Hg-X(2)	2.45	2.57	2.70	2.46	2.57	2.70
Hg-Centroid*	3.51	3.51	3.35	3.56	3.55	3.39
E-Hg-X(1)	131.3	111.2	117.3	129.4	130.8	122.2
E-Hg-X(2)	113.0	132.4	121.2	116.9	114.8	118.2
Hg-E-C(1)	107.1	107.1	109.6	104.5	104.2	108.0
N(1)-C(1)-N(2)	111.1	110.8	110.0	111.4	112.0	109.5

* = Centroid is the geometrical center of the aromatic ring substituent

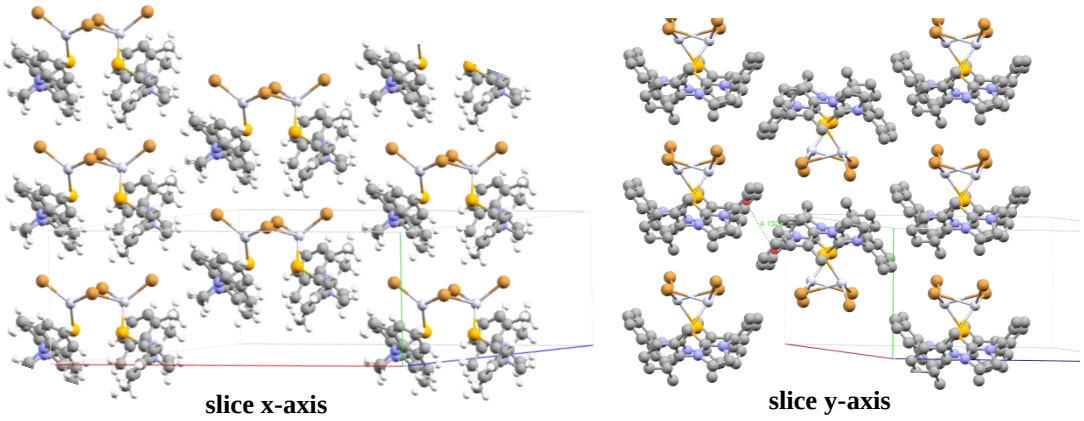

Figure 2.15: General molecular packing of (SIXyE)HgX_2 (E = S, Se; X = Cl, Br).

2.3.2 Molecular Structures of (SIMesE)HgX_2

The molecular structures of (SIMesE)HgX_2 (X = Cl, Br, I) were determined using diffraction-quality single crystals of the complexes obtained via slow evaporation of acetone (E = Se; X = Cl, Br:E = S; X = Cl), benzene (E = S; X = Br, I), or from NMR sample in $CDCl_3$ (E = Se; X = I) and solved using direct methods. In general

crystallization of the complexes was facile due to good solubility in organic solvents and the crystal structures all have R factors less than 5% (0.05). Crystals of the chloro or bromo derivatives tended to be colorless blocks, while most of the HgI_2 complexes yellow; matching the respective amorphous solid color. All complexes were synthesized with 1:1 stoichiometric ratios of metal to ligand in diethyl ether, found to be pure by elemental analysis, and the spectroscopic data shows expected changes. Solid- state structures are presented in Figures 2.17 and 2.18.

All six crystal structures for both SIMesS and SIMesSe were found to be monomeric distorted trigonal planar, typically by only 5-10°, around the mercury center. Similar strucutrally to the SIXyE mercury(II) iodide structures. Two possible stabilization methods may be gleaned from the solid-state structural data. One factor is the closer arene interaction between the mesityl moieties and the metal ion. The second factor, the donation of the sulfur's extra electron pair from the carbene into the mercury center, allowed due to the NHC's stabilization. It is easily observed in Table 2.5 that higher electronic demand from the halogens increases the energy of the association between the centroid of the aromatic ring and the metal center in solid-state. These distances are compared to literature and found to be significant, but weak for most of the solid-state structures when compared to a strong interaction length of 3.16 Å for mercury(II) to benzene.[80]

The internal N-C-N angle of the heterocyclic ring has also been related to donation ability, as previously mentioned, which is a part of the second reasoning for monomorphism for all the mercury halides. The donation ability of the saturated chalcogenone ligand is sufficient to allow the mercury ion to be stable in solid-state as a

three coordinate system, which is a less common arrangement for mercury(II). No evidence of dimerization in ^{13}C NMR spectroscopy is observed, but a noticeable increase in shielding of the methine carbon after coordination is observed, *ca.* 7 ppm upfield shift, upon coordination. This supports the mechanism for electronic interaction shown in Figure 2.16. This electronic effect in addition to the large bulk surrounding the metal may prevent the dimerization or any other kind of rearrangement after the monomeric species is formed. More so, this donation ability creates a variable donor atom. Relevant data on these structures is shown in Table 2.5. Compared to the SIXyE system the Hg-E bonds of the SIMesE ligands are very similar, but have slightly shorter bond lengths (*ca.* 0.02 Å).

Elongation of the C=E SIArE bonds (C=S ~1.6-1.7; C=Se ~1.8-1.9 Å) after coordination in the solid-state structure reflects the new dative bond to the mercury ion. Also seen in the structural data is a positive correlation of E–Hg bond energy and the electron deficiency of the mercury atom, seen in the *ca.* 0.2 Å elongation of the bond as the halogen ligand goes towards iodide. As predicated the solid-state structure shows the most stable configuration of the metal ligand bond to be in the plane of the imidazoline ring and relatively orthogonal, as sterics allow, to the chalcogenone bond. While an aromatic interaction with the metal center is observed the carbon bond lengths in either aromatic ring are consistent with one another, otherwise no perturbations in the bond lengths of the carbons in the associated ring are observed.

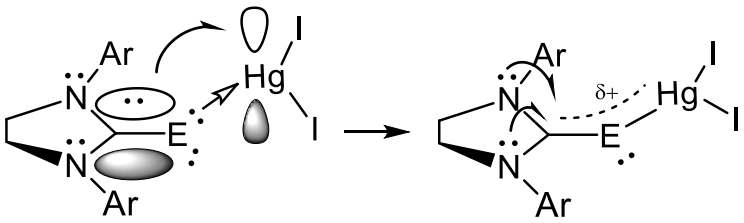

Figure 2.16: Theorized bonding in (SIArE)HgX_2.

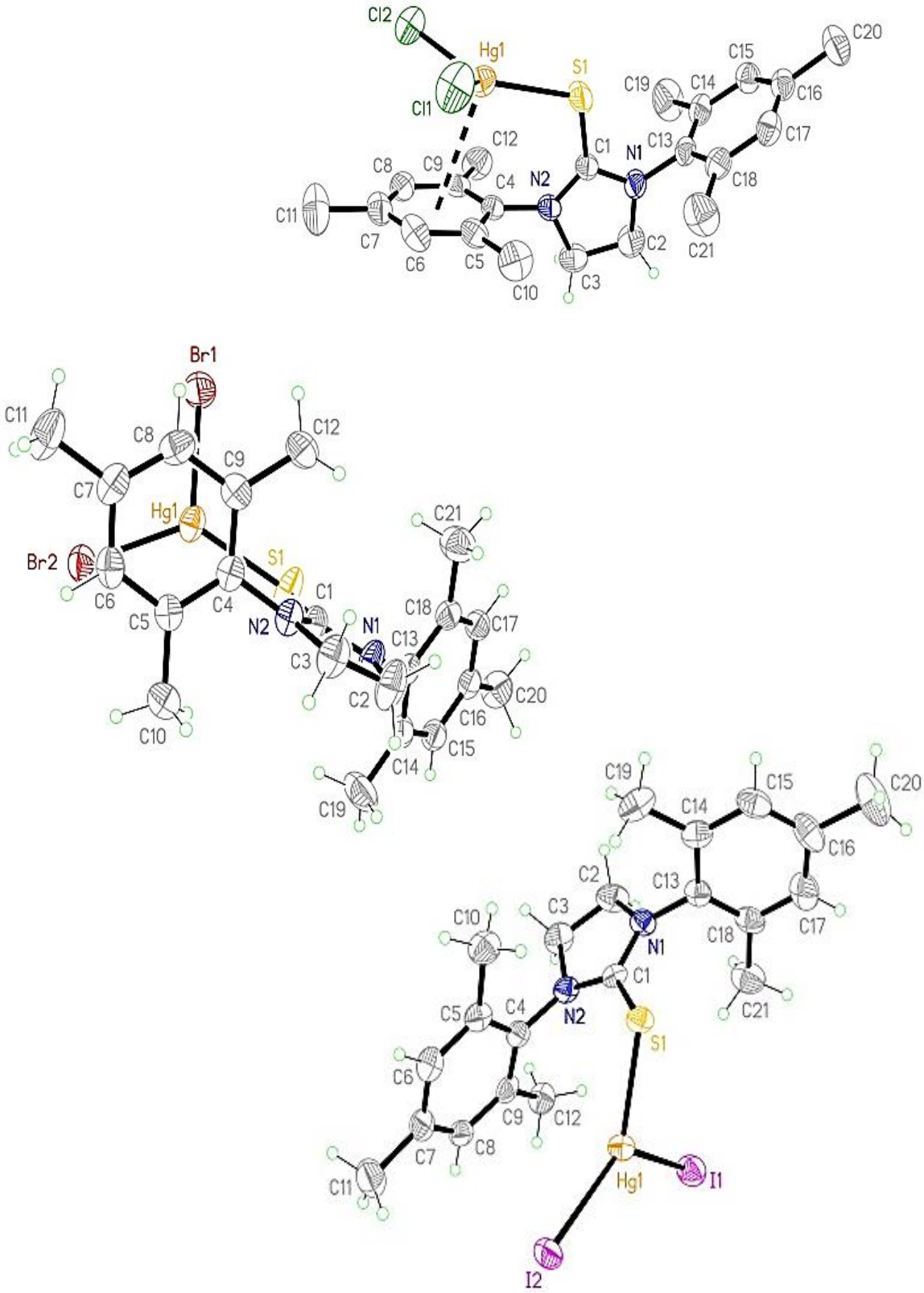

Figure 2.17: Molecular structures of (SIMesS)HgX_2 (X = Cl, Br, I).

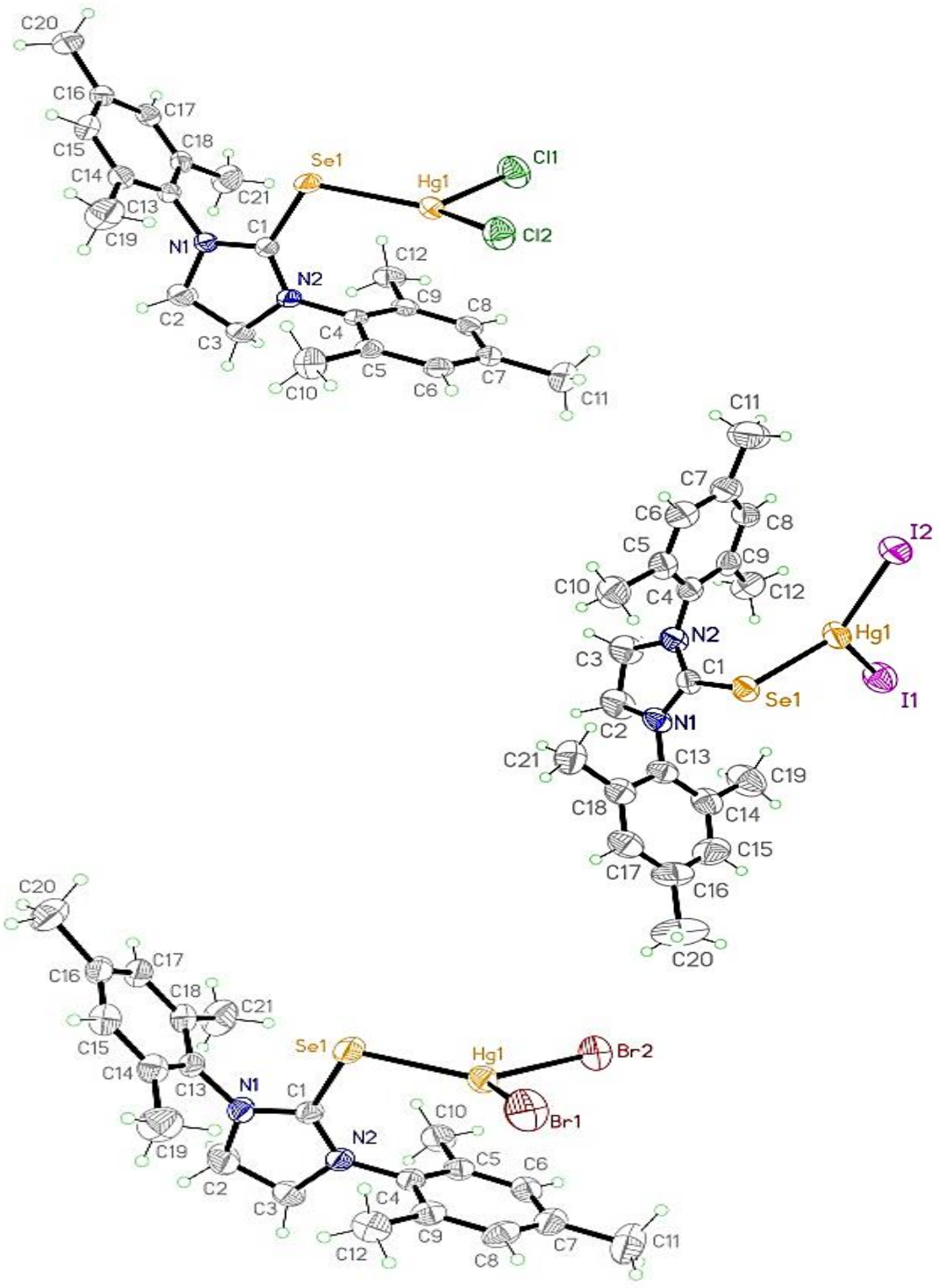

Figure 2.18: Molecular structures of (SIMesSe)HgX_2 (X = Cl, Br, I).

Table 2.5: Selected Bond Lengths (Å) And Angles (°) for (SIMesE)HgX_2.

E =	S			Se		
X =	Cl	Br	I	Cl	Br	I
Hg-E	2.42	2.45	2.50	2.51	2.53	2.57
E-C(1)	1.70	1.71	1.72	1.86	1.86	1.87
Hg-X(1)	2.39	2.52	2.66	2.41	2.53	2.66
Hg-X(2)	2.44	2.56	2.73	2.45	2.57	2.74
Hg-Centroid*	3.13	3.14	3.71	3.14	3.16	3.8
E-Hg-X(1)	117.0	116.1	108.0	117.7	117.4	111.9
E-Hg-X(2)	130.7	130.7	130.2	131.4	130.6	128.8
Hg-E-C(1)	110.6	110.7	103.6	107.7	107.6	100.7
N(1)-C(1)-N(2)	111.1	110.7	111.3	111.5	111.5	100.7

* = Centroid is the geometrical center of the aromatic ring substituent

2.3.3 Molecular Structures of (SIDippE)HgX_2

The SIDippE ligands were challenging to synthesize at first due to the purification of the imidazolinium salt intermediate. After discovering that the salt is soluble in 0 °C acetone, the reported solvent used for trituration, exploration of alternative solvents for purification ensued. Cold to room temperature ethyl acetate was found to be a suitable solvent to remove the Hünigs HCl adduct from the product, allowing for synthesis yields around 70%. The following chalcogenation step was never an issue, yielding high pure material after refluxing in n-propyl alcohol.

Most of the mercury complexes for the thione were synthesized successfully and achieved in good yields using diethyl ether as a solvent, the products were noticed to have higher solubility than the SIMesE ligands requiring the concentration of the suspension to isolate the complex in good yields. Molecular structures of (SIDippS)HgX_2

(X = Cl, Br, I) were determined using single crystals obtained at room temperature by slow evaporation of solutions of the complexes in dichloromethane (E = Se; X = Br, I) or from filtrate of the reaction and acetone washings from the frit used for the isolation (E = S; X = Cl, Br, I & E = Se; X = Cl).

In general the SIDippE mercury complexes are similar to the SIMesE and (SIXyE)HgI_2 complexess in geomertical proportions, Figures 2.19 and 2.20. All 6 solid-state structures were found to be isomorphic by direct methods. The steric bulk of the isopropyl groups observably only cause small changes in the ligand's interaction with the metal. Expectidly, the bulk of the Dipp groups prevents close association of the aromatic ring and the metal ion, resulting in the comparitavily longer mercury to aromatic center, seen in Table 2.6. The Hg-E bond lengths of the SIDippE are the shortest of the SIArE systems, but only by 0.03 Å on average. Compared to smaller NHT or NHSe systems, without bulky aromatic N-groups, the SIDippE ligands form significantly shorter metal bond lengths of about 0.1 Å on average.[77-81]

The positioning of the metal ion in front of the ring is still present in the solid-state, despite the longer distance, indicating a mild attraction still being present in the solid-state. The bond length of the chalcogenone is very similar to the SIMesE complexes as well as the chalcogen mercury bond legnths. This is expected as the electronics of the system are not drastically different as determined from ^{77}Se NMR, but does show that steric hinderance around the donor atom is not a large factor for the reactivity. The SIDippE mercury(II) complexes were notibly more soluibly in oragnic solvents that the mesitly analogs, like in part due to the larger moelculear surface area and hydrogen bonding sites.

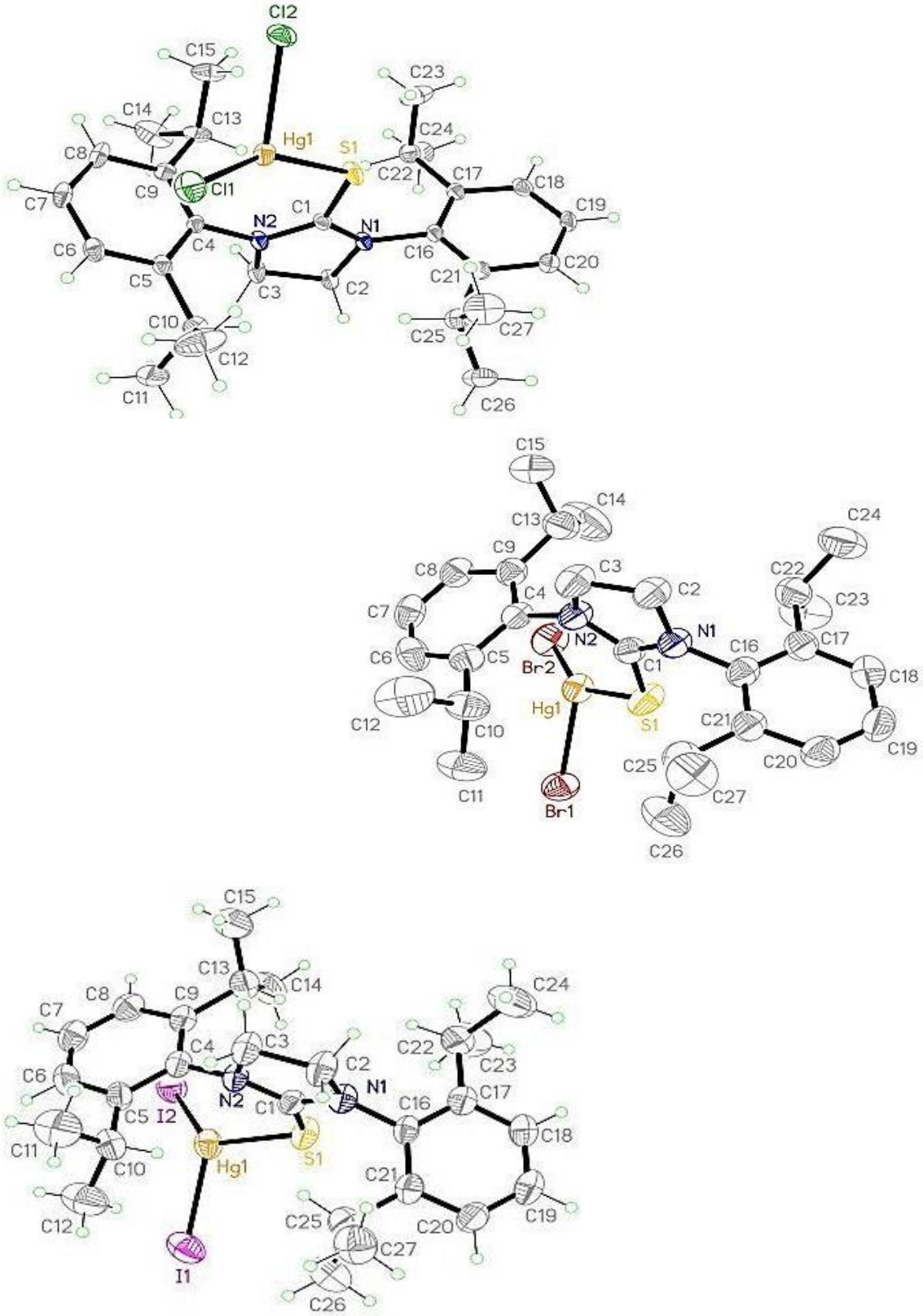

Figure 2.19: Molecular structures of (SIDippS)HgX_2 (X = Cl, Br, I).

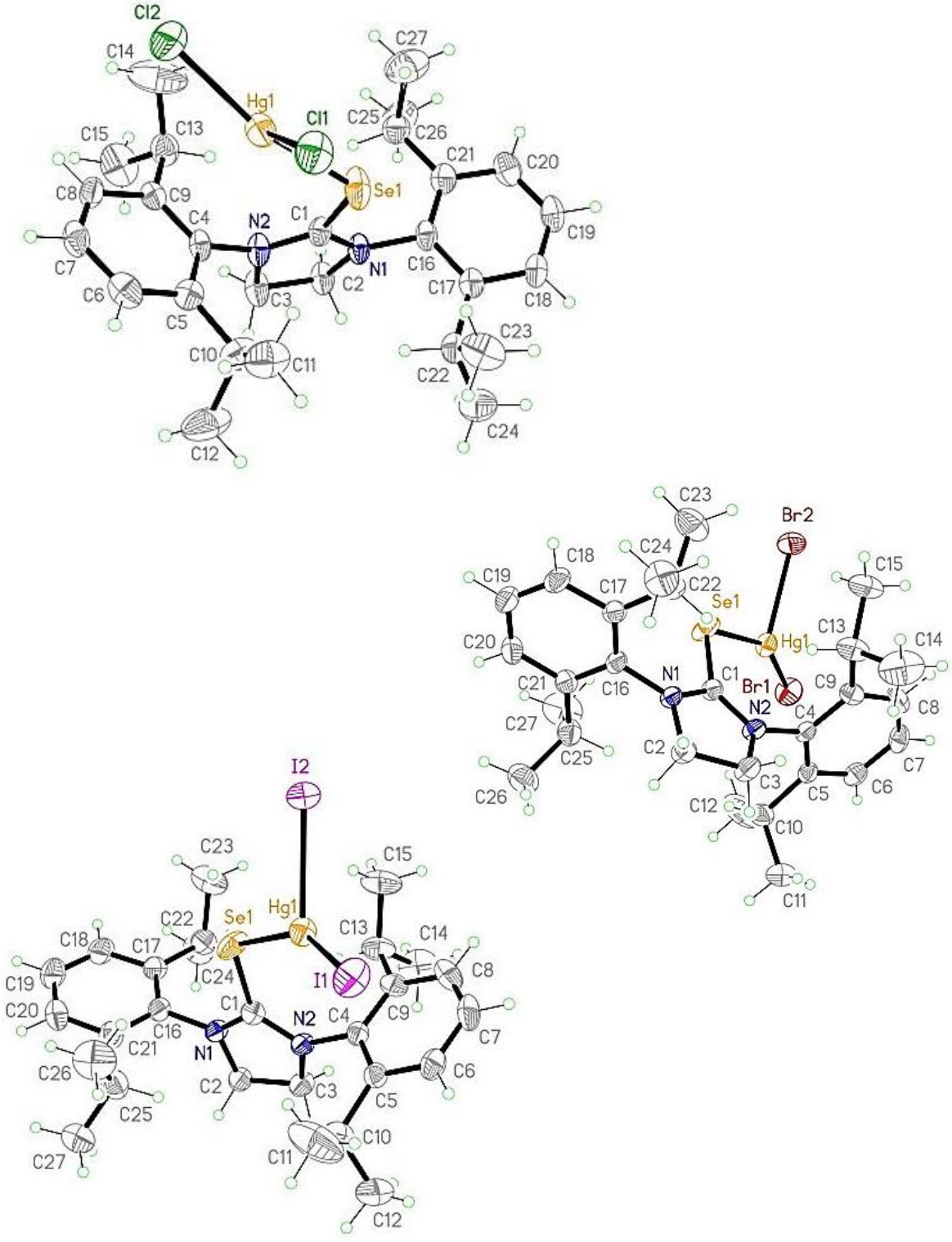

Figure 2.20: Molecular structures of (SIDippSe)HgX_2 (X = Cl, Br, I).

Table 2. 6: Selected Bond Lengths (Å) And Angles (°) for (SIDippE)HgX_2.

E =	S			Se		
X =	Cl	Br	I	Cl	Br	I
Hg-E	2.42	2.43	2.49	2.50	2.52	2.54
E-C(1)	1.71	1.71	1.71	1.87	1.87	1.87
Hg-X(1)	2.35	2.47	2.67	2.35	2.47	2.64
Hg-X(2)	2.52	2.62	2.71	2.54	2.64	2.79
Hg-Centroid*	3.40	3.42	3.42	3.47	3.48	3.51
E-Hg-X(1)	151.5	149.9	129.6	153.7	152.4	149.8
E-Hg-X(2)	99.7	100.3	107.7	96.7	97.4	97.9
Hg-E-C(1)	112.1	113.4	113.4	110.3	110.9	112.4
N(1)-C(1)-N(2)	110.4	110.6	110.7	111.7	110.8	111.4

* = Centroid is the geometrical center of the aromatic ring substituent

2.3.4 Molecular Structures of $Hg_2(SIMesS)X_4$

A small example of environment based morphism was produced after accidental use of excess mercury(II) iodide in an attempted synthesis of (SIMesS)HgI_2, in the same manner as Scheme 2.5. After elemental analysis produced elemental proportions more reasonable for a 2:1 (metal:ligand) stoichiometric product. Following this the 2:1 complexes were attempted for SIMesE ligands (Scheme 2.6). The reaction and isolation of product mirrors the 1:1 reactions with mercuric halides. NMR spectroscopy of the complexes show a minor electronic difference, with all peaks appearing slightly deshielded when compared to their 1:1 analogs in the same deuterated solvent, Figure 2.21, but this deshielding is not observed to significantly affect the spectrum. This also makes identifying the 2:1 complex difficult if not impossible by NMR.

Scheme 2.6: Synthesis of $Hg_2(SIMesS)X_4$ (X = Br, I).

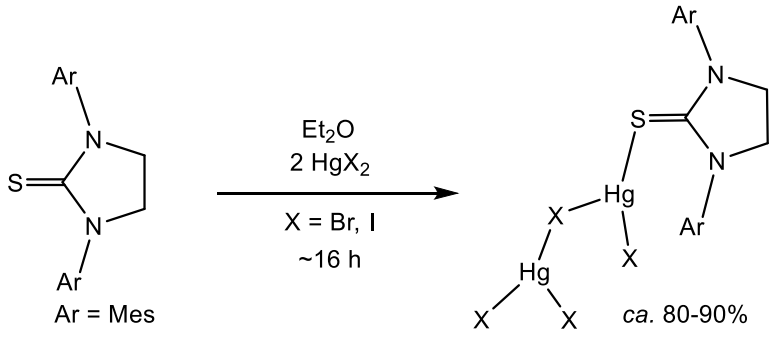

While attempts to synthesize all 6 possible complexes with SIMesE were done, only two passed EA and formed diffraction quality crystals. None of the SIMesSe 2:1 complexes resulted in stable 2:1 complexes, even though the HgI_2 reaction did yield a yellow powder the low yield and ^1H NMR spectrum indicated a 1:1 product. Crystals suitable for XRD were grown from acetonitrile mixed with acetone (X = Br) or acetonitrile (X = I).

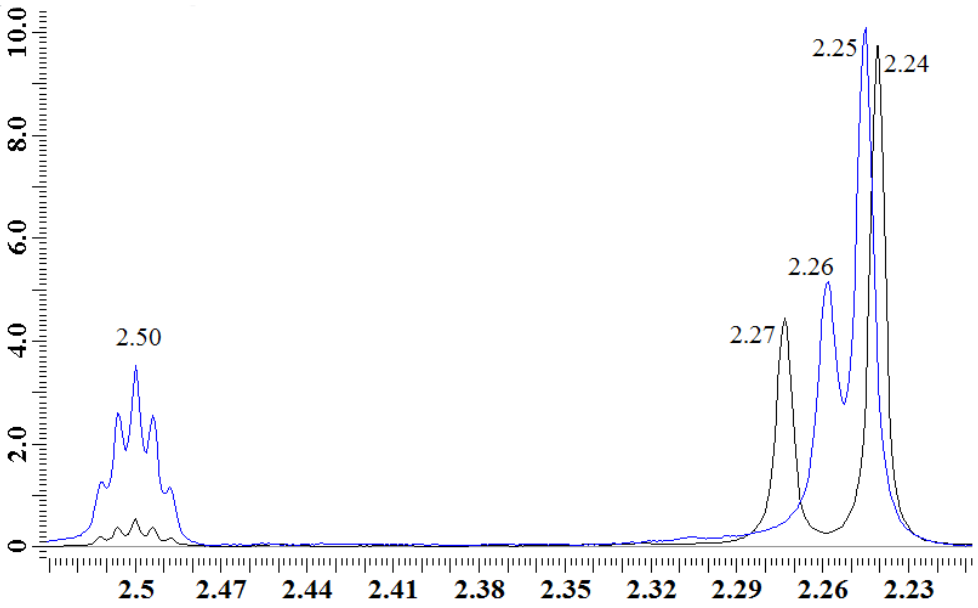

Figure 2.21: ^1H NMR spectra of $(SIMesS)HgI_2$ and $Hg_2(SIMesS)I_4$ (blue) both in d_6–DMSO.

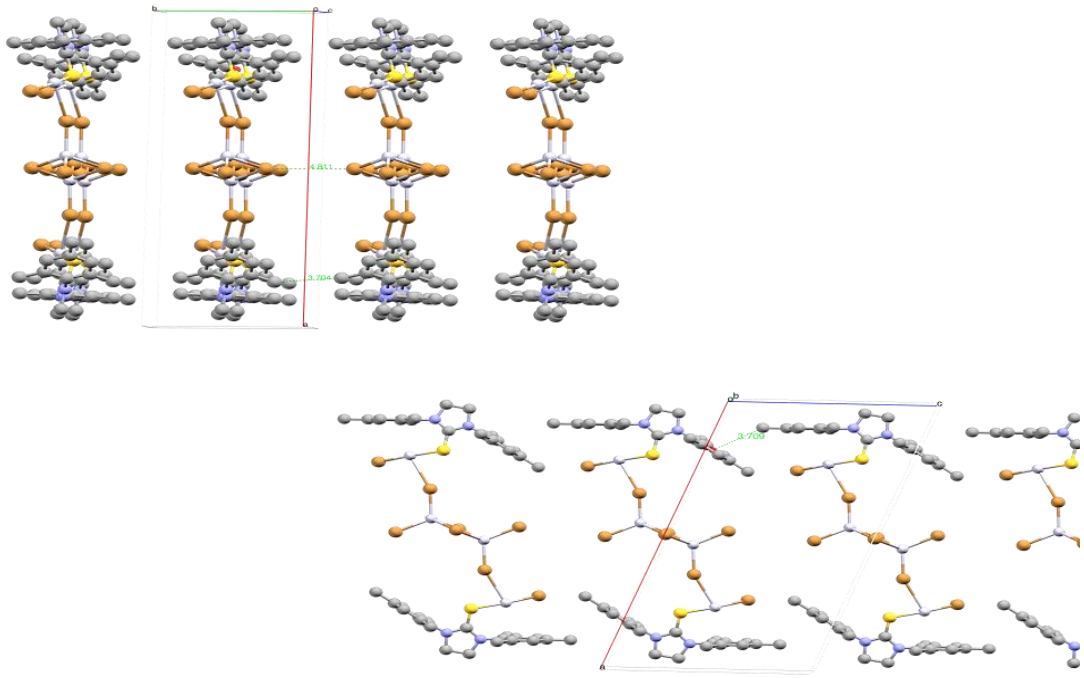

Figure 2.22: General crystal packing of $Hg_2(SIMesS)X_4$ (X = Cl, Br).

Table 2.7: Selected Bond Lengths (Å) And Angles (°) for $Hg_2(SIMesS)X_4$.

X =	Br	I
Hg-S	2.35	2.37
S-C(1)	1.73	1.72
Hg-X(1)	2.41	2.58
Hg-X(2)	3.18	3.28
Hg-X(1)’	3.39	3.48
Hg-Centroid*	3.38	3.35
S-Hg-X(1)	102.7	104.2
S-Hg-X(2)	92.2	96.1
Hg-S-C(1)	106.6	108.1
N(1)-C(1)-N(2)	111.8	111.2

* = Centroid is the geometrical center of the mesityl ring

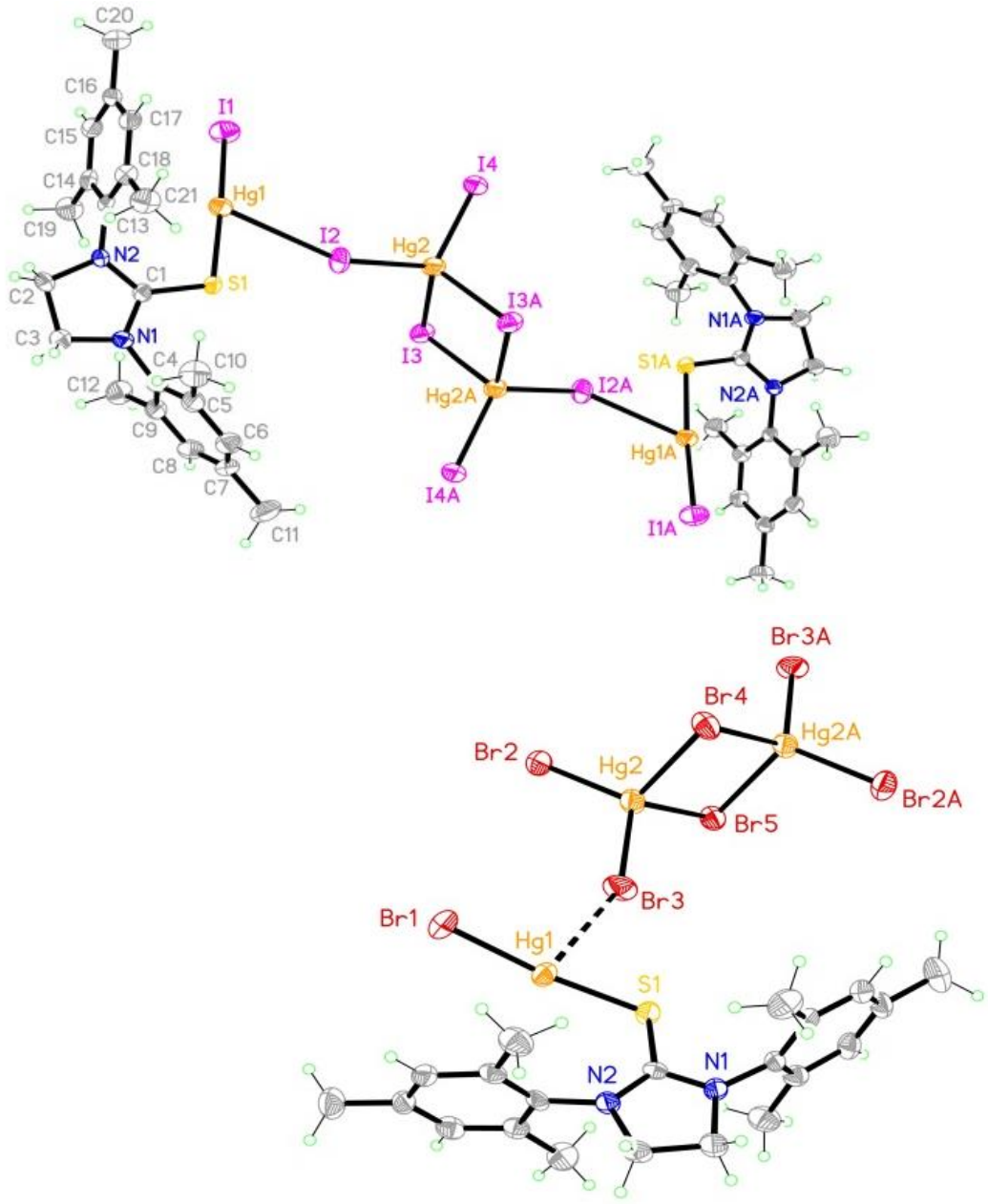

Figure 2.23: Molecular structures of $Hg_2(SIMesS)X_4$ (X = Cl, Br)

Solid-state structures of the two compounds were identical, barring halogen identity. The crystalline material was seemingly micelle like in nature, with the alkyl groups orienting towards one another and the metal ions clustered inward. The repeating units, shown in Figure 2.22, make it apparent why the solved structure was originally identified as polymeric. The true nature is more discrete, because the actual subunits, shown in Figure 2.23, are very ionic in nature. A large anion, $[Hg_2I_6]^{2-}$, is seen weakly bonding with the SIArE coordinated mercury cation. This anion being $[Hg_2I_6]^{2-}$ and not Hg_2I_4 is supported by the mercury halogen bond lengths in Table 2.7. One of the halide bonds to the cation is a relatively normal mercury halide bond length, especially when compared to the other monomeric SIArE species shown, while the other is abnormally long indicating a weak halogen bond, similar to a hydrogen bond. This tetranuclear centrosymmetric structure has not previously been seen in thione coordination chemistry, but the $[Hg_2I_6]^{2-}$ anion has been reported and structures containing this anion are in the CSD.

2.3.5 Solid Angle Data Analysis of (SIArE)HgX_2

One fundamental issue within the field of coordination chemistry is an appropriate measurement of the electronic and steric factors a ligand has when coordinated to a metal. Tolman electronic parameter (TEP) and cone angle have dominated these measurement techniques.[7] TEP is a mathematical relationship between the electronic donation of the ligand to the metal, specifically in a π fashion, and the IR frequency of an attached carbonyl ligand. Change of the stretching band in IR spectroscopy of the uncoordinated and coordinated carbonyl complex give insight into donation. This is useful for certain types of ligands, and less so for other since the

measurement generally ignores σ type interactions and sterics. Cone angle is another useful but too specific measurement as the ligand must have a center of rotation type symmetry; C_{2v}, C_{3v}, *etc.* This limits this kind of analysis to ligands similar to NHCs, phosphines, or isonitriles as they all will rotate around the metal center freely, in theory. Both of these methods have multiple flaws, one solution to this issue was developed by Guize *et al.*. Utilizing solid angle of the obtained crystallographic data to generate space models that offer direct analysis of surface area cover on the metal in a program called SolidG, within the SolidAngle package.[81]

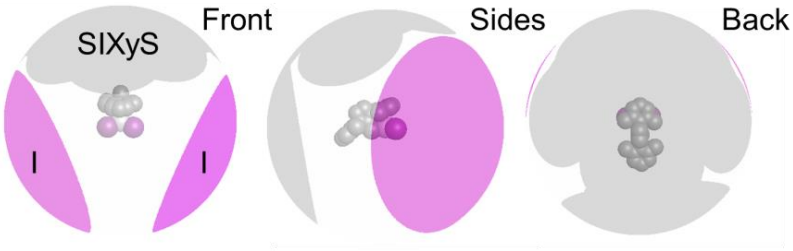

Figure 2.24: SolidG projection of (SIXyS)HgI_2. In grey is the surface area coverage of SIXyS ligand; the purple, iodide

To further analyze the steric protection of these ligands, the crystal structure data and the program SolidG were used to develop surface area maps of the metal complexes to evaluate the steric protection of the SIArE ligands.[81] Shown in Figure 2.24 is an example of the shadow map of a SIArE ligand coordinated to a Hg(II) dihalide.

The structures shown is static; using solid-state structures, so the % coverage values in Table 2.7 are calculated without considering free rotation around the chalcogen-metal bond.

Static coverage of the ligands is fairly impressive, with *ca.* 40% coverage on average, but this isn't useful unless it is compared against similar structures. Using the

CSD, multiple structures of various mononuclear mercury(II) dihalide solid-state data were obtained and % coverage calculated using SolidG, shown in Table 2.7. After reviewing the relative % coverages of similar bulky ligands *vs.* the small halogens it was determined that SIArE ligands fall into the same class of sterically hindering as NHCs or bulky phosphines in terms of surface coverage. This is to be expected due to the similarity. Unlike bulky NHC ligands, SIArE ligands have no need for activation, meaning a one-step metalation reaction akin to phosphine ligands, and the donor atom instead of being pi acidic to any degree will more likely be pi basic, supported by the elongation of the C=E bond in free ligand *vs.* complexed in crystallographic data. Unlike the phosphine ligands, however, SIArE ligands are benchtop stable, easily handled, and synthesized.

Table 2.7: (SIArE)HgX_2 *vs.* Similar Mononuclear HgX_2 Ligand Complexes.

Metal Salt	Ligand	% Coverage*
HgI_2	SIArE	35.9-41.0
$HgBr_2$	SIArE	35.8-41.6
$HgCl_2$	SIArE	35.8-42.1
$HgBr_2$	$P(C_6H_2(OMe)_3)_3$	42.3
$HgCl_2$	IDipp	40.3
$HgBr_2$	Br	20.6
$HgCl_2$	IMes	34.1
$HgCl_2$	Cl	14.4
HgI_2	$P(C_6H_2(OMe)_3)_3$	43.1
HgI_3^-	I	23.8
HgI_2	Spym[H]S	23.5
HgI_2	Im[H]S	21.7

* = Normalized to M-L = 2.28 Å

2.4 Synthesis of Gold(I) Complexes

The soft nature of the mercury(II) ion was determined to be favorable for the SIArE ligands, following suit gold(I) was chosen for reactivity. Gold(I) starting reagents are less available and expensive. To prepare a suitable reagent for reactivity experiments, a procedure synthesizing tetrahydrofuran gold(I) halides was utilized.[82]

Scheme 2.7: Synthesis of (SIArS)AuX.

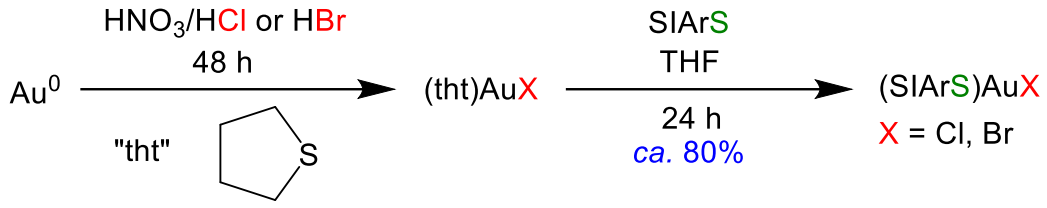

The particular trick for this reaction is the use of tetrahydrothiophene (THT), an odiferous liquid, and a solution commonly referred to as *aqua regia*, a 1:3 aqueous mixture of concentrated nitric and hydrochloric acids, this can also be done with hydrobromic acid. The harsh acid solution is required to oxidize the notoriously stable gold solid. After a couple of days the gold dissolves into the acid. Following some solvent changes, THT is added dropwise, resulting in the precipitation of the gold(I) complex in near quantitative yields.

After obtaining the starting reagent, synthesis of SIArE gold complexes is relatively simple, Scheme 2.7. It was determined that the reaction did not need to take place in a N_2 atmosphere as reported, but the THF used did required degassing to yield clean product.[51] The reagents both dissolve well in THF, but most precipitate out after mixing for around an hour baring SIDippS. After concentrating the mixture the product was precipitated with diethyl ether and alkanes.

The off white solids were found to have reasonable solubility in organic solvents, but the more polar solvents were found to displace the SIArS ligands from the metal center. Shown in Figure 2.25, the ^{1}H NMR spectra of (SIMesS)AuCl in DMSO *vs.* DCM *vs.* $CDCl_3$ clearly indicates higher dissociation rate in more polar solvents. This is not inherently a negative factor, as this indicates possible reactivity at the metal center initiated by ligand dissociation in common organic solvents. More interestingly, neither of the peaks corresponds to free ligand demonstrating some dynamic equilibrium, like that shown in Scheme 2.8, in various solvents at room temperature between one coordination arrangement and another. This is seen in other similar gold(I) chalcogen complexes and in previously reported crystal structures by Nolan *et al.* using SIDippSe.

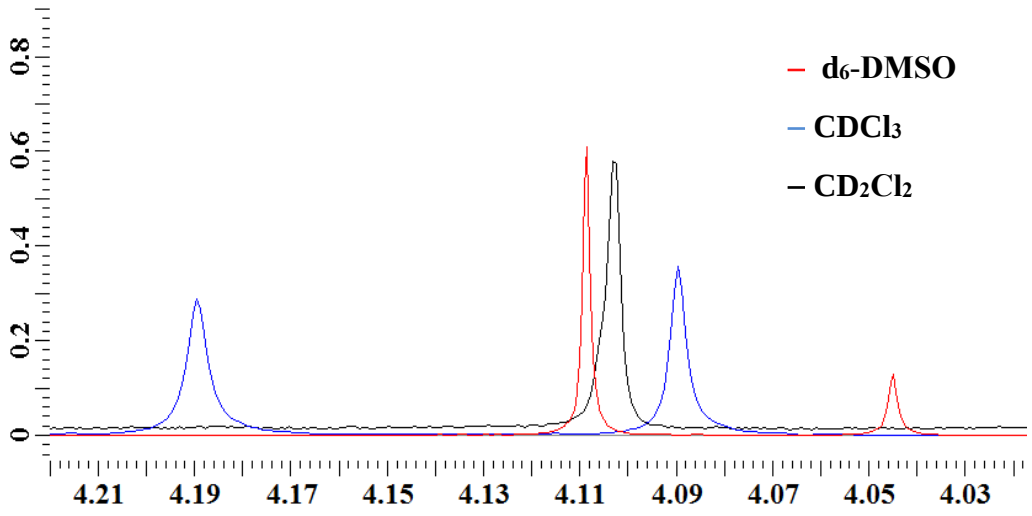

Figure 2.25: ^{1}H NMR spectra of the Methylene Backbone Peaks of (SIMesS)AuCl in Various Deuterated Solvents.

Scheme 2.8: Possible Solution State Equilibrium of SIArE Gold(I) Halides.

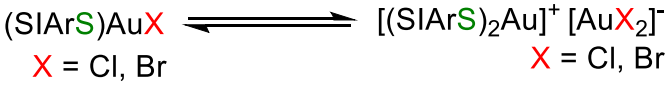

Using Hartree-Fock level theory and pseudopotential calculations for the heavy metal, M.O.s of (SIDippS)AuCl were calculated to investigate the reason for the observed dissociation, Figure 2.26.[83] In the linear arrangement it's obvious that there is strain on the σ orbital of the gold-chalcogen bond. One may imagine that a rotation of the metal to favor the ligand bond weakens the halogen bond. The π interaction stabilizes the gold, but weakly when compare to π* interaction. This observation may also described the beginning mechanism in the formation of a homoleptic charged complex in the solid-state or in solution, observed for (SIDippS)AuBr in the solid-state (Figure 2.29).

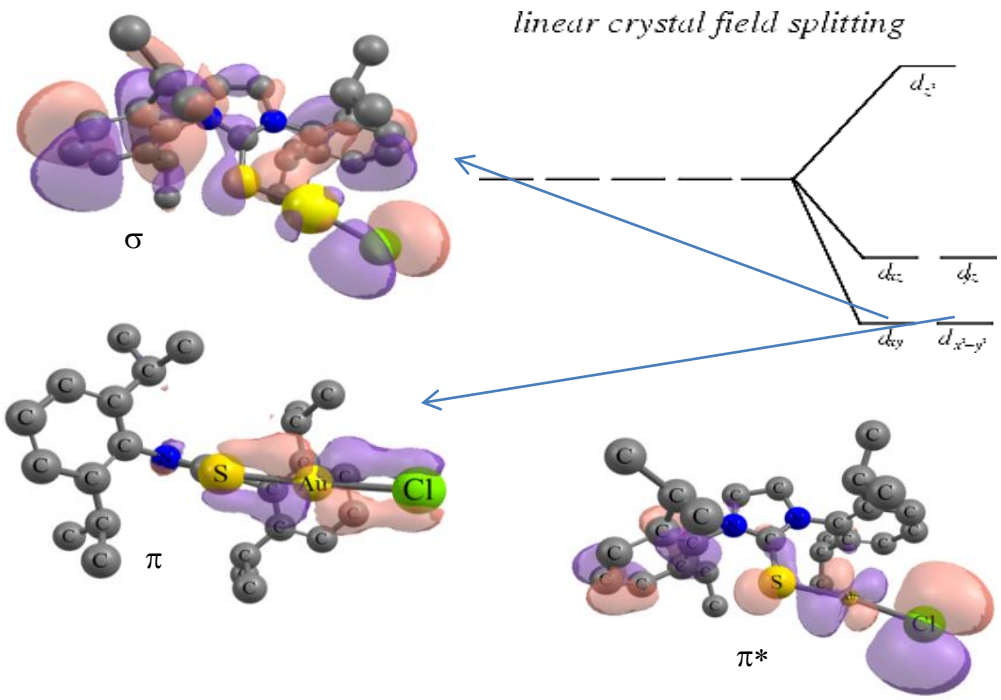

Figure 2.26: Molecular orbital isosurface of (SIDippS)AuCl of relevant ligand-metal orbital interactions.

2.4.1 Molecular Structures of (SIArS)AuX

The white to off-white solids were found to be pure by elemental analysis and were noted to have good stability in open air. It was quickly determined that THF not degassed beforehand or dry caused a reduction of the gold(I) ion, resulting in gold plating of the reaction vial. While the solvent purity was required for good yields, the reactions could be worked up in open air after the formation of the white precipitate without issue. For the gold(I) bromide reactions, washing with diethyl ether was performed to get rid of the bromine observed, due to dark red coloration The crystal structures of the gold(I) complexes were obtained from slow evaporation of solutions in deuterated chloroform (Ar = Xy; X = Cl; Ar = Mes; X = Cl, Br) or THF (Ar = Dipp; X = Cl, Br) yielding colourless diffraction quality crystals. The solid-state structure for most of the complexes show a linear arrangement and, again, close aromatic distance to the metal ion, Table 2.9.

Table 2.9 : Selected Bond Lengths (Å) And Angles (°) for (SIArS)AuX

	SIXyS	SIMesS		SIDippS	
X =	Cl	Cl	Br	Cl	Br
Au-S	2.25	2.25	2.26	2.25	2.28
S-C(1)	1.71	1.71	1.71	1.70	1.70
Au-X	2.27	2.27	2.39	2.27	--
Au-Centroid*	3.27	3.33	3.30	3.40	3.24
S-Au-X	173.5	173.8	173.8	170.0	180.0
Au-S-C(1)	109.0	108.9	108.6	113.4	110.5
N(1)-C(1)-N(2)	111.2	110.7	110.8	109.9	110.3

* Centroid is the geometrical center of the aromatic ring substituent.

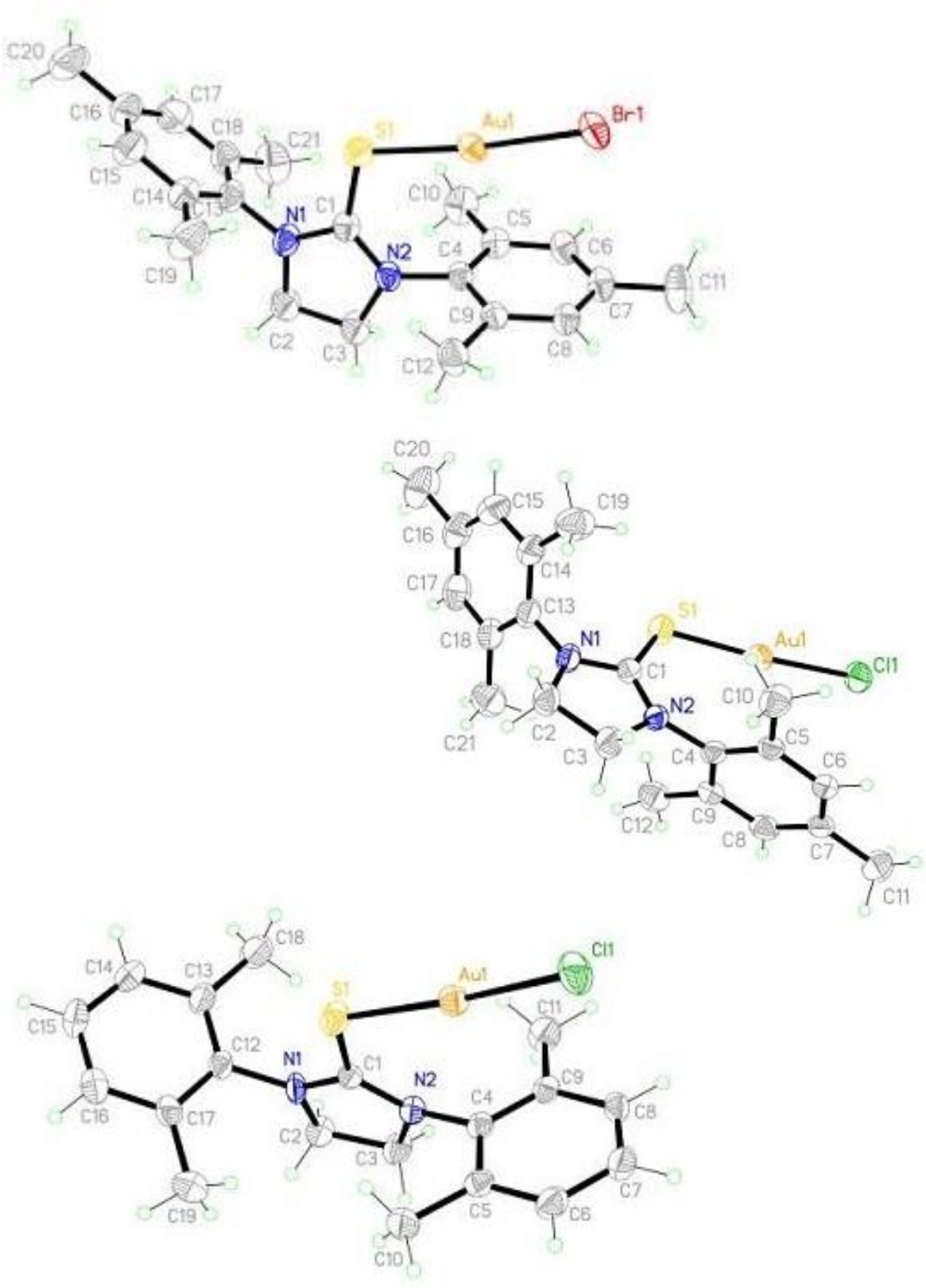

Figure 2.27: Molecular structures of (SIXyS)AuCl and (SIMesS)AuX (X = Cl, Br).

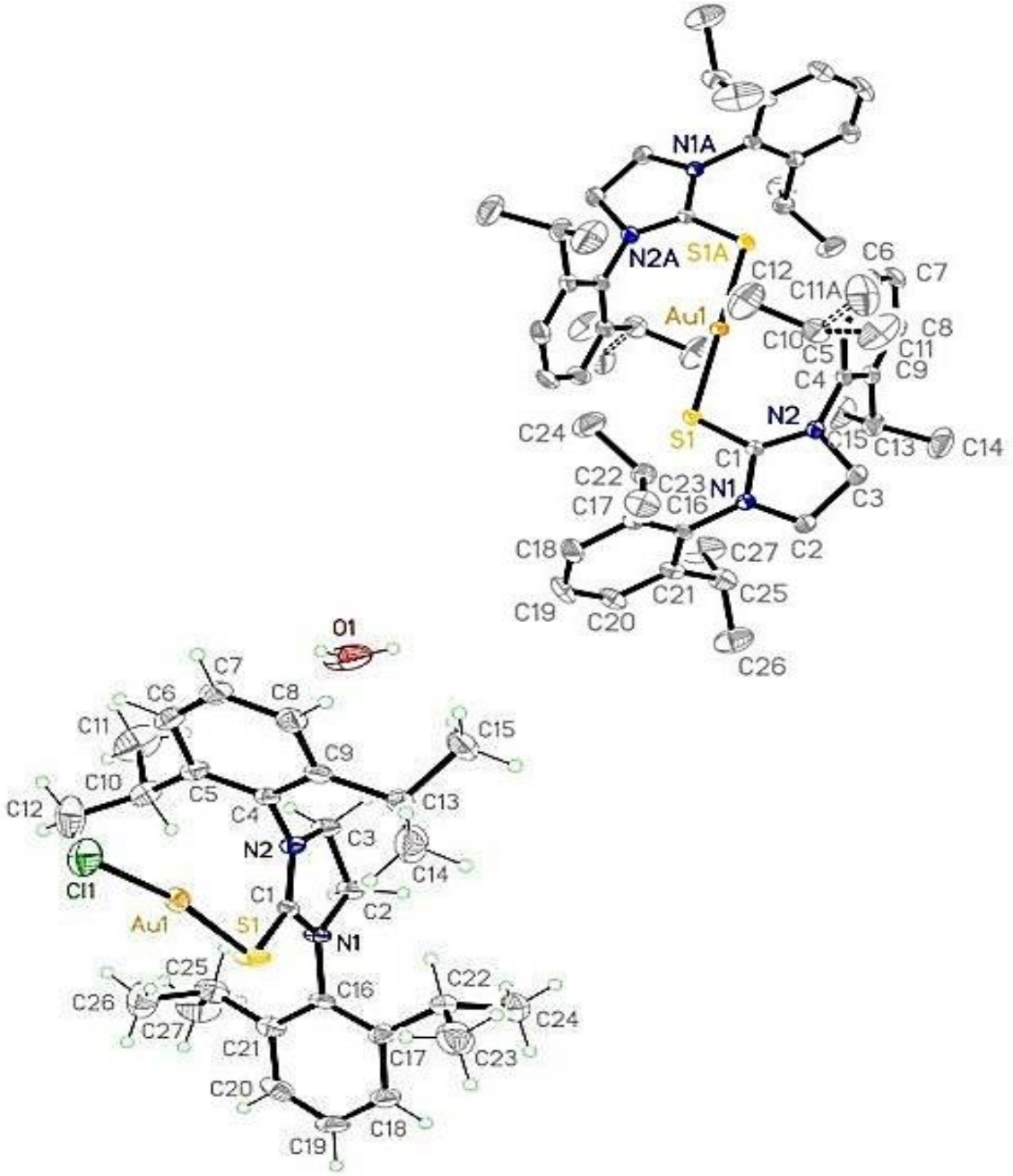

Figure 2.28: Molecular structure of (SIDippS)AuX (X = Cl, Br).

These complexes (Figure 2.27 and 2.28) are near isomorphic to the mercury complexes of SIArE, as expected, except for the (SIDippS)AuBr complex. The outlier dimeric structure is the result of a ligand metathesis on a gold center resulting in a dibromo aurate(I) anion. It's unclear if the formation of this dimer is due to the

contribution of aromatic stacking in the solid-state, the enthalpic gain of the new complex ionic system, or due to the solvent use to crystallize the complex. The thione and selone bond lengths respond similarly to that of the mercury complexes with elongated of the C=E bond compared to the free lignad. Similarly the ^{13}C NMR resonance for the thione carbon is more shielded than the free ligand typically by. While the rearrangement in various solvents has been mentioned, it is important to recognize that of the two species, neither is free ligand (Figure 2.29).

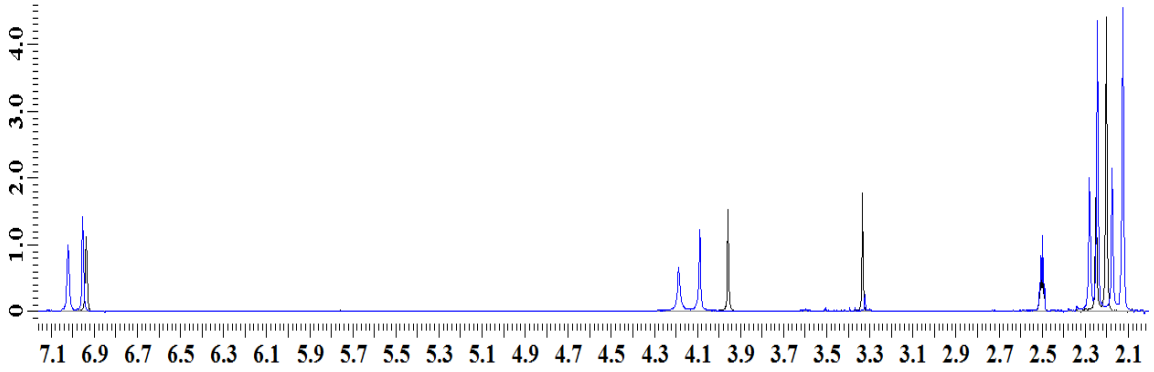

Figure 2.29: ^{1}H NMR spectra of SIMesS (black) & (SIMesS)AuBr (blue) in d_6-DMSO.

Similar gold(I) chloride complexes were previously prepared by Nolan *et al.* using NHSe ligands. Included in the surveyed NHSe ligands were SIDippSe and SIMesSe. Both SIArSe ligands formed stable gold(I) chloride complexes and solid-state data shows identical geometry to that in Figure 2.28 for SIMesS.[51] The SIDippSe ligand however formed a homoleptic charged strucutre, similar to (SIDippS)AuBr (Figure 2.26). Within the same study ^{77}Se NMR spectra were collected on the new gold(I) complexes. Interestingly, their results for the two SIArSe ligands shows a shielding in the selenium resonance peak with upfield shifts of *ca.*30 ppm for SIMesSe and *ca.*55 ppm for SIDippSe. Another group in 2002 studied similar NHSe ligands with gold(I) cyanate

specifically to deduce the equilibirum of Scheme 2.7 in solution.[84] In summary, their work indicates a solution state preference for the homoleptic charged stucutre, with K_{eq} values generally above 1. Their extended work with phosphines indicates the homoleptic strucutre is more favoured with higher σ donation from the ligand.[85] To futhur analyze these SIArE gold(I) complexes comparison with their unstaturated counterparts published work by Lavoie *et al.*should afford a idea of difference a saturated backbone imparts.[10] The solid-state arrangement of the unstaturated analog of SIMesS shows the same mononuclear neutral geometry and C=S bond length of 1.71 (Table 2.9). One obvious difference is the S-Au bond length, when using an unsaturated SIMesS ligand a 0.02 Å elongation of the chalcogen metal bond is observed.

CHAPTER 3: EXPERIMENTAL

3.1 General Consideration

All reactions were performed under aerobic conditions or under dry oxygen-free nitrogen in an Innovative Technology System One-M-DC glove box where indicated. Solvents were purified and degassed by standard procedures and all commercially available reagents were used as received. (tht)AuCl was prepared following literature procedures.[82] ^{1}H and ^{13}C NMR spectra were obtained on JEOL ECX-300 (300 MHz) or JEOL ECA-500 (500 MHz) FT spectrometers. ^{1}H and ^{13}C chemical shifts are reported in ppm and were referenced internally with respect to the residual solvent resonances[86] (^{1}H: 2.50 ppm for d_6-DMSO, 7.26 ppm $CDCl_3$; ^{13}C: 39.52 ppm for d_6-DMSO, 77.16 for $CDCl_3$; ^{77}Se: 463 ppm for PhSeSePh[87]); coupling constants are reported in Hertz (Hz). IR spectra were recorded as pure solids on a Perkin-Elmer Spectrum 100 FT-IR spectrometer and are reported in cm^{-1}; relative intensities of the absorptions are indicated in parentheses (vs = very strong, s = strong, m = medium, w = weak). Elemental analyses were determined by Atlantic Microlab, Inc. (Norcross, GA). Crystallographic data were collected using a Bruker D8 Venture X-ray instrument with MoKα radiation. All calculations were carried out with the GAUSSIAN 03 program.[88] The reported molecular orbital (M.O.) energies were evaluated at the RHF/6-311G(d) level of theory to avoid poor estimates of the ionization potentials. LANL2DZ effective core pseudopotentials were used for calculations involving I, Au, or Hg atoms.[83]

3.2 Precursor Synthesis to SIArE

The formamidines ArN=CHNHAr (Ar = Mes, Dipp) and their corresponding imidazolinium chloride derivatives were prepared as reported;[74] the 2,6-xylyl (Xy) analogues were prepared similarly from 2,6 dimethylaniline. The 2,6-diisopropylphenyl derivative [SIDippH]Cl was obtained in spectroscopically pure form after trituration with ethyl acetate, instead of acetone, and washing the resulting solid with diethyl ether.

3.3 Synthesis of SIXyS

Under an argon atmosphere, a stirred suspension of 1,3-bis(2,6-dimethylphenyl)imidazolinium chloride (1.613 g, 5.123 mmol), potassium carbonate (0.854 g, 6.179 mmol), and elemental sulfur (0.183 g, 5.708 mmol) in ethanol (30 mL) was heated to reflux for 17 h. The reaction mixture was allowed to cool to room temperature and the solvent was removed under reduced pressure to yield a pale brown solid residue. The product was extracted into dichloromethane (3 x 20 mL) and the combined extracts were washed with DI water (3 x 30 mL). The organic phase was dried over a small amount of $MgSO_4$, filtered, and the solvent was removed from the solution under vacuum to yield the off white product, which was washed with pentane (30 mL) and dried *in vacuo* for 16 h (1.243 g, 78%). Anal. Calc. for $C_{19}H_{22}N_2S$: C, 73.5; H, 7.1; N, 9.0. Found: C, 73.2; H, 7.1; N, 9.0%. ^{1}H NMR spectroscopic data match those previously reported.[89]

3.4 Synthesis of SIXySe

Under an argon atmosphere, a stirred suspension of 1,3-bis(2,6-dimethylphenyl)imidazolinium chloride (0.911 g, 2.893 mmol), potassium carbonate (0.544 g, 3.936 mmol), and gray selenium (0.275 g, 3.483 mmol) in

ethanol (100 mL) was heated to reflux for 20 h. The reaction mixture was allowed to cool to room temperature and the solvent was removed under reduced pressure to yield a dark solid residue. The product was extracted into dichloromethane (3 x 20 mL) and the combined extracts were washed with DI water (3 x 30 mL). The organic phase was dried over a small amount of $MgSO_4$, filtered, and the solvent was removed from the solution under vacuum to yield the off white product, which was dried *in vacuo* for 16 h (0.634 g, 61%). Mp = 258-260 °C (dec.). NMR data (in d_6-DMSO): ^{1}H δ 2.27 (s, 12 H, C*H*$_3$), 4.02 (s, 4 H, C*H*$_2$), 7.13-7.21 (m, 6 H, *C*$_6$*H*$_3$); ^{13}C δ 17.4 (q, $^1J_{C-H}$ = 127, 4 C, *C*H$_3$), 48.4 (t, $^1J_{C-H}$ = 148, 2 C, *C*H$_2$), 128.1 (d, $^1J_{C-H}$ = 160, 2 C, *C*$_6$H$_3$), 128.3 (d, $^1J_{C-H}$ = 160, 4 C, *C*$_6$H$_3$), 136.5 (s, 2 C, *C*$_6$H$_3$), 137.8 (s, 4 C, *C*$_6$H$_3$), 177.8 (s, 1 C, *C*=Se). IR data: 2943 (w), 2908 (w), 2849 (w), 1484 (s), 1466 (m), 1449 (m), 1402 (m), 1369 (w), 1277 (vs), 1253 (m), 1183 (w), 1156 (w), 1098 (m), 1033 (m), 986 (w), 947 (w), 915 (w), 786 (vs), 714 (m). Anal. Calc. for $C_{19}H_{22}N_2Se$: C, 63.9; H, 6.3; N, 7.8. Found: C, 64.1; H, 6.2; N, 7.9%.

3.5 Synthesis of SIMesS

Under an argon atmosphere, a stirred suspension of 1,3-bis(2,4,6 trimethylphenyl)imidazolinium chloride (1.020 g, 2.975 mmol), potassium carbonate (0.534 g, 3.864 mmol), and elemental sulfur (0.117 g, 3.649 mmol) in ethanol (30 mL) was heated to reflux for 16 h. The reaction mixture was allowed to cool to room temperature and the solvent was removed under reduced pressure to yield a pale brown solid residue. The product was extracted into dichloromethane (3 x 20 mL) and the combined extracts were washed with DI water (3 x 30 mL). The organic phase was dried over a small amount of $MgSO_4$, filtered, and the solvent was removed from the solution

under vacuum to yield the off white product, which was washed with pentane (30 mL) and dried *in vacuo* for 18 h (0.852 g, 85%). ^{1}H NMR spectroscopic data match those previously reported.[52]

3.6 Synthesis of SIMesSe

Under an argon atmosphere, a stirred suspension of 1,3-bis(2,4,6-trimethylphenyl)imidazolinium chloride (1.006 g, 2.934 mmol), potassium carbonate (0.533 g, 3.856 mmol), and gray selenium (0.302 g, 3.825 mmol) in ethanol (100 mL) was heated to reflux for 22 h. The reaction mixture was allowed to cool to room temperature and the solvent was removed under reduced pressure to yield a dark solid residue. The product was extracted into dichloromethane (3 x 20 mL) and the combined extracts were washed with DI water (3 x 30 mL). The organic phase was dried over a small amount of $MgSO_4$, filtered, and the solvent was removed from the solution under vacuum to yield the off-white product, which was washed with pentane (30 mL) and dried *in vacuo* for 16 h (1.051 g, 93%). ^{1}H NMR spectroscopic data match those previously reported.[47,51]

3.7 Synthesis of SIDippS

Under an argon atmosphere, a stirred suspension of 1,3-bis(2,6-diisopropylphenyl)imidazolinium chloride (2.638 g, 6.177 mmol), potassium carbonate (1.111 g, 8.039 mmol), and elemental sulfur (0.238 g, 7.424 mmol) in methanol (100 mL) was heated to reflux for 24 h. The reaction mixture was allowed to cool to room temperature and the solvent was removed under reduced pressure to yield a pale brown solid residue. The product was extracted into dichloromethane (3 x 30 mL) and the combined extracts were washed with DI water (3 x 30 mL). The organic phase was dried

over a small amount of $MgSO_4$, filtered, and the solvent was removed from the solution under vacuum to yield the off white product, which was washed with pentane (30 mL) and dried *in vacuo* for 16 h (1.815 g, 70%). ^{1}H NMR spectroscopic data match those previously reported.[52]

3.8 Synthesis of SIDippSe

Under an argon atmosphere, a stirred suspension of 1,3-bis(2,6-diisopropylphenyl)imidazolinium chloride (1.521 g, 3.561 mmol), potassium carbonate (0.823 g, 5.955 mmol), and gray selenium (0.439 g, 5.560 mmol) in ethanol (50 mL) was heated to reflux for 48 h. The reaction mixture was allowed to cool to room temperature and the solvent was removed under reduced pressure to yield a black solid residue. The product was extracted into dichloromethane (3 x 20 mL) and the combined extracts were washed with DI water (3 x 30 mL). The organic phase was dried over a small amount of $MgSO_4$, filtered, and the solvent was removed from the solution under vacuum to yield the off-white product, which was washed with pentane (30 mL) and dried *in vacuo* for 16 h (1.228 g, 73%). ^{1}H NMR spectroscopic data match those previously reported.[64]

3.9 Synthesis of (SIXyS)I_2

SIXyS (0.060 g, 0.193 mmol) was added in small portions to a stirred solution of I_2 (0.052 g, 0.204 mmol) in diethyl ether (10 mL), resulting in the slow formation of a red solid and a burgundy solution. After stirring for 1 h, the suspension was treated with pentane (10 mL), and the product was isolated by filtration, washed with a small amount of cold diethyl ether, and air-dried for 10 min (0.067 g, 62%). Mp = 200-202 °C (dec.). NMR data (in $CDCl_3$): ^{1}H δ 2.37 (s, 12 H, CH_3), 4.07 (s, 4 H, CH_2), 7.15 7.30 (m, 6 H, C_6H_3); ^{13}C δ 18.3 (q, $^1J_{C-H}$ = 126, 4 C, CH_3), 48.8 (t, $^1J_{C-H}$ = 149, 2 C, CH_2), 129.2 (d, $^1J_{C-}$

$_H$ = 160, 4 C, C_6H_3), 129.6 (d, $^1J_{C-H}$ = 160, 2 C, C_6H_3), 135.9 (s, 2 C, C_6H_3), 136.8 (s, 4 C, C_6H_3), 176.7 (s, 1 C, C=S). IR data: 3025 (w), 2950 (w), 2915 (w), 2892 (w), 2852 (w), 1592 (w), 1497 (s), 1484 (w), 1466 (w), 1458 (m), 1408 (s), 1373 (m), 1303 (s), 1276 (vs), 1258 (m), 1203 (w), 1187 (m), 1162 (m), 1097 (m), 1028 (m), 987 (w), 956 (m), 918 (w), 893 (w), 864 (w), 823 (w), 773 (vs), 752 (w), 727 (m). Anal. Calc. for $C_{19}H_{22}I_2N_2S$: C, 40.4; H, 3.9; N, 5.0. Found: C, 40.3; H, 4.0.1; N, 4.9%.

3.10 Synthesis of (SIMesS)I_2

SIMesS (0.085 g, 0.251 mmol) was added in small portions to a stirred solution of I_2 (0.065 g, 0.256 mmol) in diethyl ether (10 mL), resulting in the slow formation of a red solid and a burgundy solution. After stirring for 1 h, the suspension was treated with pentane (10 mL), and the product was isolated by filtration, washed with a small amount of cold diethyl ether, and air-dried for 10 min (0.101 g, 68%). Mp = 150-153 °C (dec.). NMR data (in $CDCl_3$): ^{1}H δ 2.32 (s, 12 H, C*H*$_3$), 2.33 (s, 6 H, C*H*$_3$), 4.05 (s, 4 H, C*H*$_2$), 7.00 (s, 4 H, aryl *H*); ^{13}C δ 18.1 (q, $^1J_{C-H}$ = 127, 4 C, CH_3), 21.3 (q, $^1J_{C-H}$ = 122, 2 C, *C*H$_3$), 48.9 (t, $^1J_{C-H}$ = 147, 2 C, *C*H$_2$), 130.0 (d, $^1J_{C-H}$ = 160, 4 C, *C*$_6$H$_2$), 133.4 (s, 2 C, *C*$_6$H$_2$), 136.4 (s, 4 C, *C*$_6$H$_2$), 139.6 (s, 2 C, *C*$_6$H$_2$), 176.9 (s, 1 C, *C*=S). IR data: 2973 (w), 2949 (w), 2916 (w), 2854 (w), 1606 (m), 1505 (s), 1484 (m), 1458 (m), 1438 (m), 1413 (m), 1371 (m), 1315 (w), 1301 (s), 1274 (vs), 1215 (w), 1189 (w), 1169 (m), 1099 (w), 1028 (m), 1012 (m), 987 (w), 969 (m), 936 (m), 886 (w), 853 (s), 801 (m), 728 (m). Anal. Calc. for $C_{21}H_{26}I_2$N2S: C, 42.6; H, 4.4; N, 4.7. Found: C, 42.5; H, 4.4; N, 4.7%.

3.11 Synthesis of (SIMesSe)I_2

SIMesSe (0.086 g, 0.223 mmol) was added in small portions to a stirred solution of I_2 (0.057 g, 0.225 mmol) in diethyl ether (10 mL), resulting in the slow formation of a

red solid and a burgundy solution. After stirring for 1 h, the suspension was treated with pentane (10 mL) and the product was isolated by filtration, washed with a small amount of cold diethyl ether, and air-dried for 10 min (0.106 g, 80%). Mp = 202-204 °C (dec.). NMR data (in $CDCl_3$): ^1H δ 2.31 (s, 12 H, CH_3), 2.35 (s, 6 H, CH_3), 4.12 (s, 4 H, CH_2), 7.01(s, 4 H, aryl H); ^{13}C δ 18.2 (q, $^1J_{C-H}$ = 126, 4 C, CH_3), 21.4 (q, $^1J_{C-H}$ = 126, 2 C, CH_3), 50.5 (t, $^1J_{C-H}$ = 148, 2 C, CH_2), 130.2 (d, $^1J_{C-H}$ = 155, 4 C, C_6H_2), 133.0 (s, 2 C, C_6H_2), 136.1 (s, 4 C, C_6H_2), 140.5 (s, 2 C, C_6H_2), 171.3 (s, 1 C, C=Se). IR data: 2976 (w), 2948 (w), 2914 (w), 2853 (w), 1605 (m), 1515 (vs), 1481 (m), 1459 (m), 1416 (m), 1372 (m), 1296 (s), 1274 (vs), 1212 (w), 1190 (m), 1169 (w), 1098 (w), 1030 (m), 984 (w), 955 (w), 925 (m), 855 (s), 805 (w), 728 (w). Anal. Calc. for $C_{21}H_{26}I_2N_2Se$: C, 39.5; H, 4.1; N, 4.4. Found: C, 39.6; H, 4.1; N, 4.4%.

3.12 Synthesis of (SIDippS)I_2

SIDippS (0.065 g, 0.154 mmol) was added in small portions to a stirred solution of I2 (0.041 g, 0.163 mmol) in diethyl ether (10 mL), resulting in the slow formation of a red solid and a burgundy solution. After stirring for 24 h, the suspension was concentrated under reduced pressure to ca. 2 mL, treated with pentane (10 mL), and the product was isolated by filtration, washed with small amount of cold diethyl ether (0.072 g, 69%). Mp = 176-178 °C (dec.). .). NMR data (in $CDCl_3$): ^1H δ 1.38 (d, $^3J_{H-H}$ = 6.6, 12 H, CH_3), 1.46 (d, $^3J_{H-H}$ = 6.6, 12 H, CH_3), 3.14 (septet, $^3J_{H-H}$ = 6.8, 4 H, C*H*), 4.63 (s, 4 H, CH_2), 7.32 (d, $^3J_{H-H}$ = 7.8, 4 H, C_6H_3), 7.54 (t, $^3J_{H-H}$ = 7.8, 2 H, C_6H_3); ^{13}C δ 24.1 (q, $^1J_{C-H}$ = 129, 4 C, CH_3), 26.1 (d, $^1J_{C-H}$ = 127, 4 C, CH_3), 29.7 (d, $^1J_{C-H}$ = 127, 4 C, *C*H), 55.6 (t, $^1J_{C-H}$ = 151, 2 C, CH_2), 125.6 (d, $^1J_{C-H}$ = 159, 4 C, C_m in C_6H_3), 129.7 (s, 2 C, C_{ipso} in C_6H_3), 132.3 (d, $^1J_{C-H}$ = 160, 2 C, C_p in C_6H_3), 147.3 (s, 4 C, C_o in C_6H_3), 163.4 (s, 1 C,

C=S). IR data: 2965 (m), 2921 (w), 2866 (w), 1589 (w), 1493 (s), 1458 (s), 1412 (s), 1382 (w), 1343 (w), 1325 (w), 1300 (vs), 1278 (vs), 1179 (w), 1146 (w), 1107 (w), 1049 (m), 966 (m), 936 (w), 801 (vs), 757 (m), 730 (w), 704 (w).Anal. Calc. for $C_{21}H_{26}I_2N_2S$: C, 47.9; H, 5.7; N, 4.1. Found: C, 47.9; H, 5.5; N, 4.1%.

3.13 Synthesis of (SIDippSe)I_2

SIDippSe (0.058 g, 0.124 mmol) was added in small portions to a stirred solution of I_2 (0.033 g, 0.130 mmol) in diethyl ether (10 mL), resulting in the slow formation of a red solid and a burgundy solution. After stirring for 22 h, the suspension was concentrated under reduced pressure to ca. 2 mL, treated with pentane (10 mL), and the product was isolated by filtration, washed with a small amount of cold diethyl ether and pentane, and air-dried for 10 min (0.070 g, 78%). Mp = 205 208 °C (dec.). NMR data (in CDCl3): ^{1}H δ 1.33 (d, $^3J_{H-H}$ = 6.9, 12 H, C*H*$_3$), 1.42 (d, $^3J_{H-H}$ = 6.9, 12 H, C*H*$_3$), 2.94 (septet, $^3J_{H-H}$ = 6.8, 4 H, C*H*), 4.14 (s, 4 H, C*H*$_2$), 7.28 (d, $^3J_{H-H}$ = 8.0, 4 H, C$_6$*H*$_3$), 7.50 (t, $^3J_{H-H}$ = 8.0, 2 H, C$_6$*H*$_3$); ^{13}C δ 24.3 (q, $^1J_{C-H}$ = 129, 4 C, *C*H$_3$), 25.4 (d, $^1J_{C-H}$ = 131, 4 C, *C*H$_3$), 29.5 (d, $^1J_{C-H}$ = 122, 4 C, *C*H), 52.9 (t, $^1J_{C-H}$ = 150, 2 C, *C*H$_2$), 125.3 (d, $^1J_{C-H}$ = 158, 4 C, C$_m$ in *C*$_6$H$_3$), 131.1 (d, $^1J_{C-H}$ = 159, 2 C, C$_p$ in *C*$_6$H$_3$), 132.9 (s, 2 C, C$_{ipso}$ in *C*$_6$H$_3$), 146.9 (s, 4 C, C$_o$ in *C*$_6$H$_3$), 175.3 (s, 1 C, *C*=Se). IR data: 2961 (m), 2925 (w), 2902 (w), 2865 (w), 1589 (m), 1502 (s), 1486 (m), 1457 (m), 1419 (s), 1383 (m), 1363 (w), 1339 (w), 1321 (w), 1280 (vs), 1229 (w), 1186 (m), 1106 (w), 1058 (m), 1049 (m), 941 (m), 936 (m), 803 (s), 768 (w), 757 (m), 729 (w). Anal. Calc. for $C_{21}H_{26}I_2N_2Se$: C, 44.8; H, 5.3; N, 3.9. Found: C, 44.2; H, 5.2; N, 3.9%.

3.14 Synthesis of (SIXyS)$HgCl_2$

Acetonitrile (10 mL) was added to a mixture of $HgCl_2$ (0.060 g, 0.222 mmol) and SIXyS (0.070 g, 0.226 mmol), resulting in the slow formation of a white solid and a colorless solution. After stirring the suspension for 23 h, the product was isolated by filtration and dried *in vacuo* for 18 h (0.073 g, 57%). Mp = 314-316 °C (dec.). NMR data (in d_6-DMSO): ^{1}H δ 2.29 (s, 12 H, C*H*$_3$), 4.12 (s, 4 H, C*H*$_2$), 7.17-7.28 (m, 6 H, *C*$_6$*H*$_3$); ^{13}C δ 17.3 (q, $^1J_{C\text{-}H}$ = 128, 4 C, *C*H$_3$), 48.1 (t, $^1J_{C\text{-}H}$ = 150, 2 C, *C*H$_2$), 128.8 (d, $^1J_{C\text{-}H}$ = 160, 6 C, *C*$_6$H$_3$), 136.0 (s, 2 C, *C*$_6$H$_3$), 136.6 (s, 4 C, *C*$_6$H$_3$), 176.9 (s, 1 C, *C*=S). IR data: 3022 (w), 2981 (w), 2920 (w), 2853 (w), 1628 (m), 1585 (w), 1508 (s), 1462 (m), 1442 (w), 1416 (m), 1381 (w), 1319 (s), 1283 (s), 1261 (w), 1204 (w), 1170 (w), 1100 (w), 1031 (w), 989 (w), 961 (w), 919 (w), 827 (w), 780 (vs), 723 (w), 674 (w). Anal. Calc. for $C_{19}H_{22}Cl_2HgN_2S$: C, 39.2; H, 3.8; N, 4.8. Found: C, 39.5; H, 3.9; N, 4.9%.

3.15 Synthesis of (SIXyS)$HgBr_2$

Diethyl ether (10 mL) was added to a mixture of $HgBr_2$ (0.075 g, 0.208 mmol) and SIXyS (0.065 g, 0.209 mmol), resulting in the slow formation of a white solid and a colorless solution. After stirring the suspension for 23 h, the product was isolated by filtration and dried in vacuo for 30 min (0.092 g, 66%). Mp = 294-296 °C (dec.). NMR data (in d_6-DMSO): ^{1}H δ 2.29 (s, 12 H, C*H*$_3$), 4.12 (s, 4 H, C*H*$_2$), 7.16-7.28 (m, 6 H, aryl H); ^{13}C δ 17.4 (q, $^1J_{C\text{-}H}$ = 128, 4 C, *C*H$_3$), 48.1 (t, $^1J_{C\text{-}H}$ = 149, 2 C, *C*H$_2$), 128.9 (d, $^1J_{C\text{-}H}$ = 160, 6 C, *C*$_6$H$_3$), 136.0 (s, 2 C, *C*$_6$H$_3$), 136.7 (s, 4 C, *C*$_6$H$_3$), 176.5 (s, 1 C, *C*=S). IR data: 3022 (w), 2961 (w), 2914 (w), 2853 (w), 1672 (w), 1591 (w), 1507 (s), 1461 (s), 1439 (m), 1414 (s), 1379 (m), 1319 (s), 1282 (s), 1260 (m), 1208 (w), 1197 (m), 1169 (m),

1100 (m), 1029 (m), 990 (w), 961 (w), 918 (w), 868 (w), 777 (vs), 751 (w), 723 (w). Anal. Calc. for $C_{19}H_{22}Br_2HgN_2S$: C, 34.0; H, 3.3; N, 4.2. Found: C, 34.3; H, 3.2; N, 4.2%.

3.16 Synthesis of (SIXyS)HgI_2

Diethyl ether (8 mL) was added to a mixture of HgI_2 (0.100 g, 0.220 mmol) and SIXyS (0.071 g, 0.229 mmol), resulting in the slow formation of an off-white solid and a colorless solution. After stirring the suspension for 24 h, the product was isolated by filtration and dried *in vacuo* for 30 min (0.132 g, 78%). Mp = 263-265 °C (dec.). NMR data (in d_6-DMSO): ^{1}H δ 2.28 (s, 12 H, C*H*$_3$), 4.09 (s, 4 H, C*H*$_2$), 7.15-7.26 (m, 6 H, C_6*H*$_3$); ^{13}C δ 17.4 (q, $^1J_{C\text{-}H}$ = 125, 4 C, *C*H$_3$), 47.8 (t, $^1J_{C\text{-}H}$ = 151, 2 C, *C*H$_2$), 128.6 (d, $^1J_{C\text{-}H}$ = 160, 2 C, *C*$_6$H$_3$), 128.7 (d, $^1J_{C\text{-}H}$ = 159, 4 C, *C*$_6$H$_3$), 136.5 (s, 2 C, *C*$_6$H$_3$), 136.7 (s, 4 C, *C*$_6$H$_3$), 177.6 (s, 1 C, *C*=S). IR data: 2964 (w), 2915 (w), 2846 (w), 1591 (w), 1500 (s), 1460 (m), 1415 (m), 1376 (m), 1309 (s), 1284 (s), 1256 (m), 1197 (w), 1096 (m), 1033 (m), 988 (w), 962 (w), 847 (w), 799 (m), 788 (vs), 751 (w), 732 (w), 708 (w). Anal. Calc. for $C_{19}H_{22}HgI_2N_2S$: C, 29.8; H, 2.9; N, 3.7. Found: C, 30.1; H, 2.9; N, 3.7%.

3.17 Synthesis of (SIXySe)$HgCl_2$

Acetonitrile (10 mL) was added to a mixture of $HgCl_2$ (0.102 g, 0.375 mmol) and SIXySe (0.134 g, 0.374 mmol), resulting in the formation a small amount of a white solid in a colorless solution. After stirring for 19 h, the suspension was concentrated under reduced pressure to ca. 1 mL, treated with diethyl ether (10 mL), and the product was isolated by filtration and dried in vacuo for 12 h (0.129 g, 55%). Mp = 302-305 °C (dec.). NMR data (in d_6-DMSO): ^{1}H δ 2.31 (s, 12 H, C*H*$_3$), 4.24 (s, 4 H, C*H*$_2$), 7.21-7.33 (m, 6 H, C_6*H*$_3$); ^{13}C δ 17.4 (q, $^1J_{C\text{-}H}$ = 128, 4 C, *C*H$_3$), 49.9 (t, $^1J_{C\text{-}H}$ = 151, 2 C, *C*H$_2$),

129.5 (d, $^{1}J_{C-H}$ = 161, 4 C, *C*$_6$H$_3$), 129.8 (d, $^{1}J_{C-H}$ = 161, 2 C, *C*$_6$H$_3$), 135.2 (s, 2 C, *C*$_6$H$_3$), 136.2 (s, 4 C, *C*$_6$H$_3$), 171.3 (s, 1 C, *C*=Se). IR data: 3025 (w), 2961 (w), 2920 (w), 1591 (w), 1516 (s), 1491 (w), 1464 (m), 1440 (w), 1416 (m), 1381 (w), 1308 (s), 1284 (s), 1261 (w), 1207 (w), 1196 (w), 1169 (w), 1098 (w), 1028 (w), 986 (w), 942 (w), 868 (w), 779 (vs), 741 (w), 722 (w). Anal. Calc. for $C_{19}H_{22}Cl_2HgN_2Se$: C, 36.3; H, 3.5; N, 4.5. Found: C, 36.5; H, 3.5; N, 4.5%.

3.18 Synthesis of (SIXySe)HgBr$_2$

Acetonitrile (10 mL) was added to a mixture of $HgBr_2$ (0.055 g, 0.153 mmol) and SIXySe (0.054 g, 0.151 mmol), resulting in the formation a small amount of a white solid in a colorless solution. After stirring for 19 h, the suspension was concentrated under reduced pressure to ca. 1 mL, treated with diethyl ether (10 mL), and the product was isolated by filtration and dried *in vacuo* for 12 h (0.055 g, 51%). Mp = 318-320 °C (dec.). NMR data (in d$_6$-DMSO): ^{1}H δ 2.31 (s, 12 H, C*H*$_3$), 4.23 (s, 4 H, C*H*$_2$), 7.21-7.33 (m, 6 H, *C*$_6$H$_3$); ^{13}C δ 17.5 (q, $^{1}J_{C-H}$ = 127, 4 C, *C*H$_3$), 49.8 (t, $^{1}J_{C-H}$ = 152, 2 C, *C*H$_2$), 129.5 (d, $^{1}J_{C-H}$ = 160, 4 C, *C*$_6$H$_3$), 129.7 (d, $^{1}J_{C-H}$ = 161, 2 C, *C*$_6$H$_3$), 135.5 (s, 2 C, *C*$_6$H$_3$), 136.2 (s, 4 C, *C*$_6$H$_3$), 172.2 (s, 1 C, *C*=Se). IR data: 3027 (w), 2958 (w), 2915 (w), 1514 (vs), 1490 (w), 1462 (m), 1439 (w), 1414 (m), 1380 (w), 1307 (s), 1283 (s), 1260 (w), 1207 (w), 1195 (w), 1169 (w), 1097 (w), 1027 (w), 984 (w), 942 (w), 918 (w), 866 (w), 777 (vs), 740 (w), 723 (w). Anal. Calc. for $C_{19}H_{22}Br_2HgN_2Se$: C, 31.8; H, 3.1; N, 3.9. Found: C, 32.0; H, 3.1; N, 4.0%.

3.19 Synthesis of (SIXySe)HgI$_2$

Acetonitrile (10 mL) was added to a mixture of HgI_2 (0.078 g, 0.172 mmol) and SIXySe (0.061 g, 0.171 mmol), resulting in the formation of a small amount of a pale

yellow solid and a colorless solution. After stirring for 23 h, the suspension was concentrated under reduced pressure to ca. 1 mL, treated with diethyl ether (10 mL), and the product was isolated by filtration and dried *in vacuo* for 16 h (0.109 g, 78%). Mp = 322-326 °C (dec.). NMR data (in d_6-DMSO): ^{1}H δ 2.31 (s, 12 H, C*H*$_3$), 4.19 (s, 4 H, C*H*$_2$), 7.19-7.31 (m, 6 H, C_6*H*$_3$); ^{13}C δ 17.4 (q, $^{1}J_{C-H}$ = 128, 4 C, *C*H$_3$), 49.5 (t, $^{1}J_{C-H}$ = 147, 2 C, *C*H$_2$), 129.2 (d, $^{1}J_{C-H}$ = 160, 6 C, *C*$_6$H$_3$), 135.9 (s, 2 C, *C*$_6$H$_3$), 136.1 (s, 4 C, *C*$_6$H$_3$), 173.6 (s, 1 C, *C*=Se). IR data: 2947 (w), 2914 (w), 2855 (w), 1590 (w), 1506 (s), 1484 (w), 1460 (w), 1413 (m), 1375 (m), 1298 (s), 1282 (vs), 1258 (m), 1193 (w), 1093 (m), 1030 (m), 982 (m), 940 (w), 800 (w), 787 (vs), 750 (w), 730 (w). Anal. Calc. for $C_{19}H_{22}HgI_2N_2Se$: C, 28.1; H, 2.7; N, 3.5. Found: C, 28.2; H, 2.6; N, 3.5%.

3.20 Synthesis of (SIMesS)HgCl$_2$

Diethyl ether (10 mL) was added to a mixture of HgCl2 (0.054 g, 0.199 mmol) and SIMesS (0.078 g, 0.231 mmol), resulting in the slow formation of a white solid and a colorless solution. After stirring the suspension for 21 h, the product was isolated by filtration and dried in vacuo for 18 h (0.089 g, 73%). Mp = 261-263 °C (dec.). NMR data (in d_6-DMSO): ^{1}H δ 2.22 (s, 12 H, C*H*$_3$), 2.26 (s, 6 H, C*H*$_3$), 4.11 (s, 4 H, C*H*$_2$), 6.99 (s, 4 H, aryl H); ^{13}C δ 17.3 (q, $^{1}J_{C-H}$ = 128, 4 C, *C*H$_3$), 20.7 (q, $^{1}J_{C-H}$ = 130, 2 C, *C*H$_3$), 48.0 (t, $^{1}J_{C-H}$ = 149, 2 C, *C*H$_2$), 129.4 (d, $^{1}J_{C-H}$ = 161, 4 C, *C*$_6$H$_2$), 133.7 (s, 2 C, *C*$_6$H$_2$), 136.2 (s, 4 C, *C*$_6$H$_2$), 138.1 (s, 2 C, *C*$_6$H$_2$), 177.0 (s, 1 C, *C*=S). IR data: 3013 (w), 2966 (w), 2950 (w), 2918 (w), 2860 (w), 1606 (m), 1508 (s), 1483 (m), 1460 (w), 1442 (m), 1417 (m), 1379 (m), 1320 (s), 1278 (vs), 1220 (w), 1193 (w), 1033 (m), 969 (w), 939 (w), 871 (w), 853 (m), 732 (w). Anal. Calc. for $C_{21}H_{26}Cl_2HgN_2S$: C, 41.4; H, 4.3; N, 4.6. Found: C, 41.3; H, 4.3; N, 4.5%.

3.21 Synthesis of (SIMesS)$HgBr_2$

Diethyl ether (10 mL) was added to a mixture of HgBr2 (0.075 g, 0.208 mmol) and SIMesS (0.071 g, 0.211 mmol), resulting in the slow formation of a white solid and a colorless solution. After stirring the suspension for 21 h, the product was isolated by filtration and dried *in vacuo* for 18 h (0.136 g, 94%). Mp = 239-242 °C (dec.). NMR data (in d_6-DMSO): ^{1}H δ 2.23 (s, 12 H, C*H*$_3$), 2.26 (s, 6 H, C*H*$_3$), 4.07 (s, 4 H, C*H*$_2$), 6.99 (s, 4 H, aryl H); ^{13}C δ 17.3 (q, $^1J_{C\text{-}H}$ = 128, 4 C, *C*H$_3$), 20.7 (q, $^1J_{C\text{-}H}$ = 128, 2 C, *C*H$_3$), 48.0 (t, $^1J_{C\text{-}H}$ = 149, 2 C, *C*H$_2$), 129.4 (d, $^1J_{C\text{-}H}$ = 159, 4 C, *C*$_6$H$_2$), 133.6 (s, 2 C, *C*$_6$H$_2$), 136.2 (s, 4 C, *C*$_6$H$_2$), 138.2 (s, 2 C, *C*$_6$H$_2$), 176.9 (s, 1 C, *C*=S). IR data: 3016 (w), 2971 (w), 2912 (w), 2852 (w), 1600 (m), 1501 (vs), 1480 (m), 1459 (m), 1436 (w), 1413 (m), 1378 (m), 1322 (s), 1308 (m), 1276 (vs), 1226 (w), 1189 (w), 1191 (w), 1031 (m), 972 (w), 936 (w), 863 (m), 848 (s), 737 (w). Anal. Calc. for $C_{21}H_{26}Br_2HgN_2S$: C, 36.1; H, 3.8; N, 4.0. Found: C, 36.4; H, 3.5; N, 4.0%.

3.22 Synthesis of Hg_2(SIMesS)Br_4

Diethyl ether (8 mL) was added to a mixture of $HgBr_2$ (0.149 g, 0.413 mmol) and SIMesS (0.073 g, 0.216 mmol), resulting in the slow formation of a pale yellow solid and a colorless solution. After stirring the suspension for 24 h, the product was isolated by filtration and dried *in vacuo* for 24 h (0.185 g, 85%). Mp = 202-203 °C. NMR data (in d_6-DMSO): ^{1}H δ 2.24 (s, 12 H, C*H*$_3$), 2.28 (s, 6 H, C*H*$_3$), 4.15 (s, 4 H, C*H*$_2$), 7.03 (s, 4 H, aryl H); ^{13}C δ 17.2 (q, $^1J_{C\text{-}H}$ = 127, 4 C, *C*H$_3$), 20.7 (q, $^1J_{C\text{-}H}$ = 126, 2 C, *C*H$_3$), 48.6 (t, $^1J_{C\text{-}H}$ = 150, 2 C, *C*H$_2$), 129.8 (d, $^1J_{C\text{-}H}$ = 159, 4 C, *C*$_6$H$_2$), 132.7 (s, 2 C, *C*$_6$H$_2$), 136.2 (d, $^2J_{C\text{-}H}$ = 6, 4 C, *C*$_6$H$_2$), 139.0 (d, $^2J_{C\text{-}H}$ = 7, 2 C, *C*$_6$H$_2$), 174.8 (s, 1 C, *C*=S). IR data: 2951 (w), 2916 (w), 2846 (w), 1606 (m), 1525 (s), 1482 (m), 1444 (s), 1377 (m), 1320 (m),

1311 (m), 1279 (vs), 1222 (w), 1196 (w), 1171 (w), 1024 (m), 984 (w), 967 (w), 935 (w), 862 (w), 853 (s), 734 (w), 725 (w). Anal. Calc. for $C_{21}H_{26}Br_4Hg_2N_2S$: C, 23.8; H, 2.5; N, 2.6. Found: C, 24.3; H, 2.5; N, 2.7%.

3.23 Synthesis of (SIMesS)HgI_2

Diethyl ether (8 mL) was added to a mixture of HgI2 (0.240 g, 0.528 mmol) and SIMesS (0.180 g, 0.532 mmol), resulting in the slow formation of a pale yellow solid and a colorless solution. After stirring the suspension for 36 h, the product was isolated by filtration and dried *in vacuo* for 6 h (0.367 g, 88%). Mp = 191-193 °C. NMR data (in d_6-DMSO): ^{1}H δ 2.23 (s, 12 H, C*H*$_3$), 2.36 (s, 6 H, C*H*$_3$), 4.04 (s, 4 H, C*H*$_2$), 6.98 (s, 4 H, aryl H); ^{13}C δ 17.3 (q, $^1J_{C\text{-}H}$ = 126, 4 C, *C*H_3), 20.7 (q, $^1J_{C\text{-}H}$ = 127, 2 C, *C*H_3), 47.8 (t, $^1J_{C\text{-}H}$ = 149, 2 C, *C*H_2), 129.3 (d, $^1J_{C\text{-}H}$ = 157, 4 C, *C*$_6H_2$), 134.0 (s, 2 C, *C*$_6H_2$), 136.2 (s, 4 C, *C*$_6H_2$), 137.9 (s, 2 C, *C*$_6H_2$), 177.7 (s, 1 C, *C*=S). IR data: 2975 (w), 2899 (w), 1604 (m), 1499 (s), 1479 (m), 1458 (m), 1435 (w), 1409 (m), 1374 (m), 1308 (s), 1274 (vs), 1218 (w), 1192 (w), 1027 (m), 971 (w), 935 (w), 879 (w), 858 (w), 846 (s), 734 (w). Anal. Calc. for $C_{21}H_{26}HgI_2N_2S$: C, 31.8; H, 3.3; N, 3.5. Found: C, 31.9; H, 3.3; N, 3.5%.

3.24 Synthesis of Hg_2(SIMesS)I_4

Diethyl ether (8 mL) was added to a mixture of HgI_2 (0.190 g, 0.418 mmol) and SIMesS (0.071 g, 0.210 mmol), resulting in the slow formation of a bright yellow solid and a colorless solution. After stirring the suspension for 28 h, the product was isolated by filtration and dried *in vacuo* for 18 h (0.207 g, 79%). Mp = 190-192 °C. NMR data (in d_6-DMSO): ^{1}H δ 2.24 (s, 12 H, C*H*$_3$), 2.27 (s, 6 H, C*H*$_3$), 4.12 (s, 4 H, C*H*$_2$), 7.01 (s, 4 H, aryl H); ^{13}C δ 17.4 (q, $^1J_{C\text{-}H}$ = 128, 4 C, *C*H_3), 20.7 (q, $^1J_{C\text{-}H}$ = 126, 2 C, *C*H_3), 48.4

(t, $^{1}J_{C-H}$ = 149, 2 C, *C*H_2), 129.8 (d, $^{1}J_{C-H}$ = 155, 4 C, *C*$_6H_2$), 133.0 (s, 2 C, *C*$_6H_2$), 136.1 (d, $^{2}J_{C-H}$ = 5, 4 C, *C*$_6H_2$), 138.6 (d, $^{2}J_{C-H}$ = 6, 2 C, *C*$_6H_2$), 175.8 (s, 1 C, *C*=S). IR data: 2938 (w), 2910 (w), 2846 (w), 1605 (m), 1522 (vs), 1480 (m), 1442 (s), 1385 (w), 1376 (m), 1318 (m), 1308 (w), 1279 (vs), 1220 (w), 1194 (w), 1171 (w), 1157 (w), 1018 (m), 983 (w), 965 (w), 934 (m), 861 (w), 853 (s), 819 (w), 734 (w), 726 (w). Anal. Calc. for $C_{21}H_{26}Hg_2I_4N_2S$: C, 20.2; H, 2.1; N, 2.3. Found: C, 19.9; H, 2.1; N, 2.2%.

3.25 Synthesis of (SIMesSe)HgCl$_2$

Diethyl ether (10 mL) was added to a mixture of $HgCl_2$ (0.054 g, 0.199 mmol) and SIMesSe (0.081 g, 0.210 mmol), resulting in the formation of a white solid and a colorless solution. After stirring the suspension for 26 h, the product was isolated by filtration and dried *in vacuo* for 16 h (0.100 g, 76%). Mp = 132-135 °C. NMR data (in d$_6$-DMSO): ^{1}H δ 2.24 (s, 12 H, C*H*$_3$), 2.25 (s, 6 H, C*H*$_3$), 4.19 (s, 4 H, C*H*$_2$), 7.03 (s, 4 H, aryl H); ^{13}C δ 17.3 (q, $^{1}J_{C-H}$ = 129, 4 C, *C*H_3), 20.7 (q, $^{1}J_{C-H}$ = 128, 2 C, *C*H_3), 49.8 (t, $^{1}J_{C-H}$ = 150, 2 C, *C*H_2), 130.1 (d, $^{1}J_{C-H}$ = 159, 4 C, *C*$_6H_2$), 132.8 (s, 2 C, *C*$_6H_2$), 135.8 (s, 4 C, *C*$_6H_2$), 139.4 (s, 2 C, *C*$_6H_2$), 172.0 (s, 1 C, *C*=Se). IR data: 2949 (w), 2914 (w), 2853 (w), 1607 (m), 1516 (s), 1481 (m), 1438 (m), 1418 (w), 1379 (m), 1303 (s), 1280 (vs), 1189 (w), 1030 (m), 985 (w), 926 (w), 899 (w), 853 (s), 737 (w). Anal. Calc. for $C_{21}H_{26}Cl_2HgN_2Se$: C, 38.4; H, 4.0; N, 4.3. Found: C, 37.9; H, 3.8; N, 4.3%.

3.26 Synthesis of (SIMesSe)HgBr$_2$

Diethyl ether (10 mL) was added to a mixture of HgBr2 (0.046 g, 0.128 mmol) and SIMesSe (0.051 g, 0.132 mmol), resulting in the formation of a white solid in a colorless solution. After stirring the suspension for 26 h, the product was isolated by filtration and dried *in vacuo* for 16 h (0.080 g, 84%). Mp = 270-274 °C (dec.). NMR

data (in d_6-DMSO): ^{1}H δ 2.24 (s, 18 H, C*H*$_3$), 4.19 (s, 4 H, C*H*$_2$), 7.02 (s, 4 H, aryl H); ^{13}C δ 17.4 (q, $^1J_{C-H}$ = 127, 4 C, *C*H$_3$), 20.7 (q, $^1J_{C-H}$ = 127, 2 C, *C*H$_3$), 49.9 (t, $^1J_{C-H}$ = 150, 2 C, *C*H$_2$), 130.1 (d, $^1J_{C-H}$ = 157, 4 C, *C*$_6$H$_2$), 132.7 (s, 2 C, *C*$_6$H$_2$), 135.8 (s, 4 C, *C*$_6$H$_2$), 139.4 (s, 2 C, *C*$_6$H$_2$), 172.0 (s, 1 C, *C*=Se). IR data: 2947 (w), 2915 (w), 2853 (w), 1605 (m), 1510 (vs), 1484 (m), 1462 (w), 1438 (w), 1415 (w), 1380 (m), 1303 (s), 1277 (vs), 1188 (w), 1031 (w), 1017 (m), 981 (w), 927 (w), 861 (m), 848 (s), 735 (w). Anal. Calc. for $C_{21}H_{26}Br_2HgN_2Se$: C, 33.8; H, 3.5; N, 3.8. Found: C, 33.8; H, 3.6; N, 3.8%.

3.27 Synthesis of (SIMesSe)HgI$_2$

Diethyl ether (10 mL) was added to a mixture of HgI_2 (0.043 g, 0.095 mmol) and SIMesSe (0.039 g, 0.101 mmol), resulting in the formation of a pale yellow solid and a colorless solution. After stirring the suspension for 26 h, the product was isolated by filtration and dried *in vacuo* for 16 h (0.062 g, 79%). Mp = 221-222 °C (dec.). NMR data (in d_6-DMSO): ^{1}H δ 2.25 (s, 18 H, C*H*$_3$), 4.18 (s, 4 H, C*H*$_2$), 7.02 (s, 4 H, aryl H); ^{13}C δ 17.6 (q, $^1J_{C-H}$ = 127, 4 C, *C*H$_3$), 20.8 (q, $^1J_{C-H}$ = 123, 2 C, *C*H$_3$), 49.8 (t, $^1J_{C-H}$ = 152, 2 C, *C*H$_2$), 130.2 (d, $^1J_{C-H}$ = 163, 4 C, *C*$_6$H$_2$), 133.1 (s, 2 C, *C*$_6$H$_2$), 135.7 (s, 4 C, *C*$_6$H$_2$), 139.2 (s, 2 C, *C*$_6$H$_2$), 172.9 (s, 1 C, *C*=Se). IR data: 2950 (w), 2914 (w), 2846 (w), 1606 (m), 1507 (s), 1479 (m), 1458 (w), 1437 (w), 1414 (w), 1375 (m), 1301 (s), 1277 (vs), 1218 (w), 1192 (w), 1167 (w), 1094 (w), 1028 (m), 1016 (m), 979 (w), 925 (w), 855 (w), 846 (s), 734 (w). Anal. Calc. for $C_{21}H_{26}HgI_2N_2Se$: C, 30.0; H, 3.1; N, 3.3. Found: C, 30.1; H, 3.3; N, 3.4%.

3.28 Synthesis of (SIDippS)HgCl$_2$

Diethyl ether (10 mL) was added to a mixture of $HgCl_2$ (0.070 g, 0.258 mmol) and SIDippS (0.108 g, 0.256 mmol), resulting in the slow formation of a white solid and

a colorless solution. After stirring the suspension for 20 h, the product was isolated by filtration and dried *in vacuo* for 2 h (0.134 g, 75%). Mp = 250-253 °C. NMR data (in d_6-DMSO): ^{1}H δ 1.24 (d, $^3J_{H-H}$ = 6.9, 12 H, C*H*$_3$), 1.27 (d, $^3J_{H-H}$ = 6.9, 12 H, C*H*$_3$), 3.02 (septet, $^3J_{H-H}$ = 6.9, 4 H, C*H*), 4.03 (s, 4 H, C*H*$_2$), 7.24-7.41 (m, 6 H, C$_6$*H*$_3$); ^{13}C δ 24.2 (q, $^1J_{C-H}$ = 126, 8 C, *C*H$_3$), 28.4 (d, $^1J_{C-H}$ = 126, 4 C, *C*H), 50.5 (t, $^1J_{C-H}$ = 147, 2 C, *C*H$_2$), 124.3 (d, $^1J_{C-H}$ = 158, 4 C, C$_m$ in C$_6$H$_3$), 129.2 (d, $^1J_{C-H}$ = 160, 2 C, C$_p$ in *C*$_6$H$_3$), 134.4 (s, 2 C, C$_{ipso}$ in *C*$_6$H$_3$), 147.0 (s, 4 C, C$_o$ in *C*$_6$H$_3$), 182.4 (s, 1 C, *C*=S). IR data: 2962 (m), 2927 (w), 2868 (w), 1589 (w), 1508 (s), 1463 (s), 1426 (s), 1386 (w), 1364 (w), 1343 (m), 1313 (m), 1300 (m), 1282 (s), 1223 (w), 1200 (w), 1186 (w), 1107 (w), 1057 (m), 1027 (w), 966 (w), 935 (w), 809 (vs), 761 (s), 729 (w), 708 (w). Anal. Calc. for $C_{27}H_{38}Cl_2HgN_2S$: C, 46.7; H, 5.5; N, 4.0. Found: C, 46.7; H, 5.6; N, 4.1%.

3.29 Synthesis of (SIDippS)HgBr$_2$

Ethanol (10 mL) was added to a mixture of $HgBr_2$ (0.082 g, 0.228 mmol) and SIDippS (0.102 g, 0.241 mmol), resulting in the slow formation of a white solid and a colorless solution. After stirring for 20 h, the suspension was concentrated under reduced pressure to ca. 1 mL and the product was isolated by filtration and dried *in vacuo* for 3 h (0.135 g, 76%). Mp = 249-252 °C. NMR data (in d_6-DMSO): ^{1}H δ 1.24 (d, $^3J_{H-H}$ = 6.9, 12 H, C*H*$_3$), 1.27 (d, $^3J_{H-H}$ = 6.9, 12 H, C*H*$_3$), 3.01 (septet, $^3J_{H-H}$ = 6.9, 4 H, C*H*), 4.04 (s, 4 H, C*H*$_2$), 7.25-7.43 (m, 6 H, C$_6$*H*$_3$); ^{13}C δ 24.2 (q, $^1J_{C-H}$ = 126, 8 C, *C*H$_3$), 28.4 (d, $^1J_{C-H}$ = 127, 4 C, *C*H), 50.5 (t, $^1J_{C-H}$ = 148, 2 C, *C*H$_2$), 124.3 (d, $^1J_{C-H}$ = 157, 4 C, C$_m$ in *C*$_6$H$_3$), 129.3 (d, $^1J_{C-H}$ = 160, 2 C, C$_p$ in *C*$_6$H$_3$), 134.3 (s, 2 C, C$_{ipso}$ in *C*$_6$H$_3$), 147.0 (s, 4 C, C$_o$ in *C*$_6$H$_3$), 181.6 (s, 1 C, *C*=S). IR data: 2960 (m), 2925 (w), 2867 (w), 1589 (w), 1506 (s), 1461 (s), 1424 (s), 1386 (w), 1364 (w), 1342 (m), 1311 (m), 1299 (m), 1282 (s), 1199

(w), 1186 (w), 1107 (w), 1056 (m), 1027 (w), 990 (w), 966 (w), 935 (w), 808 (vs), 760 (s), 730 (w), 708 (w). Anal. Calc. for $C_{27}H_{38}Br_2HgN_2S$: C, 41.4; H, 4.9; N, 3.6. Found: C, 41.4; H, 5.0; N, 3.6%.

3.30 Synthesis of (SIDippS)HgI_2

Ethanol (10 mL) was added to a mixture of HgI_2 (0.083 g, 0.182 mmol) and SIDippS (0.081 g, 0.192 mmol), resulting in the slow formation of a pale yellow solid and a colorless solution. After stirring for 24 h, the suspension was concentrated under reduced pressure to ca. 1 mL and the product was isolated by filtration and dried *in vacuo* for 24 h (0.084 g, 53%). Mp = 221-223 °C (dec.). NMR data (in d_6-DMSO): ^{1}H δ 1.23 (d, $^3J_{H-H}$ = 6.7, 12 H, C*H*$_3$), 1.27 (d, $^3J_{H-H}$ = 6.9, 12 H, C*H*$_3$), 3.03 (septet, $^3J_{H-H}$ = 6.8, 4 H, C*H*), 4.01 (s, 4 H, C*H*$_2$), 7.22-7.40 (m, 6 H, C$_6$*H*$_3$); ^{13}C δ 24.2 (q, $^1J_{C-H}$ = 126, 8 C, *C*H$_3$), 28.4 (d, $^1J_{C-H}$ = 127, 4 C, *C*H), 50.2 (t, $^1J_{C-H}$ = 147, 2 C, *C*H$_2$), 124.0 (d, $^1J_{C-H}$ = 157, 4 C, C_m in *C*$_6$H$_3$), 128.9 (d, $^1J_{C-H}$ = 160, 2 C, C_p in *C*$_6$H$_3$), 134.8 (s, 2 C, C_{ipso} in *C*$_6$H$_3$), 147.0 (s, 4 C, C_o in C$_6$H$_3$), 182.8 (s, 1 C, *C*=S). IR data: 3033 (w), 2957 (m), 2920 (m), 2866 (w), 1611 (w), 1487 (s), 1438 (w), 1422 (s), 1401 (m), 1328 (m), 1304 (s), 1268 (vs), 1183 (w), 1098 (w), 1057 (m), 1032 (m), 978 (w), 964 (w), 935 (w), 901 (m), 873 (m), 854 (m), 803 (m), 758 (m), 730 (w), 708 (w). Anal. Calc. for $C_{27}H_{38}HgI_2N_2S$: C, 37.0; H, 4.4; N, 3.2. Found: C, 37.1; H, 4.4; N, 3.2%.

3.31 Synthesis of (SIDippSe)$HgCl_2$

Diethyl ether (10 mL) was added to a mixture of HgCl2 (0.056 g, 0.206 mmol) and SIDippSe (0.099 g, 0.211 mmol), resulting in the slow formation of a white solid and a colorless solution. After stirring the suspension for 20 h, the product was isolated by filtration and dried *in vacuo* for 24 h (0.097 g, 64%). Mp = 282-285 °C (dec.). NMR

data (in d_6-DMSO): ^{1}H δ 1.28 (d, $^3J_{H-H}$ = 6.9, 12 H, *C*H_3), 1.31 (d, $^3J_{H-H}$ = 6.9, 12 H, C*H*$_3$), 2.97 (septet, $^3J_{H-H}$ = 6.8, 4 H, C*H*), 4.19 (s, 4 H, CH_2), 7.32-7.51 (m, 6 H, C_6H_3); ^{13}C δ 24.1 (q, $^1J_{C-H}$ = 126, 4 C, *C*H3), 24.6 (q, $^1J_{C-H}$ = 126, 4 C, *C*H_3), 28.5 (d, $^1J_{C-H}$ = 126, 4 C, *C*H), 52.3 (t, $^1J_{C-H}$ = 150, 2 C, *C*H_2), 125.0 (d, $^1J_{C-H}$ = 159, 4 C, C_m in *C*$_6$H$_3$), 130.3 (d, $^1J_{C-H}$ = 161, 2 C, C_p in *C*$_6$H$_3$), 133.5 (s, 2 C, C_{ipso} in C_6H_3), 146.4 (s, 4 C, C_o in *C*$_6$H$_3$), 176.8 (s, 1 C, *C*=Se). IR data: 2963 (m), 2925 (w), 2867 (w), 1589 (w), 1516 (s), 1489 (w), 1464 (m), 1442 (w), 1427 (m), 1386 (w), 1364 (w), 1339 (w), 1321 (w), 1307 (w), 1298 (w), 1283 (s), 1225 (w), 1197 (m), 1186 (w), 1149 (w), 1105 (w), 1057 (m), 1021 (w), 989 (w), 935 (w), 809 (vs), 761 (m), 729 (w), 708 (w). Anal. Calc. for $C_{27}H_{38}Cl_2HgN_2Se$: C, 43.8; H, 5.2; N, 3.8. Found: C, 43.9; H, 5.2; N, 3.8%.

3.32 Synthesis of (SIDippSe)HgBr$_2$

Diethyl ether (10 mL) was added to a mixture of $HgBr_2$ (0.069 g, 0.191 mmol) and SIDippSe (0.092 g, 0.196 mmol), resulting in the slow formation of a white solid and a colorless solution. After stirring the suspension for 20 h, the product was isolated by filtration and dried *in vacuo* for 24 h (0.107 g, 67%). Mp = 286-289 °C (dec.). NMR data (in d_6-DMSO): ^{1}H δ 1.28 (d, $^3J_{H-H}$ = 6.9, 12 H, C*H*$_3$), 1.31 (d, $^3J_{H-H}$ = 6.9, 12 H, C*H*$_3$), 3.00 (septet, $^3J_{H-H}$ = 6.8, 4 H, C*H*), 4.17 (s, 4 H, CH_2), 7.31-7.50 (m, 6 H, C_6H_3); ^{13}C δ 24.2 (q, $^1J_{C-H}$ = 126, 4 C, *C*H_3), 24.6 (q, $^1J_{C-H}$ = 126, 4 C, *C*H_3), 28.5 (d, $^1J_{C-H}$ = 127, 4 C, *C*H), 52.2 (t, $^1J_{C-H}$ = 151, 2 C, *C*H_2), 125.0 (d, $^1J_{C-H}$ = 159, 4 C, C_m in *C*$_6$H$_3$), 130.2 (d, $^1J_{C-H}$ = 161, 2 C, C_p in *C*$_6$H$_3$), 133.7 (s, 2 C, C_{ipso} in *C*$_6$H$_3$), 146.5 (s, 4 C, C_o in *C*$_6$H$_3$), 177.4 (s, 1 C, *C*=Se). IR data: 2961 (m), 2924 (w), 2867 (w), 1590 (w), 1515 (s), 1488 (w), 1463 (m), 1426 (m), 1386 (w), 1364 (w), 1339 (w), 1321 (w), 1306 (w), 1297 (w), 1283 (s), 1225 (w), 1197 (w), 1186 (w), 1106 (w), 1057 (m), 1021 (w), 989 (w), 935 (w),

808 (vs), 759 (m), 729 (w), 710 (w). Anal. Calc. for $C_{27}H_{38}Br_2HgN_2Se$: C, 39.1; H, 4.6; N, 3.4. Found: C, 39.3; H, 4.7; N, 3.2%.

3.33 Synthesis of (SIDippSe)HgI_2

Diethyl ether (10 mL) was added to a mixture of HgI_2 (0.076 g, 0.167 mmol) and SIDippSe (0.080 g, 0.170 mmol), resulting in the slow formation of a pale yellow solid and a colorless solution. After stirring the suspension for 20 h, the product was isolated by filtration and dried *in vacuo* for 24 h (0.106 g, 69%). Mp = 246-249 °C (dec.). NMR data (in d_6-DMSO): ^{1}H δ 1.28 (d, $^3J_{H-H}$ = 7.3, 12 H, C*H*$_3$), 1.30 (d, $^3J_{H-H}$ = 7.3, 12 H, C*H*$_3$), 2.99 (septet, $^3J_{H-H}$ = 6.9, 4 H, C*H*), 4.15 (s, 4 H, C*H*$_2$), 7.30-7.51 (m, 6 H, C$_6$*H*$_3$); ^{13}C δ 24.2 (q, $^1J_{C-H}$ = 126, 4 C, *C*H$_3$), 24.5 (q, $^1J_{C-H}$ = 126, 4 C, *C*H$_3$), 28.5 (d, $^1J_{C-H}$ = 126, 4 C, *C*H), 52.1 (t, $^1J_{C-H}$ = 149, 2 C, *C*H$_2$), 124.9 (d, $^1J_{C-H}$ = 158, 4 C, C$_m$ in *C*$_6$H$_3$), 130.2 (d, $^1J_{C-H}$ = 161, 2 C, C$_p$ in *C*$_6$H$_3$), 133.9 (s, 2 C, C$_{ipso}$ in *C*$_6$H$_3$), 146.5 (s, 4 C, C$_o$ in *C*$_6$H$_3$), 178.1 (s, 1 C, *C*=Se). IR data: 2959 (m), 2923 (w), 2865 (w), 1589 (w), 1509 (s), 1459 (m), 1440 (w), 1422 (s), 1385 (w), 1364 (w), 1338 (w), 1321 (w), 1294 (m), 1281 (s), 1226 (w), 1195 (m), 1186 (m), 1148 (w), 1106 (w), 1055 (m), 1021 (w), 984 (w), 934 (w), 805 (vs), 758 (m), 729 (w), 711 (w). Anal. Calc. for $C_{27}H_{38}HgI_2N_2Se$: C, 35.1; H, 4.2; N, 3.0. Found: C, 35.0; H, 4.1; N, 3.0%.

3.34 Synthesis of (SIXyS)AuCl

Tetrahydrofuran (10 mL) was added to a mixture of (tht)AuCl (0.061 g, 0.190 mmol) and SIXyS (0.061 g, 0.197 mmol), resulting in the slow formation of an white solid and a colorless solution. After stirring the suspension for 24 h, the mixture was concentration under reduced pressure to ca. 2 mL. The white product was precipitated in 15 mL of pentane, isolated by filtration, and dried *in vacuo* for 16 h (0.067 g, 65%). Mp

= 258-263 °C (dec.). NMR data (in $CDCl_3$): ^1H δ 2.35 (s, 12 H, C*H*$_3$), 4.14 (s, 4 H, C*H*$_2$), 7.21-7.37 (m, 6 H, C_6H_3); ^{13}C δ 17.9 (q, $^1J_{C-H}$ = 127, 4 C, *C*H_3), 49.3 (t, $^1J_{C-H}$ = 157, 2 C, *C*H_2), 129.8 (d, $^1J_{C-H}$ = 157, 2 C, *C*$_6H_3$), 130.3 (d, $^1J_{C-H}$ = 161, 4 C, *C*$_6H_3$), 135.2 (s, 2 C, *C*$_6H_3$), 136.4 (s, 4 C, *C*$_6H_3$), 176.9 (s, 1 C, *C*=Se). IR data: 2940 (w), 2910 (w), 2855 (w), 1590 (w), 1510 (s), 1467 (m), 1445 (m), 1413 (m), 1371 (w), 1303 (s), 1283 (vs), 1259 (m), 1214 (w), 1188 (w), 1164 (w), 1095 (m), 1021 (m), 985 (w), 890 (w), 795 (m), 780 (vs), 716 (w). Anal. Calc. for $C_{19}H_{22}AuClN_2S$: C, 42.0; H, 4.1; N, 5.2. Found: C, 42.3; H, 4.3; N, 5.2%.

3.35 Synthesis of (SIXyS)AuBr

Tetrahydrofuran (5 mL) was added to a mixture of (tht)AuBr (0.048 g, 0.130 mmol) and SIXyS (0.047 g, 0.152 mmol), resulting in the slow formation of an white solid and a red solution. After stirring the suspension for 24 h, the mixture was concentration under reduced pressure to ca. 1 mL. The white product was precipitated in a mixture of pentane and ether (10 mL : 5 mL), isolated by filtration, and dried *in vacuo* for 16 h (0.054 g, 71%). Mp = 270-274 °C (dec.). NMR data (in $CDCl_3$): ^1H δ 2.34 (s, 12 H, C*H*$_3$), 4.14 (s, 4 H, C*H*$_2$), 7.20-7.43 (m, 6 H, C_6H_3); ^{13}C δ 17.9 (q, $^1J_{C-H}$ = 127, 4 C, *C*H_3), 49.2 (t, $^1J_{C-H}$ = 147, 2 C, *C*H_2), 129.8 (d, $^1J_{C-H}$ = 161, 2 C, *C*$_6H_3$), 130.3 (d, $^1J_{C-H}$ = 163, 4 C, *C*$_6H_3$), 135.2 (s, 2 C, *C*$_6H_3$), 136.4 (s, 4 C, *C*$_6H_3$), 176.8 (s, 1 C, *C*=S). IR data: 2921 (w), 2860 (w), 1591 (w), 1509 (s), 1462 (m), 1440 (m), 1416 (m), 1374 (w), 1318 (s), 1282 (vs), 1260 (m), 1210 (w), 1191 (w), 1167 (w), 1098 (m), 1029 (m), 776 (vs), 721 (w). Anal. Calc. for $C_{19}H_{22}AuBrN_2S$: C, 38.9; H, 3.8; N, 4.8. Found: C, 38.9; H, 3.8; N, 4.8%.

3.36 Synthesis of (SIMesS)AuCl

Tetrahydrofuran (15 mL) was added to a mixture of (tht)AuCl (0.099 g, 0.309 mmol) and SIMesS (0.119 g, 0.351 mmol), resulting in the slow formation of an white solid and a colorless solution. After stirring the suspension for 24 h, the mixture was concentration under reduced pressure to *ca.* 2 mL. The white product was precipitated in a mixture of pentane and ether (10 mL : 10 mL), isolated by filtration, and dried *in vacuo* for 1 h (0.156 g, 88%). Mp = 268-272 °C (dec.). NMR data (in $CDCl_3$): ^{1}H δ 2.28 (s, 12 H, C*H*$_3$), 2.36 (s, 6 H, C*H*$_3$), 4.10 (s, 4 H, C*H*$_2$), 7.03 (s, 4 H, C_6H_2); ^{13}C δ 17.8 (q, $^1J_{C\text{-}H}$ = 124, 4 C, *C*H$_3$), 21.4 (q, $^1J_{C\text{-}H}$ = 124, 2 C, *C*H$_3$), 49.2 (t, $^1J_{C\text{-}H}$ = 147, 2 C, *C*H$_2$), 130.4 (d, $^1J_{C\text{-}H}$ = 158, 4 C, *C*$_6$H$_2$), 132.54 (s, 2 C, *C*$_6$H$_2$), 135.9 (s, 4 C, *C*$_6$H$_2$), 140.6 (s, 2 C, *C*$_6$H$_2$), 176.5 (s, 1 C, *C*=S). IR data: 2917 (w), 2856 (w), 1609 (m), 1505 (s), 1479 (m), 1457 (m), 1413 (s), 1374 (w), 1321 (s), 1305 (m), 1275 (vs), 1221 (w), 1191 (w), 1131 (w), 1030 (m), 970 (w), 934 (w), 864 (m), 843 (w), 736 (w). Anal. Calc. for $C_{21}H_{26}AuClN_2S$: C, 44.2; H, 4.6; N, 4.9. Found: C, 43.9; H, 4.5; N, 4.9%.

3.37 Synthesis of (SIMesS)AuBr

Tetrahydrofuran (10 mL) was added to a mixture of (tht)AuBr (0.072 g, 0.198 mmol) and SIMesS (0.068 g, 0.202 mmol), resulting in the slow formation of an white solid and a colorless solution. After stirring the suspension for 24 h, the mixture was concentration under reduced pressure to *ca.* 2 mL. The white product was precipitated in ether (10 mL), isolated by filtration, and dried *in vacuo* for 16 h (0.094 g, 77%). Mp = 278-281 °C (dec.). NMR data (in $CDCl_3$): ^{1}H δ 2.28 (s, 12 H, C*H*$_3$), 2.37 (s, 6 H, C*H*$_3$), 4.10 (s, 4 H, C*H*$_2$), 7.03 (s, 4 H, C$_6$*H*$_2$); ^{13}C δ 17.8 (q, $^1J_{C\text{-}H}$ = 127, 4 C, *C*H$_3$), 21.4 (q, $^1J_{C\text{-}H}$ = 127, 2 C, *C*H$_3$), 49.2 (t, $^1J_{C\text{-}H}$ = 148, 2 C, *C*H$_2$), 130.5 (d, $^1J_{C\text{-}H}$ = 158, 4 C, C_6H_2),

132.6 (s, 2 C, *C*$_6$H$_2$), 135.9 (s, 4 C, *C*$_6$H$_2$), 140.6 (s, 2 C, *C*$_6$H$_2$), 176.7 (s, 1 C, *C*=S). IR data: 2953 (w), 2916 (w), 2856 (w), 1609 (m), 1503 (s), 1479 (m), 1455 (m), 1415 (w), 1374 (m), 1321 (m), 1305 (m), 1275 (vs), 1220 (w), 1190 (w), 1099 (w), 1030 (m), 970 (w), 934 (w), 862 (m), 844 (w), 816 (w), 736 (w). Anal. Calc. for $C_{21}H_{26}AuBrN_2S$: C, 40.9; H, 4.3; N, 4.6. Found: C, 40.9; H, 4.2; N, 4.5%.

3.38 Synthesis of (SIDippS)AuCl

Tetrahydrofuran (10 mL) was added to a mixture of (tht)AuCl (0.080 g, 0.250 mmol) and SIDippS (0.109 g, 0.258 mmol), resulting in the slow formation of a white solid and a colorless solution. After stirring for 25 h, the suspension was concentrated under reduced pressure to *ca.* 1 mL and the product was isolated by filtration and dried *in vacuo* for 24 h (0.115 g, 70%). Mp = 293-296 °C (dec.). NMR data (in $CDCl_3$): ^{1}H δ 1.32 (d, $^3J_{H-H}$ = 6.9, 12 H, C*H*$_3$), 1.41 (d, $^3J_{H-H}$ = 6.7, 12 H, C*H*$_3$), 2.90 (septet, $^3J_{H-H}$ = 6.9, 4 H, C*H*), 4.14 (s, 4 H, C*H*$_2$), 7.28-7.55 (m, 6 H, C$_6$*H*$_3$); ^{13}C δ 24.5 (q, $^1J_{C-H}$ = 127, 4 C, *C*H$_3$), 25.1 (q, $^1J_{C-H}$ = 127, 4 C, *C*H$_3$), 29.4 (d, $^1J_{C-H}$ = 130, 4 C, *C*H), 51.9 (t, $^1J_{C-H}$ = 147, 2 C, *C*H$_2$), 125.5 (d, $^1J_{C-H}$ = 157, 4 C, C_m in C_6H_3), 131.1 (d, $^1J_{C-H}$ = 159, 2 C, C_p in C_6H_3), 132.7 (s, 2 C, C_{ipso} in C_6H_3), 146.8 (s, 4 C, C_o in C_6H_3), 179.4 (s, 1 C, *C*=S). IR data: 2859 (m), 2924 (w), 2866 (w), 1590 (w), 1490 (s), 1459 (s), 1416 (s), 1384 (w), 1364 (w), 1341 (m), 1321 (w), 1298 (m), 1274 (s), 1179 (m), 1149 (w), 1100 (w), 1051 (m), 1028 (w), 967 (w), 935 (m), 908 (w), 803 (vs), 765 (m), 755 (m), 730 (w), 709 (w). Anal. Calc. for $C_{27}H_{38}AuClN_2S$: C, 49.5; H, 5.9; N, 4.3. Found: C, 49.6; H, 5.9; N, 4.2%.

3.39 Synthesis of (SIDippS)AuBr

Tetrahydrofuran (10 mL) was added to a mixture of (tht)AuBr (0.077 g, 0.211 mmol) and SIDippS (0.091 g, 0.215 mmol), resulting in the slow formation of an off-white solid and a red solution. After stirring for 24 h, the suspension was concentrated under reduced pressure to *ca.* 1 mL and the product was isolated by filtration and dried *in vacuo* for 24 h (0.052 g, 35%). Mp = 302-305 °C (dec.). NMR data (in $CDCl_3$): ^{1}H δ 1.33 (d, $^3J_{H-H}$ = 6.9, 12 H, C*H*$_3$), 1.42 (d, $^3J_{H-H}$ = 6.9, 12 H, C*H*$_3$), 2.91 (septet, $^3J_{H-H}$ = 6.9, 4 H, C*H*), 4.14 (s, 4 H, C*H*$_2$), 7.28-7.56 (m, 6 H, C_6H_3); ^{13}C δ 24.6 (q, $^1J_{C-H}$ = 127, 4 C, *C*H$_3$), 25.1 (q, $^1J_{C-H}$ = 127, 4 C, *C*H$_3$), 29.5 (d, $^1J_{C-H}$ = 127, 4 C, *C*H), 51.9 (t, $^1J_{C-H}$ = 147, 2 C, *C*H$_2$), 125.6 (d, $^1J_{C-H}$ = 158, 4 C, C_m in C_6H_3), 131.1 (d, $^1J_{C-H}$ = 160, 2 C, C_p in C_6H_3), 132.7 (s, 2 C, C_{ipso} in C_6H_3), 146.8 (s, 4 C, C_o in C_6H_3), 179.7 (s, 1 C, *C*=S). IR data: 2963 (m), 2923 (w), 2890 (w), 1590 (w), 1541 (m), 1499 (s), 1460 (s), 1419 (s), 1385 (w), 1346 (w), 1324 (s), 1303 (vs), 1281 (s), 1210 (w), 1187 (w), 1103 (w), 1078 (w), 1056 (w), 996 (w), 937 (w), 801 (s), 769 (w), 757 (m), 709 (w), 668 (w). Anal. Calc. for $C_{27}H_{38}AuBrN_2S$: C, 46.4; H, 5.5; N, 4.0. Found: C, 46.5; H, 5.6; N, 4.1%.

CHAPTER 4: CONCLUSIONS

4.1 Conclusions

The facile synthesis of SIArE ligands has been accomplished using different routes than previously published to achieve reasonable yields. Using this synthesis the new ligand SIXySe was synthesized as well. It was also shown that these ligands resist oxidation by forming adducts with iodine, indicating donation, but not ionization. Beyond this, the coordination chemistry of heterocyclic sulfur- and selenium- containing compounds with saturated five-membered rings was explored with closed-shell (d^{10}) metal ions such as mercury(II) and gold(I).

These ligands were found to favor formation of metal complexes that have good stability in open air and in solution. The bonding is consistently monodentate and favors C-E-M bond angles of about 109-112°. It was found that the higher Lewis acidity of the electrophile, e.g. mercury(II) *vs.* gold(I), the more donation from the chalcogen to the metal center. This can be seen when the ^{13}C NMR chemical shift of the free ligands chalcogenone carbon resonance is compared to those of the corresponding gold(I) and mercury(II) complexes (Figure 4.1). The more charged the metal ion is the more the molecule will donate electron density from the nitrogen atoms into the chalcogenone carbon, increasing the shielding seen in NMR spectra. This donation is obviously important for the analogues NHC ligands, but in these ligands there has been little discussion in literature about the bonding between NHT and NHSe and metal ions.

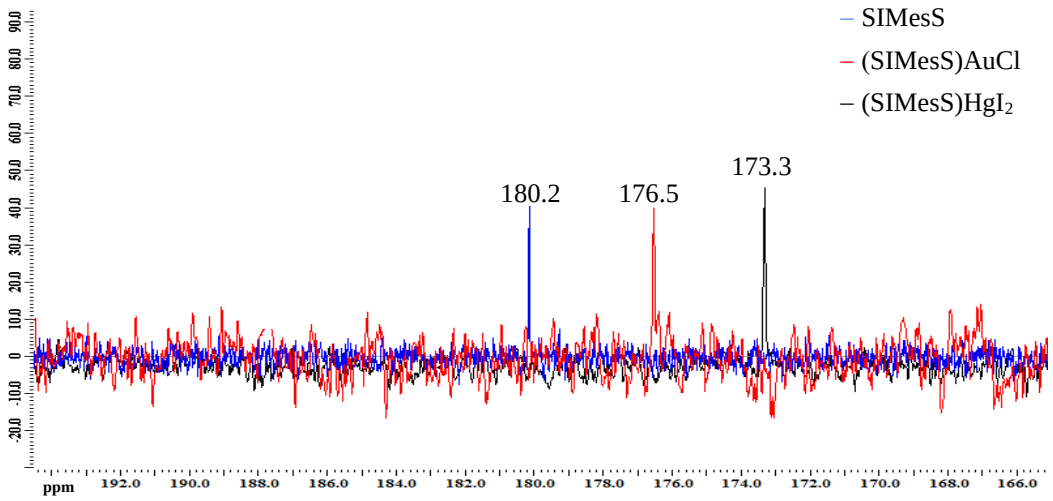

Figure 4.1: ^{13}C NMR spectra of SIMesS (*C*=S) and its complexes in $CDCl_3$.

In similar fashion to the complexes the iodine adducts also exhibit the *C*=E carbon peak shift of about 7-10 ppm upfield in their ^{13}C NMR spectra, compared to the free ligand, similar to the mercury(II) complexes (Figure 4.1). This variable interaction is in part due to the support of the nitrogen lone pairs of the NHC, but it is unclear if some sort of back donation occurs, as in the iodine compounds there is no orthogonal virtual orbital for the chalcogen to donate into. Figure 4.2 shows the theoretical bonding allowed for the NHT and NHSe ligands. This kind of donation is similar to other ligands, but these SIArE ligands are far more robust than free NHCs or most phosphines.

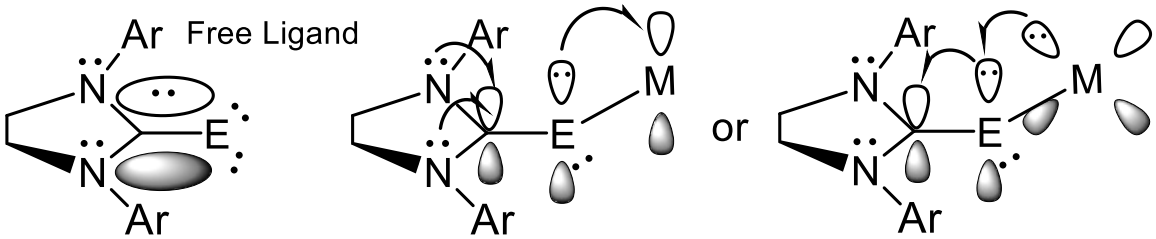

Figure 4.2: Bonding in SIArE ligands and its metal complexes.

Presented data clearly shows these Lewis bases encumbering the metal ions. Most of the mercury(II) and gold(I) structures are mononuclear. Even the few dimeric structures are most likely byproducts of solidification. In general, metal to chalcogen bonds are stronger when compared to small NHT or NHSe ligands, as discussed in Chapter 2, and strongest for the SIDippE complexes. The bonding angle of nearly 109° for C-E-M (M=metal) is common for all the metal complexes and E-M bonds range from 2.4 to 2.5 Å. This close bonding stabilization is enhanced by the steric shielding, observed by close aromatic to metal ion distances in the solid state data for many of the metal complexes. The iodine compounds lack comparable solid-state bond lengths, but do show similar bonding angles, but have more of an out of plane bonding angle, most likely due to electron repulsion of the iodine atom from the aromatic group.

NHT and NHSe ligands improve upon NHC ligands as the chalcogen allows for better orbital overlap to softer metal ions, while the bonding angle imparts good steric protection as seen in the SolidG comparison of SIArE *vs.* other common ligands. This is an important factor since the most important classic catalysis reactions involving carbon-carbon bond formation tend to use soft heavy metals. This fact coupled with the steric protection imparted by the bulky aromatic substituents affords stable complexes with SIArE ligands as well as solubility properties that the metal alone would not have. These six ligands are air-stable, exhibit good solubility in a variety of organic solvents, and readily form stable metal complexes. These factors make SIArE ligands of interest to progressing the field of coordination chemistry by, potentially, affording low-valent low oxidation state heavy metal complexes with good solubility in common solvents for reactivity applications.

4.2 Future Work

Like many other new ligands the SIArE ligands first need to be explored on a synthetic basis. The synthesis conceived in this work gives a direct route to a number of different aromatic groups or backbones. While expanding the backbone of a heterocycle has been done for NHC ligands, finding rings larger than six-membered become too unstable, this has not been investigated properly for NHT or NHSe systems.[90] One may envision any number of aromatic substituted primary amines that could afford formamidines with which to create the heterocycle, with examples shown in Figure 4.3. Using this fact a number of NHT or NHSe ligands designed for applications could be developed. Within literature very few variations of the SIArE ligands exist, as discussed in Chapter 1, but the scope of possible SIArE variants is unbounded. As these ligands already find use in biology, Figure 4.3 shows two examples of NHT or NHSe ligands functionalized for metallodrugs by containing nitro groups for better water solubility or naphthalene substituents for potentially imaging of the drug in the cell. In further efforts to stabilize metal ions, the use of pyridine N-substituted NHT or NHSe ligands could afford mixed donor atom ligands suitable for open-shell metal ions (Figure 4.3).

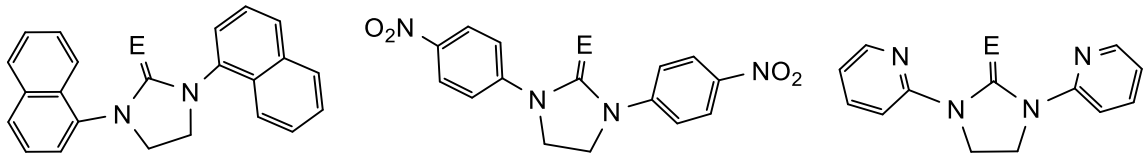

Figure 4.3: Plausible synthetically accessible NHT or NHSe ligands.

As for NHT or NHSe metal complexes, multiple groups have reported the utility of gold(I) complexes featuring NHT or NHSe ligands. Nolan, after inspiration from Ganter, isolated the first examples of NHSe gold(I) complexes.[51] This work determined the donation of the donor atom to the metal occurred in solution and was quantifiable by

analyzing the ^{77}Se chemical shift of the free ligands *vs.* the gold(I) complex, as previously discussed in Chapter 2.[51] Yang *et al.* investigated the use of similar gold complexes with bulky NHT ligands for catalyzing cyclization reactions, due to air stability highlighted by the researchers. They found these gold(I) complexes to be viable catalysts with very low loading in open air reactions resulting in high yields and shorter reaction times.[56] It is clearly evident that these ligands have useful properties for many kinds of homogenous catalysis; further investigation would be of use to the field.

A more biological use of these kinds of gold(I) NHT complexes was published by the Che group, as shown in Figure 4.4.[57] They found that p-methoxyphenyl functionalized variants of SIArS ligands were effective at killing a panel of different cancer cell lines, including the standard HeLa cells. Specifically Che *et al.* found that the SIArE gold(I) complex was particularly potent for more complex cancer cells, requiring about less concentration of the metallodrug to achieve similar results as cisplatin.

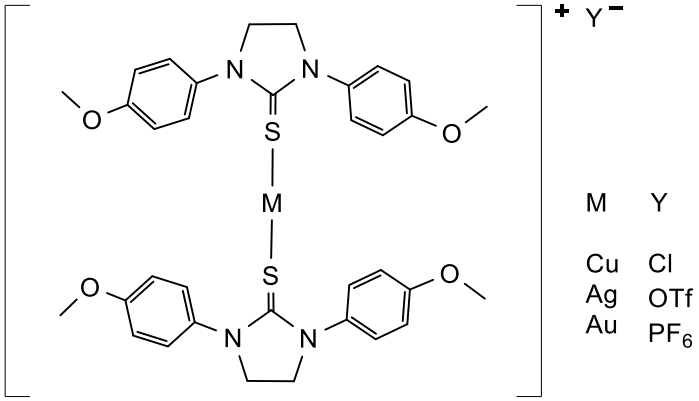

Figure 4.4: Relevant antitumor complexes from Che and coworkers.

The researchers believe the higher reactivity of this metallodrug is due to the non-reversible binding of soft donors that maintain the redox mechanisms within the cell, effectively inhibiting the enzymes necessary for control. One set of enzymes potentially

responsible for the apoptosis after inoculation with the NHT complexes are thioredoxin reductases, which are responsible for regulating redox signaling within the cell by reducing thioredoxin.[91] Almost all living organisms are known to contain this small thioredoxin protein. These medicinal applications were considered and studies are being performed by other researchers within the Rabinovich group, who will utilize the gold complexes shown here for cytotoxicity studies on HeLa cells.

In a different direction of research, gold(I) is an interesting platform for coordination chemistry to occur. The Nolan group investigated NHC gold(I) complexes and found the use of CsOH to impart a hydroxide on the gold center, creating a starting material for numerous possible gold(I) complexes, as shown in Scheme 4.1.[92] From this kind of synthesis platform a numerous variants for specific applications could be synthesized easily, since so many acidic proton containing molecule could be used. This reactivity is due to the high enthalpy of water, a product, meaning these already cytotoxic complex molecules could be equipped with a number of different heteroligands to increase water solubility, stability towards radicals, make them fluorescent, *etc*. Functionalization for use as a molecular drug would be facile and the hydroxy intermediate to the drug might also be air stable, as seen with earlier examples of NHT or NHSe metal complexes, both favorable features of a market drug.

Scheme 4.1: Synthetic Pathway for Gold(I) Hydroxides.

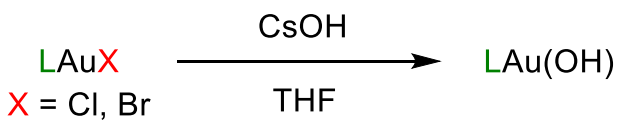

Beyond gold(I) chemistry these ligands have a unique bonding ability as noted previously in this work and in others. Coordination reactivity and studies done with metals other than those having closed-shell (d^{10}) electron configuration should elucidate the extent of the bonding abilities of these ligands. These studies are important especially after a study recently published that has isolated and characterized the first potential examples of protonated NHT and NHSe ligands.[93] This study along with the work presented here shows that these ligands have more elasticity in bonding capabilities than most soft Lewis bases.

SIArE can form stable bonds with a Lewis acid such as a proton to a large soft mercury(II) or gold(I) ion. This is similar to nucleophilic carbenes, which have been coordinated to nearly every metal available.[8] Reactivity towards alkali earth metals, early transition metals, and perhaps evaluation as a Lewis base in organic synthesis routes are pertinent for these NHT and NHSe molecules to assess the various modes of coordination possible. Other research done with palladium is a foundation to analyzing potential homogeneous catalysts that use these stabilizing ligands, especially catalytic pathways that suffer from sensitivity to air or moisture. Research efforts to use these ligands in biological applications are already underway and have been met with some success, future work utilizing them in pharmaceuticals will most likely be forthcoming. These SIArE ligands are particularly modular in their preparation and applications. Coordination chemistry has been developing for nearly 100 years and every time a new molecule is discovered that interacts with metal ions to perform some interesting chemistry it has elevated the field as a whole.

REFERENCES

1. Bourissou, D.; Guerret, O.; Gabbaï, F. P.; Bertrand, G. *Chem. Rev.* **2000,** *100*, 39-92.

2. Hopkinson, M. N.; Richter, C.; Schedler, M.; Glorius, F. *Nature* **2014,** *510*, 485-496.

3. Öfele, K. *J. Organomet. Chem.* **1968,** *12*, P42-P43.

4. Wanzlick, H. W.; Schönherr, H. J. *Angew. Chem. Int. Ed. Engl.* **1968,** *7*, 141-142.

5. Arduengo, A. J.; Harlow, R. L.; Kline, M. *J. Am. Chem. Soc.* **1991,** *113*, 361-363.

6. Herrmann, W. A.; Köcher, C. *Angew. Chem. Int. Ed. Engl.* **1997,** *36*, 2162-2187.

7. Nolan, S. P.; Diez-Gonzalez, S. *Coord. Chem. Rev.* **2007,** *251*, 874–883.

8. Wurtemberger-Pietsch, S.; Radius, U.; Marder, T. B. *Dalton Trans.* **2016,** *45*, 5880-5895.

9. Groom, C. R.; Bruno, I. J.; Lightfoot, M. P.; Ward, S. C. *Acta Cryst.* **2016,** *B72*, 171-179.

10. Alvarado, E.; Badaj, A. C.; Larocque, T. G.; Lavoie, G. G. *Chem. Eur. J.* **2012,** *18*, 12112-12121.

11. Arduengo, A. J.; Burgess, E. M. *J. Am. Chem. Soc.* **1977,** *99*, 2376-2378.

12. Benac, B. L.; Burgess, E. M.; Arduengo, A. J. *Org. Synth.* **1986,** *64*, 92.

13. Huang, J.; Schanz, H.-J.; Stevens, E. D.; Nolan, S. P.; Capps, K. B.; Bauer, A.; Hoff, C. D. *Inorg. Chem.* **2000,** *39*, 1042-1045.

14. Kuhn, N.; Kratz, T. *Synthesis* **1993,** *6*, 561-562.

15. Nelson, D. J.; Nahra, F.; Patrick, S. R.; Cordes, D. B.; Slawin, A. M. Z.; Nolan, S. P. *Organometallics* **2014,** *33*, 3640−3645.

16. Srinivas, K.; Naga Babu, C.; Prabusankar, G. *Dalton Trans.* **2015,** *44*, 15636-15644.

17. Srinivas, K.; Suresh, P.; Babu, C. N.; Sathyanarayana, A.; Prabusankar, G. *RSC Adv.* **2015,** *5*, 15579-15590.

18. Normand, A. T.; Cavell, K. J. *Eur. J. Inorg. Chem.* **2008,** *2008*, 2781-2800.

19. Kantchev, E. A. B.; O'Brien, C. J.; Organ, M. G. *Angew. Chem. Int. Ed.* **2007,** *46*, 2768-2813.

20. Enders, D.; Niemeier, O.; Henseler, A. *Chem. Rev.* **2007,** *107*, 5606-5655.

21. Hickey, J. L.; Ruhayel, R. A.; Barnard, P. J.; Baker, M. V.; Berners-Price, S. J.; Filipovska, A. *J. Am. Chem. Soc.* **2008,** *130*, 12570-12571.

22. Magill, A. M.; Cavell, K. J.; Yates, B. F. *J. Am. Chem. Soc.* **2004,** *126*, 8717-24.

23. Scholl, M.; Ding, S.; Lee, C. W.; Grubbs, R. H. *Org. Lett.* **1999,** *1*, 953-956.

24. Briel, O.; Cazin, C. S. J. N-Heterocyclic Carbene Complexes in Industrial Processes. In *N-Heterocyclic Carbenes in Transition Metal Catalysis and Organocatalysis*, Springer Netherlands: Dordrecht, 2011; pp 315-324.

25. Cortizo-Lacalle, D.; Skabara, P. J.; Westgate, T. D. Chalcogen-Rich Compounds as Electron Donors. In *Handbook of Chalcogen Chemistry: New Perspectives in Sulfur, Selenium and Tellurium (2),* The Royal Society of Chemistry: Cambridge, UK, 2013; Ch. 11.2, Vol. 2, pp 99-126.

26. Ramadan, S. E.; Razak, A. A.; Ragab, A. M.; El-Meleigy, M. *Biol. Trace Elem. Res.* **1989,** *20*, 225.

27. Cunha, R. L. O. R.; Gouvea, I. E.; Juliano, L. *An. Acad. Bras. Ciênc.* **2009,** *81*, 393-407.

28. Gruhlke, M. C.; Slusarenko, A. J. The Cellular 'Thiolstat' as an Emerging Potential Target of Some Plant Secondary Metabolites. In *Recent Advances in Redox Active Plant*

and Microbial Products: From Basic Chemistry to Widespread Applications in Medicine and Agriculture, Springer Netherlands: Dordrecht, 2014; Ch. 5, pp 235-262.

29. Hopkins, F. G. *Biochem. J.* **1928,** *22*, 1341-1348.

30. Mamoru, K.; Hideharu, I. *Curr. Org. Synth.* **2006,** *3*, 439-455.

31. Fringuelli, F.; Marino, G.; Taticchi, A.; Grandolini, G. *J. Chem. Soc., Perkin Trans. 2* **1974**, 332-337.

32. Rong, Y.; Al-Harbi, A.; Kriegel, B.; Parkin, G. *Inorg. Chem.* **2013,** *52*, 7172-7182.

33. Raper, E. S. *Coord. Chem. Rev.* **1985,** *61*, 115-184.

34. Backlund, M.; Ziller, J.; Farmer, P. J. *Inorg. Chem.* **2008,** *47*, 2864-2870.

35. Chen, Y.; Wang, Z.-O.; Ren, Z.-G.; Li, H.-X.; Li, D.-X.; Liu, D.; Zhang, Y.; Lang, J.-P. *Cryst. Growth Des.* **2009,** *9*, 4963-4968.

36. Lewis, J. A.; Puerta, D. T.; Cohen, S. M. *Inorg. Chem.* **2003,** *42*, 7455-7459.

37. Trinajstić, N. *Tetrahedron Lett.* **1968,** *9*, 1529-1532.

38. Weigand, W.; Wunsch, R.; Robl, C.; Mloston, G.; Noth, H.; Schmidt, M. *Z. Naturforsch., B: Chem.Sci.* **2000,** *55*, 453-458.

39. Petzold, H.; Görls, H.; Weigand, W.; Romanski, J.; Mloston, G. *Heteroat. Chem* **2007,** *18*, 584-590.

40. Gosselink, J. W.; Van Koten, G. *Inorg. Chem.* **1981,** *20*, 877-884.

41. Stadelman, B. S.; Brumaghim, J. L. Thione- and Selone-Containing Compounds, Their Late First Row Transition Metal Coordination Chemistry, and Their Biological Potential. In *Biochalcogen Chemistry: The Biological Chemistry of Sulfur, Selenium, and Tellurium*, American Chemical Society: New York, 2013; Ch. 3, pp 33-70.

42. Cooper , D. S. *N. Engl. J. Med.* **2005,** *352*, 905-917.

43. Kaur, M.; Rob, A.; Caton-Williams, J.; Huang, Z. Biochemistry of Nucleic Acids Functionalized with Sulfur, Selenium, and Tellurium: Roles of the Single-Atom Substitution. In *Biochalcogen Chemistry: The Biological Chemistry of Sulfur, Selenium, and Tellurium*, American Chemical Society: New York, 2013; Ch. 5, pp 89-126.

44. Xu, Q.; Heo, C. H.; Kim, G.; Lee, H. W.; Kim, H. M.; Yoon, J. *Angew. Chem. Int. Ed.* **2015,** *54*, 4890-4894.

45. Sabir, S. M.; Salman, S. M.; Rocha, J. B. T. *Environ. Toxicol. Pharmacol.* **2012,** *34*, 446-453.

46. Buhl, H.; Verlinden, K.; Ganter, C.; Novakovic, S. B.; Bogdanovic, G. A. *Eur. J. Inorg. Chem.* **2016,** *2016*, 3389-3395.

47. Verlinden, K.; Buhl, H.; Frank, W.; Ganter, C. *Eur. J. Inorg. Chem.* **2015,** 2416-2425.

48. Vummaleti, S. V. C.; Nelson, D. J.; Poater, A.; Gomez-Suarez, A.; Cordes, D. B.; Slawin, A. M. Z.; Nolan, S. P.; Cavallo, L. *Chem. Sci.* **2015,** *6*, 1895-1904.

49. Matsumura, T.; Nakada, M. *Tetrahedron Lett.* **2014,** *55*, 1412-1415.

50. Chen, W.; Li, R.; Han, B.; Li, B.-J.; Chen, Y.-C.; Wu, Y.; Ding, L.-S.; Yang, D. *Eur. J. Org. Chem.* **2006**, 1177-1184.

51. Nelson, D. J.; Nahra, F.; Patrick, S. R.; Cordes, D. B.; Slawin, A. M. Z.; Nolan, S. P. *Organometallics* **2014,** *33*, 3640-3645.

52. Paas, M.; Wibbeling, B.; Froehlich, R.; Hahn, F. E. *Eur. J. Inorg. Chem.* **2006**, 158-162.

53. Liu, S.; Lei, Y.; Yang, Z.; Lan, Y. *J. Mol. Struct.* **2014,** *1074*, 527-533.

54. Yang, D.; Chen, Y.-C. Preparation of substituted cyclic thioureas as ligands for Heck and Suzuki coupling reaction catalysts. US20050215783A1, 2005.

55. Yang, D.; Chen, Y.-C.; Zhu, N.-Y. *Org. Lett.* **2004,** *6*, 4635.

56. Pan, J.-H.; Yang, M.; Gao, Q.; Zhu, N.-Y.; Yang, D. *Synthesis* **2007**, 2539-2544.

57. Yan, K.; Lok, C.-N.; Bierla, K.; Che, C.-M. *Chem. Commun.* **2010,** *46*, 7691-7693.

58. Arduengo, A. J.; Goerlich, J. R.; Marshall, W. J. *J. Am. Chem. Soc.* **1995,** *117*, 11027-11028.

59. Arduengo, A. J.; Krafczyk, R.; Schmutzler, R. *Tetrahedron* **1999,** *55*, 14523-l 4534.

60. Arduengo, A. J. Preparation of 1,3-disubstituted imidazolium salts. US5077414, 1991.

61. Abrams, M. B.; Scott, B. L.; Baker, R. T. *Organometallics* **2000,** *19*, 4944-4956.

62. Kuhn, K.; Grubbs, R. H. Preparation of saturated imidazolinium salts and related compounds. US7109348, 2011.

63. Meschedef, L.; Limbach, H.-H. *J. Phys. Chem.* **1991,** *95*, 10267-10280.

64. Liske, A.; Verlinden, K.; Buhl, H.; Schaper, K.; Ganter, C. *Organometallics* **2013,** *32*, 5269-5272.

65. Cullen, E. R.; Guziec, F. S.; Murphy, C. J.; Wong, T. C.; Andersen, K. K. *J. Am. Chem. Soc.* **1981,** *103*, 7055-7057.

66. Paas, M.; Wibbeling, B.; Fröhlich, R.; Hahn, F. E. *Eur. J. Inorg. Chem.* **2006,** 158-162.

67. Yang, D.; Chen, Y.-C.; Zhu, N.-Y. *Org. Lett.* **2004,** *6*, 1577-1580.

68. Powell, B. M.; Torrie, B. H. *Acta Cryst. C* **1983,** *39*, 963-965.

69. Mancini, A.; Aragoni, M. C.; Bricklebank, N.; Castellano, C.; Demartin, F.; Isaia, F.; Lippolis, V.; Pintus, A.; Arca, M. *Chem. Asian J.* **2013,** *8*, 639-647.

70. van Bolhuis, F.; Koster, P. B.; Migchelsen, T. *Acta Crystallogr.* **1967,** *23*, 90-91.

71. Aragoni, M. C.; Arca, M.; Devillanova, F. A.; Grimaldi, P.; Isaia, F.; Lelj, F.; Lippolis, V. *Eur. J. Inorg. Chem.* **2006,** *2006*, 2166-2174.

72. Boyle, P. D.; Godfrey, S. M. *Coord. Chem. Rev.* **2001,** *223*, 265-299.

73. Lin, G. H.-Y.; Hope, H. *Acta Cryst. B* **1972,** *28*, 643-646.

74. Kuhn, K. M.; Grubbs, R. H. *Org. Lett.* **2008,** *10*, 2075-2077.

75. Karri, R.; Banerjee, M.; Rai, R.; Roy, G. *Proc. Natl. Acad. Sci., India, Sect. A* **2016,** *86*, 611-617.

76. Lu, W.; Barber, P. S.; Kelley, S. P.; Rogers, R. D. *Dalton Trans.* **2013,** *42*, 12908-12916.

77. Lobana, T. S.; Sandhu, A. K.; Jassal, A. K.; Hundal, G.; Mahajan, R. K.; Jasinski, J. P.; Butcher, R. J. *Polyhedron* **2015,** *87*, 17-27.

78. Isab, A. A.; Wazeer, M. I. M.; Fettouhi, M.; Ahmad, S.; Ashraf, W. *Polyhedron* **2006,** *25*, 2629-2636.

79. Choi, J.; Park, S. Y.; Yang, H. Y.; Kim, H. J.; Ihm, K.; Nam, J. H.; Ahn, J. R.; Son, S. U. *Polym. Chem.* **2011,** *2*, 2512-2517.

80. Gardinier, J. R.; Gabbai, F. P. *J. Chem. Soc., Dalton Trans.* **2000**, 2861-2865.

81. Guzei, I. A.; Wendt, M. *Dalton Trans.* **2006**, 3991-3999.

82. Uson, R.; Laguna, A.; Laguna, M. *Inorg. Synth.* 2007; 26, p 85-91.

83. Chiodo, S.; Russo, N.; Sicilia, E. *J. Chem. Phys.* **2006,** *125*, 104107.

84. Ahmad, S. *Coord. Chem. Rev.* **2004,** *248*, 231-243.

85. Isab, A. A.; Hussain, M. S.; Akhtar, M. N.; Wazeer, M. I. M.; Al-Arfaj, A. R. *Polyhedron* **1999,** *18*, 1401-1409.

86. Fulmer, G. R.; Miller, A. J. M.; Sherden, N. H.; Gottlieb, H. E.; Nudelman, A.; Stoltz, B. M.; Bercaw, J. E.; Goldberg, K. I. *Organometallics* **2010,** *29*, 2176-2179.

87. Griffin, J. M.; Knight, F. R.; Hua, G.; Ferrara, J. S.; Hogan, S. W. L.; Woollins, J. D.; Ashbrook, S. E. *J. Phys. Chem. C* **2011,** *115*, 10859-10872.

88. Frisch, M. J.; Trucks, G. W.; Schlegel, H. B.; Scuseria, G. E.; Robb, M. A.; Cheeseman, J. R.; Montgomery, J. A.; Vreven, T.; Kudin, K. N.; Burant, J. C.; Millam, J. M.; Iyengar, S. S.; Tomasi, J.; Barone, V.; Mennucci, B.; Cossi, M.; Scalmani, G.; Rega, N.; Petersson, G. A.; Nakatsuji, H.; Hada, M.; Ehara, M.; Toyota, K.; Fukuda, R.; Hasegawa, J.; Ishida, M.; Nakajima, T.; Honda, Y.; Kitao, O.; Nakai, H.; Klene, M.; Li, X.; Knox, J. E.; Hratchian, H. P.; Cross, J. B.; Bakken, V.; Adamo, C.; Jaramillo, J.; Gomperts, R.; Stratmann, R. E.; Yazyev, O.; Austin, A. J.; Cammi, R.; Pomelli, C.; Ochterski, J. W.; Ayala, P. Y.; Morokuma, K.; Voth, G. A.; Salvador, P.; Dannenberg, J. J.; Zakrzewski, V. G.; Dapprich, S.; Daniels, A. D.; Strain, M. C.; Farkas, O.; Malick, D. K.; Rabuck, A. D.; Raghavachari, K.; Foresman, J. B.; Ortiz, J. V.; Cui, Q.; Baboul, A. G.; Clifford, S.; Cioslowski, J.; Stefanov, B. B.; Liu, G.; Liashenko, A.; Piskorz, P.; Komaromi, I.; Martin, R. L.; Fox, D. J.; Keith, T.; Laham, A.; Peng, C. Y.; Nanayakkara, A.; Challacombe, M.; Gill, P. M. W.; Johnson, B.; Chen, W.; Wong, M. W.; Gonzalez, C.; Pople, J. A. Gaussian 03, Revision C.02. 2003.

89. Matsumura, T.; Nakada, M. *Tetrahedron Lett.* **2014,** *55*, 1412-1415.

90. Iglesias, M.; Beetstra, D. J.; Knight, J. C.; Ooi, L.-L.; Stasch, A.; Coles, S.; Male, L.; Hursthouse, M. B.; Cavell, K. J.; Dervisi, A.; Fallis, I. A. *Organometallics* **2008,** *27*, 3279-3289.

91. Arnér, E. S. J.; Holmgren, A. *Eur. J. Biochem.* **2000,** *267*, 6102-6109.

92. Nahra, F.; Patrick, S. R.; Collado, A.; Nolan, S. P. *Polyhedron* **2014,** *84*, 59-62.

93. Liu, L.; Zhu, D.; Cao, L. L.; Stephan, D. W. *Dalton Trans.* **2017,** *46*, 3095-3099.

APPENDIX A: CRYSTAL DATA FOR SIXyS

Empirical formula	$C_{19}H_{22}N_2S$
Formula weight	310.45
Temperature	298(2) K
Wavelength	0.71073 Å
Crystal system, space group	Monoclinic, $P2_1/c$ (No. 14)
Unit cell dimensions	a = 7.4085(8) Å α = 90° b = 8.3823(10) Å β = 94.013(3)° c = 27.619(3) Å γ = 90°
Volume	1710.9(3) $Å^3$
Z, Density (calculated)	4, 1.205 Mg/m^3
Absorption coefficient	0.188 mm^{-1}
Crystal size	0.30 x 0.25 x 0.20 mm^3
Crystal color / habit	colorless / block
Theta range for data collection	2.96 to 25.74°
Reflections collected/ Independent	30753/ 3233 [R(int) = 0.0290]
Completeness to theta = 25.25°	99.5%
Absorption correction	multi-scan / SADABS
Max. and min. transmission	0.9634 and 0.9458
Refinement method	Full-matrix least-squares on F^2
Data / restraints / parameters	3233 / 0 / 203
Goodness-of-fit on F^2	1.077
Final R indices [I>2sigma(I)]	R1 = 0.0466, wR2 = 0.1263
R indices (all data)	R1 = 0.0541, wR2 = 0.1316
Largest diff. peak and hole	0.199 and -0.218 $e.Å^{-3}$

APPENDIX B: CRYSTAL DATA FOR SIXySe

Empirical formula	$C_{19}H_{22}N_2Se$
Formula weight	357.35
Temperature	200(2) K
Wavelength	0.71073 Å
Crystal system, space group	Monoclinic, *P*2/*n* (No. 10)
Unit cell dimensions	a = 8.3392(8) Å α = 90° b = 7.4730(7) Å β = 98.786(3)° c = 13.7372(12) Å γ = 90°
Volume	846.04(14) $Å^3$
Z, Density (calculated)	2, 1.403 Mg/m^3
Absorption coefficient	2.218 mm^{-1}
Crystal size	0.18 x 0.17 x 0.14 mm^3
Crystal color / habit	colorless / block
Theta range for data collection	3.00 to 25.70°
Reflections collected/ Independent	22852 /1608 [R(int) = 0.0308]
Completeness to theta = 25.25°	99.6%
Absorption correction	mbsulti-scan / SADABS
Max. and min. transmission	0.7465 and 0.6910
Refinement method	Full-matrix least-squares on F^2
Data / restraints / parameters	1608 / 0 / 103
Goodness-of-fit on F^2	1.086
Final R indices [I>2sigma(I)]	R1 = 0.0220, wR2 = 0.0579
R indices (all data)	R1 = 0.0233, wR2 = 0.0588
Largest diff. peak and hole	0.233 and -0.312 $e.Å^{-3}$

APPENDIX C: CRYSTAL DATA FOR (SIXyS)$HgCl_2$

Empirical formula	$C_{19}H_{22}Cl_2HgN_2S$
Formula weight	581.94
Temperature	200(2) K
Wavelength	0.71073 Å
Crystal system, space group	Monoclinic, *C*2/*c* (No. 15)
Unit cell dimensions	a = 25.0259(15) Å α = 90° b = 9.3706(6) Å β = 118.728(2)° c = 19.6280(13) Å γ = 90°
Volume	4036.3(4) $Å^3$
Z, Density (calculated)	8, 1.915 Mg/m^3
Absorption coefficient	7.999 mm^{-1}
Crystal size	0.20 x 0.18 x 0.12 mm^3
Crystal color / habit	colorless / block
Theta range for data collection	3.27 to 25.75°
Reflections collected/ Independent	64964/ 3857 [R(int) = 0.0338]
Completeness to theta = 25.25°	99.8%
Absorption correction	None
Max. and min. transmission	0.4470 and 0.2976
Refinement method	Full-matrix least-squares on F^2
Data / restraints / parameters	3857 / 0 / 230
Goodness-of-fit on F^2	1.003
Final R indices [I>2sigma(I)]	R1 = 0.0162, wR2 = 0.0411
R indices (all data)	R1 = 0.0198, wR2 = 0.0441
Largest diff. peak and hole	0.332 and -1.030 e.$Å^{-3}$

APPENDIX D: CRYSTAL DATA FOR (SIXyS)$HgBr_2$

Empirical formula	$C_{19}H_{22}Br_2HgN_2S$	
Formula weight	670.86	
Temperature	200(2) K	
Wavelength	1.54178 Å	
Crystal system, space group	Monoclinic, *C*2/*c* (No. 15)	
Unit cell dimensions	a = 25.635(6) Å b = 9.392(2) Å c = 19.992(4) Å	α = 90° β = 119.769(6)° γ = 90°
Volume	4178.5(16) $Å^3$	
Z, Density (calculated)	8, 2.133 Mg/m^3	
Absorption coefficient	18.655 mm^{-1}	
Crystal size	0.20 x 0.20 x 0.20 mm^3	
Crystal color / habit	colorless / block	
Theta range for data collection	3.97 to 70.65°.	
Reflections collected/ Independent	32975/ 3966 [R(int) = 0.0616]	
Completeness to theta = 68.25°	99.3%	
Absorption correction	multi-scan / SADABS	
Max. and min. transmission	0.1180 and 0.1180	
Refinement method	Full-matrix least-squares on F^2	
Data / restraints / parameters	3966 / 0 / 231	
Goodness-of-fit on F^2	1.042	
Final R indices [I>2sigma(I)]	R1 = 0.0371, wR2 = 0.0988	
R indices (all data)	R1 = 0.0391, wR2 = 0.1011	
Largest diff. peak and hole	2.394 and -1.584 e.$Å^{-3}$	

APPENDIX E: CRYSTAL DATA FOR (SIXyS)HgI_2

Empirical formula	$C_{19}H_{22}HgI_2N_2S$	
Formula weight	764.84	
Temperature	200(2) K	
Wavelength	0.71073 Å	
Crystal system, space group	Triclinic, $P\bar{1}$ (No. 2)	
Unit cell dimensions	a = 7.3109(10) Å b = 10.6805(13) Å c = 14.934(2) Å	α= 75.519(4)° β = 80.546(5)° γ = 81.595(4)°
Volume	1106.9(3) $Å^3$	
Z, Density (calculated)	2, 2.295 Mg/m^3	
Absorption coefficient	9.840 mm^{-1}	
Crystal size	0.20 x 0.15 x 0.08 mm^3	
Crystal color / habit	colorless / block	
Theta range for data collection	2.84 to 25.80°	
Reflections collected/ Independent	50055, 4227 [R(int) = 0.0339]	
Completeness to theta = 25.25°	99.8%	
Absorption correction	multi-scan / SADABS	
Max. and min. transmission	0.5065 and 0.2436	
Refinement method	Full-matrix least-squares on F^2	
Data / restraints / parameters	4227 / 6 / 230	
Goodness-of-fit on F^2	1.058	
Final R indices	[I>2sigma(I)]R1 = 0.0241, wR2 = 0.0547	
R indices (all data)	R1 = 0.0303, wR2 = 0.0597	
Largest diff. peak and hole	0.995 and -0.805 e.$Å^{-3}$	

APPENDIX F: CRYSTAL DATA FOR (SIXySe)$HgCl_2$

Empirical formula	$C_{19}H_{22}Cl_2HgN_2Se$
Formula weight	628.84
Temperature	200(2) K
Wavelength	0.71073 Å
Crystal system, space group	Monoclinic, *C*2/*c* (No. 15)
Unit cell dimensions	a = 24.902(3) Å α = 90° b = 9.5090(10) Å β = 118.457(3)° c = 19.627(2) Å γ = 90°
Volume	4085.9(8) $Å^3$
Z, Density (calculated)	8, 2.044 Mg/m^3
Absorption coefficient	9.582 mm^{-1}
Crystal size	0.20 x 0.20 x 0.18 mm^3
Crystal color / habit	colorless / block
Theta range for data collection	3.26 to 25.45°
Reflections collected/ Independent	67717/ 3763 [R(int) = 0.0425]
Completeness to theta = 25.25°	99.8%
Absorption correction	multi-scan / SADABS
Max. and min. transmission	0.2774 and 0.2502
Refinement method	Full-matrix least-squares on F^2
Data / restraints / parameters	3763 / 0 / 230
Goodness-of-fit on F^2	1.024
Final R indices [I>2sigma(I)]	R1 = 0.0165, wR2 = 0.0422
R indices (all data)	R1 = 0.0199, wR2 = 0.0448
Largest diff. peak and hole	0.319 and -1.039 e.$Å^{-3}$

APPENDIX G: CRYSTAL DATA FOR (SIXySe)$HgBr_2$

Empirical formula	$C_{19}H_{22}Br_2HgN_2Se$
Formula weight	717.76
Temperature	200(2) K
Wavelength	0.71073 Å
Crystal system, space group	Monoclinic, *C*2/*c* (No. 15)
Unit cell dimensions	a = 25.492(3) Å α = 90° b = 9.5401(11) Å β = 119.399(4)° c = 19.895(3) Å γ = 90°
Volume	4215.3(9) $Å^3$
Z, Density (calculated)	8, 2.262 Mg/m^3
Absorption coefficient	12.826 mm^{-1}
Crystal size	0.18 x 0.15 x 0.04 mm^3
Crystal color / habit	colorless / block
Theta range for data collection	3.22 to 25.40°
Reflections collected/ Independent	50744/ 3876 [R(int) = 0.0488]
Completeness to theta = 25.25°	99.8%
Absorption correction	multi-scan / SADABS
Max. and min. transmission	0.6280 and 0.2061
Refinement method	Full-matrix least-squares on F^2
Data / restraints / parameters	3876 / 0 / 230
Goodness-of-fit on F^2	1.038
Final R indices [I>2sigma(I)]	R1 = 0.0205, wR2 = 0.0414
R indices (all data)	R1 = 0.0304, wR2 = 0.0447
Largest diff. peak and hole	0.874 and -0.566 e.$Å^{-3}$

APPENDIX H: CRYSTAL DATA FOR (SIXySe)HgI_2

Empirical formula	$C_{19}H_{22}HgI_2N_2Se$	
Formula weight	811.74	
Temperature	200(2) K	
Wavelength	0.71073 Å	
Crystal system, space group	Triclinic, $P\bar{1}$ (No. 2)	
Unit cell dimensions	a = 7.3269(13) Å b = 10.793(2) Å c = 14.791(2) Å	α = 75.360(6)° β = 80.691(6)° γ = 81.691(7)°
Volume	1110.2(3) $Å^3$	
Z, Density (calculated)	2, 2.428 Mg/m^3	
Absorption coefficient	11.357 mm^{-1}	
Crystal size	0.18 x 0.08 x 0.06 mm^3	
Crystal color / habit	colorless / block	
Theta range for data collection	3.00 to 25.48°	
Reflections collected/ Independent	4163/ 4164 [R(int) = 0.0000]	
Completeness to theta = 25.25°	98.7%	
Absorption correction	multi-scan / SADABS	
Max. and min. transmission	0.5490 and 0.2343	
Refinement method	Full-matrix least-squares on F^2	
Data / restraints / parameters	4164 / 12 / 231	
Goodness-of-fit on F^2	1.093	
Final R indices [I>2sigma(I)]	R1 = 0.0412, wR2 = 0.1195	
R indices (all data)	R1 = 0.0485, wR2 = 0.1279	
Largest diff. peak and hole	1.158 and -2.094 e.$Å^{-3}$	

APPENDIX I: CRYSTAL DATA FOR (SIMesS)$HgCl_2$

Empirical formula	$C_{21}H_{26}Cl_2HgN_2S$
Formula weight	609.99
Temperature	298(2) K
Wavelength	0.71073 Å
Crystal system, space group	Monoclinic, $P2_1/c$ (No. 14)
Unit cell dimensions	a = 8.3509(3) Å α = 90° b = 20.8489(7) Å β = 98.5200(10)° c = 13.2440(5) Å γ = 90°
Volume	2280.43(14) $Å^3$
Z, Density (calculated)	4, 1.777 Mg/m^3
Absorption coefficient	7.084 mm^{-1}
Crystal size	0.30 x 0.25 x 0.20 mm^3
Crystal color / habit	colorless / block
Theta range for data collection	2.88 to 25.73°
Reflections collected/ Independent	29271/ 4331 [R(int) = 0.0348]
Completeness to theta = 25.25°	99.8%
Absorption correction	Multi-scan / SADABS
Max. and min. transmission	0.3316 and 0.2251
Refinement method	Full-matrix least-squares on F^2
Data / restraints / parameters	4331 / 0 / 250
Goodness-of-fit on F^2	1.026
Final R indices [I>2sigma(I)]	R1 = 0.0252, wR2 = 0.0582
R indices (all data)	R1 = 0.0368, wR2 = 0.0639
Largest diff. peak and hole	0.552 and -1.084 e.$Å^{-3}$

APPENDIX J: CRYSTAL DATA FOR (SIMesS)$HgBr_2$

Empirical formula	$C_{21}H_{26}Br_2HgN_2S$
Formula weight	698.91
Temperature	200(2) K
Wavelength	0.71073 Å
Crystal system, space group	Monoclinic, $P2_1/c$ (No. 14)
Unit cell dimensions	a = 8.4657(4) Å α = 90° b = 20.9618(9) Å β = 98.3340(10)° c = 13.2594(5) Å γ = 90°
Volume	2328.12(17) $Å^3$
Z, Density (calculated)	4, 1.994 Mg/m^3
Absorption coefficient	10.142 mm^{-1}
Crystal size	0.18 x 0.18 x 0.15 mm^3
Crystal color / habit	colorless / block
Theta range for data collection	2.86 to 25.73°
Reflections collected/ Independent	57444/ 4434 [R(int) = 0.0346]
Completeness to theta = 25.25°	99.8%
Absorption correction	multi-scan / SADABS
Max. and min. transmission	0.3115 and 0.2626
Refinement method	Full-matrix least-squares on F^2
Data / restraints / parameters	4434 / 0 / 250
Goodness-of-fit on F^2	1.040
Final R indices [I>2sigma(I)]	R1 = 0.0206, wR2 = 0.0509
R indices (all data)	R1 = 0.0277, wR2 = 0.0559
Largest diff. peak and hole	0.575 and -0.862 $e.Å^{-3}$

APPENDIX K: CRYSTAL DATA FOR (SIMesS)HgI_2

Empirical formula	$C_{21}H_{26}HgI_2N_2S$	
Formula weight	792.89	
Temperature	200(2) K	
Wavelength	0.71073 Å	
Crystal system, space group	Triclinic, $P\bar{1}$ (No. 2)	
Unit cell dimensions	a = 9.8756(15) Å b = 11.3632(16) Å c = 11.5907(19) Å	α = 107.568(6)° β = 103.268(6)° γ = 91.536(6)°
Volume	1200.4(3) $Å^3$	
Z, Density (calculated)	2, 2.194 Mg/m^3	
Absorption coefficient	9.078 mm-1	
Crystal size	0.25 x 0.13 x 0.12 mm^3	
Crystal color / habit	block / pale yellwo	
Theta range for data collection	2.88 to 25.79°	
Reflections collected/ Independent	29438/ 4567 [R(int) = 0.0439]	
Completeness to theta = 25.25°	99.9%	
Absorption correction	multi-scan / SADABS	
Max. and min. transmission	0.4088 and 0.2099	
Refinement method	Full-matrix least-squares on F^2	
Data / restraints / parameters	4567 / 0 / 250	
Goodness-of-fit on F^2	1.037	
Final R indices [I>2sigma(I)]	R1 = 0.0243, wR2 = 0.0555	
R indices (all data)	R1 = 0.0322, wR2 = 0.0594	
Largest diff. peak and hole	0.682 and -1.110 e.$Å^{-3}$	

APPENDIX L: CRYSTAL DATA FOR (SIMesSe)$HgCl_2$

Empirical formula	$C_{21}H_{26}Cl_2HgN_2Se$
Formula weight	656.89
Temperature	200(2) K
Wavelength	0.71073 Å
Crystal system, space group	Monoclinic, $P2_1/c$ (No. 14)
Unit cell dimensions	a = 8.2263(9) Å α = 90° b = 20.998(2) Å β = 97.231(4)° c = 13.2152(14) Å γ = 90°
Volume	2264.6(4) $Å^3$
Z, Density (calculated)	4, 1.927 Mg/m^3
Absorption coefficient	8.649 mm^{-1}
Crystal size	0.20 x 0.18 x 0.10 mm^3
Crystal color / habit	colorless / block
Theta range for data collection	2.93 to 25.71°
Reflections collected/ Independent	46775/ 4299 [R(int) = 0.0401]
Completeness to theta = 25.25°	99.9%
Absorption correction	multi-scan / SADABS
Max. and min. transmission	0.4784 and 0.2766
Refinement method	Full-matrix least-squares on F^2
Data / restraints / parameters	4299 / 0 / 250
Goodness-of-fit on F^2	1.080
Final R indices [I>2sigma(I)]	R1 = 0.0216, wR2 = 0.0417
R indices (all data)	R1 = 0.0301, wR2 = 0.0442
Largest diff. peak and hole	1.068 and -1.083 e.$Å^{-3}$

APPENDIX M: CRYSTAL DATA FOR (SIMesSe)$HgBr_2$

Empirical formula	$C_{21}H_{26}Br_2HgN_2Se$
Formula weight	745.81
Temperature	200(2) K
Wavelength	0.71073 Å
Crystal system, space group	Monoclinic, $P2_1/c$ (No. 14)
Unit cell dimensions	a = 8.3916(5) Å α = 90° b = 21.1726(12) Å β = 97.430(2)° c = 13.3252(7) Å γ = 90°
Volume	2347.6(2) $Å^3$
Z, Density (calculated)	4, 2.110 Mg/m^3
Absorption coefficient	11.519 mm^{-1}
Crystal size	0.20 x 0.18 x 0.18 mm^3
Crystal color / habit	colorless / block
Theta range for data collection	2.88 to 25.71°
Reflections collected/ Independent	57696/ 4456 [R(int) = 0.0432]
Completeness to theta = 25.25°	99.7%
Absorption correction	multi-scan / SADABS
Max. and min. transmission	0.2309 and 0.2066
Refinement method	Full-matrix least-squares on F^2
Data / restraints / parameters	4456 / 0 / 250
Goodness-of-fit on F^2	1.036
Final R indices [I>2sigma(I)]	R1 = 0.0249, wR2 = 0.0641
R indices (all data)	R1 = 0.0326, wR2 = 0.0701
Largest diff. peak and hole	0.971 and -0.849 e.$Å^{-3}$

APPENDIX N: CRYSTAL DATA FOR (SIMesSe)HgI_2

Empirical formula	$C_{21}H_{26}HgI_2N_2Se$	
Formula weight	839.79	
Temperature	296(2) K	
Wavelength	0.71073 Å	
Crystal system, space group	Triclinic, $P\bar{1}$ (No. 2)	
Unit cell dimensions	a = 10.0059(7) Å b = 11.5003(7) Å c = 11.6659(8) Å	α = 106.721(2)° β = 105.484(2)° γ = 91.104(2)°
Volume	1232.25(14) $Å^3$	
Z, Density (calculated)	2, 2.263 Mg/m^3	
Absorption coefficient	10.236 mm^{-1}	
Crystal size	0.30 x 0.15 x 0.12 mm^3	
Crystal color / habit	yellow / block	
Theta range for data collection	2.97 to 25.78°	
Reflections collected/ Independent	41784/ 4693 [R(int) = 0.0341]	
Completeness to theta = 25.25°	99.8%	
Absorption correction	multi-scan / sadabs	
Max. and min. transmission	0.3730 and 0.1492	
Refinement method	Full-matrix least-squares on F^2	
Data / restraints / parameters	4693 / 0 / 250	
Goodness-of-fit on F^2	1.087	
Final R indices [I>2sigma(I)]	R1 = 0.0285, wR2 = 0.0628	
R indices (all data)	R1 = 0.0387, wR2 = 0.0707	
Largest diff. peak and hole	0.983 and -1.277 e.$Å^{-3}$	

APPENDIX O: CRYSTAL DATA FOR (SIDippS)$HgCl_2$

Empirical formula	$C_{27}H_{38}Cl_2HgN_2S$
Formula weight	694.14
Temperature	200(2) K
Wavelength	0.71073 Å
Crystal system, space group	Monoclinic, $P2_1/c$ (No. 14)
Unit cell dimensions	a = 10.3342(6) Å α = 90° b = 16.9093(11) Å β = 101.496(2)° c = 16.5710(11) Å γ = 90°
Volume	2837.6(3) $Å^3$
Z, Density (calculated)	4, 1.625 Mg/m^3
Absorption coefficient	5.704 mm^{-1}
Crystal size	0.20 x 0.14 x 0.10 mm^3
Crystal color / habit	colorless / block
Theta range for data collection	3.13 to 25.38°
Reflections collected/ Independent	43333/ 5206 [R(int) = 0.0446]
Completeness to theta = 25.25°	99.7%
Absorption correction	multi-scan / SADABS
Max. and min. transmission	0.5993 and 0.3950
Refinement method	Full-matrix least-squares on F^2
Data / restraints / parameters	5206 / 18 / 306
Goodness-of-fit on F^2	1.020
Final R indices [I>2sigma(I)]	R1 = 0.0248, wR2 = 0.0639
R indices (all data)	R1 = 0.0359, wR2 = 0.0735
Largest diff. peak and hole	0.997 and -0.659 e.$Å^{-3}$

APPENDIX P: CRYSTAL DATA FOR (SIDippS)$HgBr_2$

Empirical formula	$C_{27}H_{38}Br_2HgN_2S$
Formula weight	783.06
Temperature	200(2) K
Wavelength	1.54178 Å
Crystal system, space group	Monoclinic, $P2_1/c$ (No. 14)
Unit cell dimensions	a = 10.384(3) Å α = 90° b = 16.904(4) Å β = 100.855(10)° c = 16.890(4) Å γ = 90°
Volume	2911.8(12) $Å^3$
Z, Density (calculated)	4, 1.786 Mg/m^3
Absorption coefficient	13.486 mm^{-1}
Crystal size	0.18 x 0.18 x 0.10 mm^3
Crystal color / habit	colorless / block
Theta range for data collection	3.73 to 68.80°
Reflections collected/ Independent	35018/ 5332 [R(int) = 0.0475]
Completeness to theta = 68.25°	99.3%
Absorption correction	multi-scan / SADABS
Max. and min. transmission	0.3457 and 0.1951
Refinement method	Full-matrix least-squares on F^2
Data / restraints / parameters	5332 / 6 / 306
Goodness-of-fit on F^2	1.005
Final R indices [I>2sigma(I)]	R1 = 0.0286, wR2 = 0.0776
R indices (all data)	R1 = 0.0327, wR2 = 0.0832
Largest diff. peak and hole	0.755 and -0.692 $e.Å^{-3}$

APPENDIX Q: CRYSTAL DATA FOR (SIDippS)HgI_2

Empirical formula	$C_{27}H_{38}HgI_2N_2S$
Formula weight	877.04
Temperature	200(2) K
Wavelength	1.54178 Å
Crystal system, space group	Monoclinic, $P2_1/n$ (No. 11)
Unit cell dimensions	a = 12.1245(12) Å α = 90° b = 19.527(2) Å β = 94.811(4)° c = 13.3314(13) Å γ = 90°
Volume	3145.1(5) $Å^3$
Z, Density (calculated)	4, 1.852 Mg/m^3
Absorption coefficient	24.923 mm^{-1}
Crystal size	0.20 x 0.16 x 0.08 mm^3
Crystal color / habit	colorless / block
Theta range for data collection	4.02 to 68.64°
Reflections collected/ Independent	40829/ 5762 [R(int) = 0.0540]
Completeness to theta = 68.25°	99.4%
Absorption correction	multi-scan / SADABS
Max. and min. transmission	0.2404 and 0.0824
Refinement method	Full-matrix least-squares on F^2
Data / restraints / parameters	5762 / 0 / 306
Goodness-of-fit on F^2	1.063
Final R indices [I>2sigma(I)]	R1 = 0.0346, wR2 = 0.0911
R indices (all data)	R1 = 0.0378, wR2 = 0.0943
Largest diff. peak and hole	0.968 and -1.269 e.$Å^{-3}$

APPENDIX R: CRYSTAL DATA FOR (SIDippSe)$HgCl_2$

Empirical formula	$C_{27}H_{38}Cl_2HgN_2Se$
Formula weight	741.04
Temperature	200(2) K
Wavelength	0.71073 Å
Crystal system, space group	Monoclinic, $P2_1/c$ (No. 14)
Unit cell dimensions	a = 10.2791(5) Å α = 90° b = 16.8967(7) Å β = 100.892(2)° c = 16.7008(7) Å γ = 90°
Volume	2848.4(2) $Å^3$
Z, Density (calculated)	4, 1.728 Mg/m^3
Absorption coefficient	6.887 mm^{-1}
Crystal size	0.21 x 0.20 x 0.19 mm^3
Crystal color / habit	colorless / block
Theta range for data collection	3.13 to 25.41°.
Reflections collected/ Independent	69404/ 5246 [R(int) = 0.0343]
Completeness to theta = 25.25°	99.8%
Absorption correction	multi-scan / SADABS
Max. and min. transmission	0.3545 and 0.3257
Refinement method	Full-matrix least-squares on F^2
Data / restraints / parameters	5246 / 0 / 306
Goodness-of-fit on F^2	1.025
Final R indices [I>2sigma(I)]	R1 = 0.0226, wR2 = 0.0625
R indices (all data)	R1 = 0.0316, wR2 = 0.0729
Largest diff. peak and hole	0.660 and -1.034 e.$Å^{-3}$

APPENDIX S: CRYSTAL DATA FOR (SIDippSe)$HgBr_2$

Empirical formula	$C_{27}H_{38}Br_2HgN_2Se$
Formula weight	829.96
Temperature	200(2) K
Wavelength	0.71073 Å
Crystal system, space group	Monoclinic, $P2_1/c$ (No. 14)
Unit cell dimensions	a = 10.3159(4) Å α = 90° b = 16.9046(6) Å β = 100.703(10)° c = 17.0028(6) Å γ = 90°
Volume	2913.47(18) $Å^3$
Z, Density (calculated)	4, 1.892 Mg/m^3
Absorption coefficient	9.292 mm^{-1}
Crystal size	0.20 x 0.18 x 0.15 mm^3
Crystal color / habit	colorless / block
Theta range for data collection	3.10 to 25.75°
Reflections collected/ Independent	72856/ 5565 [R(int) = 0.0386]
Completeness to theta = 25.25°	99.8%
Absorption correction	multi-scan / SADABS
Max. and min. transmission	0.3362 and 0.2580
Refinement method	Full-matrix least-squares on F^2
Data / restraints / parameters	5565 / 0 / 306
Goodness-of-fit on F^2	1.075
Final R indices [I>2sigma(I)]	R1 = 0.0259, wR2 = 0.0691
R indices (all data)	R1 = 0.0353, wR2 = 0.0811
Largest diff. peak and hole	0.816 and -1.411 e.$Å^{-3}$

APPENDIX T: CRYSTAL DATA FOR (SIDippSe)HgI_2

Empirical formula	$C_{27}H_{38}HgI_2N_2Se$
Formula weight	923.94
Temperature	200(2) K
Wavelength	0.71073 Å
Crystal system, space group	Monoclinic, $P2_1/c$ (No. 14)
Unit cell dimensions	a = 10.4609(10) Å α = 90° b = 17.1014(18) Å β = 100.763(3)° c = 17.4634(18) Å γ = 90°
Volume	3069.2(5) Å
Z, Density (calculated)	4, 2.000 Mg/m^3
Absorption coefficient	8.229 mm^{-1}
Crystal size	0.19 x 0.14 x 0.10 mm^3
Crystal color / habit	yellow / block
Theta range for data collection	3.10 to 25.76°.
Reflections collected/ Independent	57264/ 5843 [R(int) = 0.0461]
Completeness to theta = 25.25°	99.8%
Absorption correction	multi-scan / SADABS
Max. and min. transmission	0.4933 and 0.3039
Refinement method	Full-matrix least-squares on F^2
Data / restraints / parameters	5843 / 0 / 306
Goodness-of-fit on F^2	1.030
Final R indices [I>2sigma(I)]	R1 = 0.0241, wR2 = 0.0620
R indices (all data)	R1 = 0.0340, wR2 = 0.0711
Largest diff. peak and hole	0.887 and -1.219 e.$Å^{-3}$

APPENDIX U: CRYSTAL DATA FOR $Hg_2(SIMesS)Br_4$

Empirical formula	$C_{21}H_{26}Br_4Hg_2N_2S$	
Formula weight	1059.32	
Temperature	200(2) K	
Wavelength	0.71073 Å	
Crystal system, space group	Monoclinic, *C*2 (No. 5)	
Unit cell dimensions	a = 24.4349(13) Å	α = 90°.
	b = 8.6874(5) Å	β = 107.726(10)°.
	c = 13.2190(7) Å	γ = 90°.
Volume	2672.9(3) $Å^3$	
Z, Density (calculated)	4, 2.632 Mg/m^3	
Absorption coefficient	17.544 mm^{-1}	
Crystal size	0.20 x 0.19 x 0.16 mm^3	
Crystal color / habit	colorless / block	
Theta range for data collection	3.12 to 25.72°	
Reflections collected/ Independent	27553/ 5073 [R(int) = 0.0273]	
Completeness to theta = 25.25°	99.8%	
Absorption correction	multi-scan / SADABS	
Max. and min. transmission	0.1657 and 0.1272	
Refinement method	Full-matrix least-squares on F^2	
Data / restraints / parameters	5073 / 1 / 279	
Goodness-of-fit on F^2	1.076	
Final R indices [I>2sigma(I)]	R1 = 0.0182, wR2 = 0.0379	
R indices (all data)	R1 = 0.0210, wR2 = 0.0388	
Largest diff. peak and hole	1.001 and -0.745 e.$Å^{-3}$	

APPENDIX V: CRYSTAL DATA FOR $Hg_2(SIMesS)I_4$

Empirical formula	$C_{21}H_{26}Hg_2I_4N_2S$
Formula weight	1247.28
Temperature	200(2) K
Wavelength	0.71073 Å
Crystal system, space group	Monoclinic, $P2_1/n$ (No. 11)
Unit cell dimensions	a = 13.5906(11) Å $\alpha = 90°$ b = 8.8175(7) Å $\beta = 103.032(2)°$ c = 24.6622(19) Å $\gamma = 90°$
Volume	2879.3(4) $Å^3$
Z, Density (calculated)	4, 2.877 Mg/m^3
Absorption coefficient	15.024 mm^{-1}
Crystal size	0.21 x 0.20 x 0.15 mm^3
Crystal color / habit	yellow / block
Theta range for data collection	2.87 to 25.70°
Reflections collected/ Independent	38268/ 5451 [R(int) = 0.0299]
Completeness to theta = 25.25°	99.7%
Absorption correction	None
Max. and min. transmission	0.2115 and 0.1445
Refinement method	Full-matrix least-squares on F^2
Data / restraints / parameters	5451 / 0 / 277
Goodness-of-fit on F2	1.064
Final R indices [I>2sigma(I)]	R1 = 0.0266, wR2 = 0.0643
R indices (all data)	R1 = 0.0336, wR2 = 0.0694
Largest diff. peak and hole	0.752 and -1.458 $e.Å^{-3}$

APPENDIX W: CRYSTAL DATA FOR (SIXyS)AuCl

Empirical formula	$C_{19}H_{22}AuClN_2S$	
Formula weight	542.86	
Temperature	200(2) K	
Wavelength	0.71073 Å	
Crystal system, space group	Monoclinic, *C*2/*c* (No. 15)	
Unit cell dimensions	a = 37.343(4) Å	α = 90°
	b = 7.8798(8) Å	β = 105.833(4)°
	c = 13.4292(14) Å	γ = 90°
Volume	3801.7(7) $Å^3$	
Z, Density (calculated)	8, 1.897 Mg/m^3	
Absorption coefficient	7.992 mm^{-1}	
Crystal size	0.15 x 0.10 x 0.08 mm^3	
Crystal color / habit	colorless / block	
Theta range for data collection	3.05 to 25.73°	
Reflections collected/ Independent	41885, 3618 [R(int) = 0.0674	
Completeness to theta = 25.25°	99.8%	
Absorption correction	None	
Max. and min. transmission	0.5673 and 0.3802	
Refinement method	Full-matrix least-squares on F^2	
Data / restraints / parameters	3618 / 0 / 221	
Goodness-of-fit on F^2	1.001	
Final R indices [I>2sigma(I)]	R1 = 0.0236, wR2 = 0.0486	
R indices (all data)	R1 = 0.0389, wR2 = 0.0540	
Largest diff. peak and hole	0.546 and -0.749 $e.Å^{-3}$	

APPENDIX X: CRYSTAL DATA FOR (SIMesS)AuCl

Empirical formula	$C_{21}H_{26}AuClN_2S$
Formula weight	570.91
Temperature	200(2) K
Wavelength	0.71073 Å
Crystal system, space group	Monoclinic, $P2_1/c$ (No. 14)
Unit cell dimensions	a = 41.681(4) Å α = 90° b = 7.9389(7) Å β = 99.687(3)° c = 13.2534(11) Å γ = 90°
Volume	4323.0(6) $Å^3$
Z, Density (calculated)	8, 1.754 Mg/m^3
Absorption coefficient	7.033 mm^{-1}
Crystal size	0.20 x 0.16 x 0.15 mm^3
Crystal color / habit	colorless / block
Theta range for data collection	2.97 to 25.71°
Reflections collected/ Independent	42297/ 4113 [R(int) = 0.0326]
Completeness to theta = 25.25°	99.9%
Absorption correction	multi-scan / SADABS
Max. and min. transmission	0.4185 and 0.3336
Refinement method	Full-matrix least-squares on F^2
Data / restraints / parameters	4113 / 0 / 241
Goodness-of-fit on F^2	1.088
Final R indices [I>2sigma(I)]	R1 = 0.0185, wR2 = 0.0369
R indices (all data)	R1 = 0.0271, wR2 = 0.0394
Largest diff. peak and hole	0.326 and -0.675 $e.Å^{-3}$

APPENDIX Y: CRYSTAL DATA FOR (SIMesS)AuBr

Empirical formula	$C_{21}H_{26}AuBrN_2S$
Formula weight	615.37
Temperature	200(2) K
Wavelength	0.71073 Å
Crystal system, space group	Monoclinic, *C*2/*c* (No. 15)
Unit cell dimensions	a = 40.985(5) Å α = 90° b = 8.2138(11) Å β = 100.385(5)° c = 13.2939(15) Å γ = 90°
Volume	4402.0(9) $Å^3$
Z, Density (calculated)	8, 1.857 Mg/m^3
Absorption coefficient	8.601 mm^{-1}
Crystal size	0.20 x 0.20 x 0.20 mm^3
Crystal color / habit	colorless / block
Theta range for data collection	2.91 to 25.74°.
Reflections collected/ Independent	74270/ 4190 [R(int) = 0.0404]
Completeness to theta = 25.25°	99.9 %
Absorption correction	multi-scan / SADABS
Max. and min. transmission	0.2781 and 0.2781
Refinement method	Full-matrix least-squares on F^2
Data / restraints / parameters	4190 / 0 / 241
Goodness-of-fit on F^2	1.064
Final R indices [I>2sigma(I)]	R1 = 0.0183, wR2 = 0.0447
R indices (all data)	R1 = 0.0233, wR2 = 0.0476
Largest diff. peak and hole	0.428 and -0.814 $e.Å^{-3}$

APPENDIX Z: CRYSTAL DATA FOR (SIDippS)AuCl · H_2O

Empirical formula	$C_{27}H_{40}AuClN_2OS$
Formula weight	673.09
Temperature	200(2) K
Wavelength	0.71073 Å
Crystal system, space group	Monoclinic, *C*2/*c* (No. 15)
Unit cell dimensions	a = 24.0666(18) Å α = 90° b = 15.9552(18) Å β = 117.848(6)° c = 17.743(2) Å γ = 90°
Volume	6024.0(11) $Å^3$
Z, Density (calculated)	8, 1.484 Mg/m^3
Absorption coefficient	5.062 mm^{-1}
Crystal size	0.19 x 0.15 x 0.12 mm^3
Crystal color / habit	colorless / block
Theta range for data collection	3.09 to 25.44°.
Reflections collected/ Independent	10875/ 10877 [R(int) = 0.0000]
Completeness to theta = 25.25°	99.8%
Absorption correction	multi-scan / SADABS
Max. and min. transmission	0.5818 and 0.4464
Refinement method	Full-matrix least-squares on F^2
Data / restraints / parameters	10877 / 6 / 302
Goodness-of-fit on F^2	1.096
Final R indices [I>2sigma(I)]	R1 = 0.0391, wR2 = 0.1037
R indices (all data)	R1 = 0.0537, wR2 = 0.1143
Largest diff. peak and hole	1.741 and -0.675 e.$Å^{-3}$

APPENDIX AA: CRYSTAL DATA FOR (SIDippS)AuBr

Empirical formula	$C_{54}H_{76}Au_2Br_2N_4S_2$
Formula weight	1399.06
Temperature	200(2) K
Wavelength	0.71073 Å
Crystal system, space group	Monoclinic, $P2_1/c$ (No. 14)
Unit cell dimensions	a = 15.8319(6) Å α = 90° b = 12.0130(5) Å β = 117.058(11)° c = 16.8989(7) Å γ = 90°
Volume	2862.2(2) $Å^3$
Z, Density (calculated)	2, 1.623 Mg/m^3
Absorption coefficient	6.625 mm^{-1}
Crystal size	0.18 x 0.15 x 0.10 mm^3
Crystal color / habit	colorless / block
Theta range for data collection	3.19 to 25.71°
Reflections collected/ Independent	71136/ 5443 [R(int) = 0.0550]
Completeness to theta = 25.25°	99.8 %
Absorption correction	None
Max. and min. transmission	0.5571 and 0.3818
Refinement method	Full-matrix least-squares on F^2
Data / restraints / parameters	5443 / 2 / 319
Goodness-of-fit on F^2	1.057
Final R indices [I>2sigma(I)]	R1 = 0.0300, wR2 = 0.0628
R indices (all data)	R1 = 0.0462, wR2 = 0.0707
Largest diff. peak and hole	0.837 and -2.084 $e.Å^{-3}$

APPENDIX AB: CRYSTAL DATA FOR (SIDippS)I_2

Empirical formula	$C_{27}H_{38}I_2N_2S$
Formula weight	676.45
Temperature	200(2) K
Wavelength	0.71073 Å
Crystal system, space group	Monoclinic, $P2_1/c$ (No. 14)
Unit cell dimensions	a = 10.6682(6) Å α = 90° b = 17.3329(10) Å β = 91.404(2)° c = 15.9010(10) Å γ = 90°
Volume	2939.4(3) $Å^3$
Z/ Density (calculated)	4/ 1.529 Mg/m^3
Absorption coefficient	2.227 mm^{-1}
Crystal size	0.19 x 0.18 x 0.15 mm^3
Crystal color / habit	red / block
Theta range for data collection	3.23 to 25.39°
Reflections collected/ Independent	71533/ 5390 [R(int) = 0.0447]
Completeness to theta = 25.25°	99.8 %
Absorption correction	multi-scan / SADABS
Max. and min. transmission	0.7311 and 0.6770
Refinement method	Full-matrix least-squares on F^2
Data / restraints / parameters	5390 / 0 / 297
Goodness-of-fit on F^2	1.033
Final R indices [I>2sigma(I)]	R1 = 0.0234, wR2 = 0.0613
R indices (all data)	R1 = 0.0314, wR2 = 0.0707
Largest diff. peak and hole	0.558 and -0.876 e.$Å^{-3}$

APPENDIX AC: CRYSTAL DATA FOR (SIXySe)I_2

Empirical formula	$C_{19}H_{22}I_2N_2Se$	
Formula weight	611.15	
Temperature	200(2) K	
Wavelength	0.71073 Å	
Crystal system, space group	Triclinic, $P\bar{1}$ (No. 2)	
Unit cell dimensions	a = 8.4037(12) Å b = 14.3921(17) Å c = 18.842(3) Å	α = 70.638(4)° β = 79.149(8)° γ = 89.587(5)°
Volume	2107.8(5) $Å^3$	
Z, Density (calculated)	4, 1.926 Mg/m^3	
Absorption coefficient	4.714 mm^{-1}	
Crystal size	0.21 x 0.10 x 0.04 mm^3	
Crystal color / habit	red / block	
Theta range for data collection	3.10 to 25.40°	
Reflections collected/ Independent	6854/ 6854 [R(int) = 0.0000]	
Completeness to theta = 25.00°	88.5 %	
Absorption correction	multi-scan / TWINABS	
Max. and min. transmission	0.8338 and 0.4376	
Refinement method	Full-matrix least-squares on F^2	
Data / restraints / parameters	6858 / 0 / 442	
Goodness-of-fit on F^2	1.064	
Final R indices [I>2sigma(I)]	R1 = 0.0445, wR2 = 0.1071	
R indices (all data)	R1 = 0.0657, wR2 = 0.1263	
Largest diff. peak and hole	1.345 and -1.039 e.$Å^{-3}$	

APPENDIX AD: CRYSTAL DATA FOR $(SIMesSe)I_2$

Empirical formula	$C_{21}H_{26}I_2N_2Se$
Formula weight	639.20
Temperature	200(2) K
Wavelength	0.71073 Å
Crystal system, space group	Monoclinic, $P2_1/n$ (No. 11)
Unit cell dimensions	a = 7.5810(5) Å α = 90° b = 15.7989(11) Å β = 96.129(2)° c = 19.6134(14) Å γ = 90°
Volume	2335.7(3) $Å^3$
Z, Density (calculated)	4/ 1.818 Mg/m^3
Absorption coefficient	4.259 mm^{-1}
Crystal size	0.22 x 0.20 x 0.20 mm^3
Crystal color / habit	red / block
Theta range for data collection	2.99 to 25.38°
Reflections collected/ Independent	63976/ 4271 [R(int) = 0.0382]
Completeness to theta = 25.25°	99.6%
Absorption correction	multi-scan / SADABS
Max. and min. transmission	0.4830 and 0.4543
Refinement method	Full-matrix least-squares on F^2
Data / restraints / parameters	4271 / 0 / 241
Goodness-of-fit on F^2	1.012
Final R indices [I>2sigma(I)]	R1 = 0.0312, wR2 = 0.0793
R indices (all data)	R1 = 0.0381, wR2 = 0.0883
Largest diff. peak and hole	0.750 and -0.732 $e.Å^{-3}$